Automated Calibration of Real Water Distribution Networks: City X Case Study

by

Ayman Khedr

A thesis
presented to the University of Waterloo
in fulfillment of the
thesis requirement for the degree of
Masters of Applied Science
in
Civil Engineering

Waterloo, Ontario, Canada, 2016

AUTHOR'S DECLARATION

I hereby declare that I am the sole author of this thesis. This is a true copy of the thesis, including any required final revisions, as accepted by my examiners.

I understand that my thesis may be made electronically available to the public.

Abstract

The calibration of water distribution systems networks (WDN) is a complex non-linear problem that has traditionally been solved using manual trial-and-error methods. Over the past few decades, automated calibration techniques have been the subject of a great deal of research, and significant advancements in the field of WDN calibration have been achieved. Despite these advancements in calibration techniques, and the development and application of automated tools in numerous research settings, most practitioners still rely on engineering judgment and traditional calibration methods for WDN calibration. In an effort to bridge the gap between practitioners and researchers, the value of these advanced calibration approaches relative to traditional methods is validated and quantified in a real world scenario.

City X's WDN model has been manually calibrated by engineers familiar with the system. Their calibration procedure was mainly an expert-based approach using judgment and trial-and-error and did not rely on automated optimization tools. The purpose of this study is to resolve the corresponding calibration problem with optimization tools and compare the calibration solutions in terms of quality (closeness to measured data) and calibration parameter values. The calibration problem is posed as a multi-objective optimization problem and solved with the PA-DDS algorithm. The precise calibration objectives are roughly matched to the manual calibration objectives specified by the engineers who calibrated the model. Multi-objective optimization results are compared against the manually calibrated model, and the potential benefit of applying an automated approach is assessed. The utilization of automated calibration methods is shown to clearly assist in parameter error detection and model quality improvement.

To further improve the quality of the calibrated model, the initial results from the automated calibration are used to guide a manual calibration effort. Upon the manual adjustment of macro-calibration parameters, the automated calibration tools are used again to quantify the parameter uncertainty. As such, the calibration approach is iterative, and based upon the effective application of automated calibration tools coupled with traditional trial-and-error methods. Several thousand unique solutions of approximately equal or greater quality than the existing manually calibrated model are generated. 89 of the most robust solutions are identified in an effort to parsimoniously capture the model parameter uncertainty. Ideally, this list of candidate solutions can be used in future operational studies to ensure that operational decisions are robust to a wide range of potential network conditions.

Moreover, particularly uncertain model parameters are identified so as to focus future field studies, and data collection efforts.

Acknowledgements

I would like to thank my advisor Dr. Bryan Tolson for the guidance and support given to me in fulfillment of my degree. I would also like to thank City X officials as well as the engineers from Company Y for their efforts in supplying the real network data used for analysis in this thesis. Special thanks to Mohammadamin Jahanpour for his assistance and coding expertise.

Finally, I would like to thank my family for the relentless support they provided me during my academic pursuits.

Table of Contents

AUTHOR'S DECLARATION ii
Abstract iii
Acknowledgements v
Table of Contents vi
List of Figures viii
List of Tables x
Chapter 1 Introduction 1
1.1 Problem Statement 9
1.2 Objective 9
1.3 Scope 10
1.4 Outline 10
Chapter 2 Manual and Automated Calibration Methods 12
2.1 Manual Calibration Methods 13
2.2 Automated Calibration Methodology 16
2.2.1 Automated Calibration Objectives 17
2.2.2 Decision Variables 20
2.2.3 Software/Hardware Utilized 25
2.2.4 Summary of Automated Calibration Experiments 26
2.3 Sources of Uncertainty 27
2.3.1 Uncertainty Specific to Model Inputs and Field Data 27
2.3.2 Modeling Uncertainty 29
Chapter 3 Initial Micro-Calibration Results 32
3.1 Trade-off Curves 32
3.1.1 Independent Objective Formulations: 5 C-factor Decision Space 34
3.1.2 Aggregate Objective Formulation: 5 C-factor Decision Space 37
3.1.3 2010 vs 2011 Performance: Bi-Objective Analysis 39
3.2 Graphical Time Series Analysis 41
3.3 Summary Statistics 46
3.4 Results Summary 48
Chapter 4 Manual Adjustment of Model Parameters 50
4.1 Control Rule Adjustment 50

4.2 Demand Pattern Adjustment 56
4.3 Zone 2 Demand Shift Analysis 61
4.4 Result Summary and Adjusted Micro-Calibration Problem Formulation 63
Chapter 5 Micro-Calibration Results of Manually Adjusted Model 65
5.1 Trade-off Analysis 66
5.1.1 2010 Calibration – 5 C-factor vs 13 C-factor 66
5.1.2 2011 Calibration: 5 C-factor vs 13 C-factor 68
5.1.3 Aggregate Calibration: 5 C-factor vs. 13 C-factor 71
5.1.4 Bi-Objective Trade-off Analysis 73
5.1.5 Trade-off Summary Statistics 74
5.2 Time Series Analysis 76
5.3 Final Solution Set 78
5.4 Results Summary 81
Chapter 6 Conclusions and Recommendations 84
Appendix A Calibration Parameters for Final Solution Set 87
Bibliography 92

List of Figures

Figure 1.1: Common components of a WDN – (Figure adapted from (Mays 2010)) 1
Figure 2.1: City X WDN model components; pressure zones and demand shift highlighted 12
Figure 2.2: Standard C-factor test (Figure from Walski et .al. 2003) 14
Figure 3.1: Non-dominated solutions from the 5 C-factor grouping 2010, 2011, and manual 2010 calibration formulations presented in the 2010 objective space 35
Figure 3.2: Non-dominated solutions from the 5 C-factor grouping 2011, 2010, and manual 2011 calibration formulations presented in the 2011 objective space 36
Figure 3.3: Non-dominated solutions from the 5 C-factor grouping 2010, aggregate and manual 2010 calibration formulations presented in the 2010 objective space 38
Figure 3.4: Non-dominated solutions from the 5 C-factor grouping 2011, aggregate, and manual 2011 calibration formulations presented in the 2011 objective space 39
Figure 3.5: 2010 vs 2011 bi-objective analysis of non-dominated solutions from the 5 C-factor grouping 2010, 2011, and aggregate calibration formulations (solutions circled in red are selected for time series analysis) 40
Figure 3.6: 2010 C (a), V (b) and S (c) tanks HGL time series of field observations compared to the manually calibrated and a select automatically calibrated solution in the 5 C-factor decision space.. 42
Figure 3.7: 2011 C (a), V (b) and S (c) tanks HGL time series of field observations compared to the manually calibrated and a select automatically calibrated solution in the 5 C-factor decision space.. 43
Figure 3.8: Manually calibrated simulation results vs. field observations relating zonal inflows and outflows to tank water levels 45
Figure 4.1: University pumping station model components and inflows/outflows 52
Figure 4.2: C (a), V (b), and S (c) tanks HGL time series for manually calibrated 2010 model with original and adjusted control rules 54
Figure 4.3: C (a), V (b), and S (c) tanks HGL time series for manually calibrated 2011 model with original and adjusted control rules 55
Figure 4.4: Zone 1 demand shift and network tanks 58
Figure 4.5: C (a), V (b), and S (c) tanks HGL time series for the manually calibrated 2010 model with adjusted control rules – zone 1 demand shift analysis 59
Figure 4.6: C (a), V (b), and S (c) tanks HGL time series for the manually calibrated 2011 model with adjusted control rules – zone 1 demand shift analysis 60

Figure 4.7: Zone 2 demand shift - decreasing base demands coloured blue; increasing demands coloured red 62
Figure 4.8: 2010 (a) and 2011 (b) simulated HGL time series of S tank for the manually calibrated model with adjusted control rules and diurnal demand curves – zone 2 demand shift analysis 63
Figure 5.1: Non-dominated solutions from the 2010 5 C-factor and 13 C-factor decision space calibration formulations presented in the 2010 objective space 67
Figure 5.2: Non-dominated solutions from the 2010 5 C-factor and 13 C-factor decision space calibration formulations validated in the 2011 objective space 68
Figure 5.3: Non-dominated solutions from the 2011 5 C-factor and 13 C-factor decision space calibration formulations presented in the 2011 objective space 68
Figure 5.4: Non-dominated solutions from the 2011 5 C-factor and 13 C-factor decision space calibration formulations validated in the 2010 objective space 69
Figure 5.5: Non-dominated solutions of the aggregate 5 C-factor and 13 C-factor decision space calibration formulations presented in the 2010 Objective Space 72
Figure 5.6: Non-dominated solutions of the aggregate 5 C-factor and 13 C-factor decision space calibration formulations presented in the 2011 Objective Space 73
Figure 5.7: 2010 vs 2011 bi-objective analysis of non-dominated solutions from the 2010, 2011 and aggregate calibration formulations in the 5 and 13 C-factor decision spaces (solution circled in red selected for time series analysis) 74
Figure 5.8: Zonal inflow/outflow and tank water level time series of observed field data vs. an automatically generated solution simulated in 2010 network conditions 77
Figure 5.9: Zonal inflow/outflow and tank water level time series of observed field data vs. an automatically generated solution simulated in 2011 network conditions 78

List of Tables

Table 2.1: Manually calibrated C-factor settings 15
Table 2.2: Automated calibration: 5 C-factor decision space 21
Table 2.3: Lamont (1981) C-factor settings for cast iron pipes - Adapted from Walski et.al. (2003). 23
Table 2.4: C-factor groupings associated with the 13 C-factor grouping decision space 24
Table 3.1: Automated calibration solution summary 46
Table 3.2: Automated calibration solution objective function change relative to manual Solution 48
Table 4.1: Observed zonal flux and demand calculated from 2010 and 2011 SCADA data 58
Table 5.1: 5 C-factor vs. 13 C-factor solution set comparison for 2010, 2011 and aggregate objective function formulations 75
Table 5.2: Final solution set - parameter variability and summary statistics of the 46 unique solutions generated in the 5 C-factor decision space 80
Table 5.3: Final solution set - parameter variability and summary statistics of the 43 unique solutions generated in the 13 C-factor decision space 81

Chapter 1
Introduction

Simulations of water distribution network (WDN) models are essential tools for planning, operation and maintenance of WDNs. A WDN is designed and built to deliver water from an initial source, often a water treatment facility, to customers using a series of pumps, pipes, valves, and tanks. The typical components of a WDN are depicted in figure 1.1. It is often impractical, and quite expensive to perform operational analyses and experiments on a network directly. Therefore, in lieu of direct experimentation, a model describing the physical characteristics of a real network is built and simulated. Simulating a model is the process of solving the complex hydraulic equations which mathematically represent flow and pressure conditions within the real system (Walski et al. 2003). The results generated from WDN simulations are regularly used by professionals in the municipal water industry to facilitate infrastructure investment (Engineering Computer Applications Committee 1999)

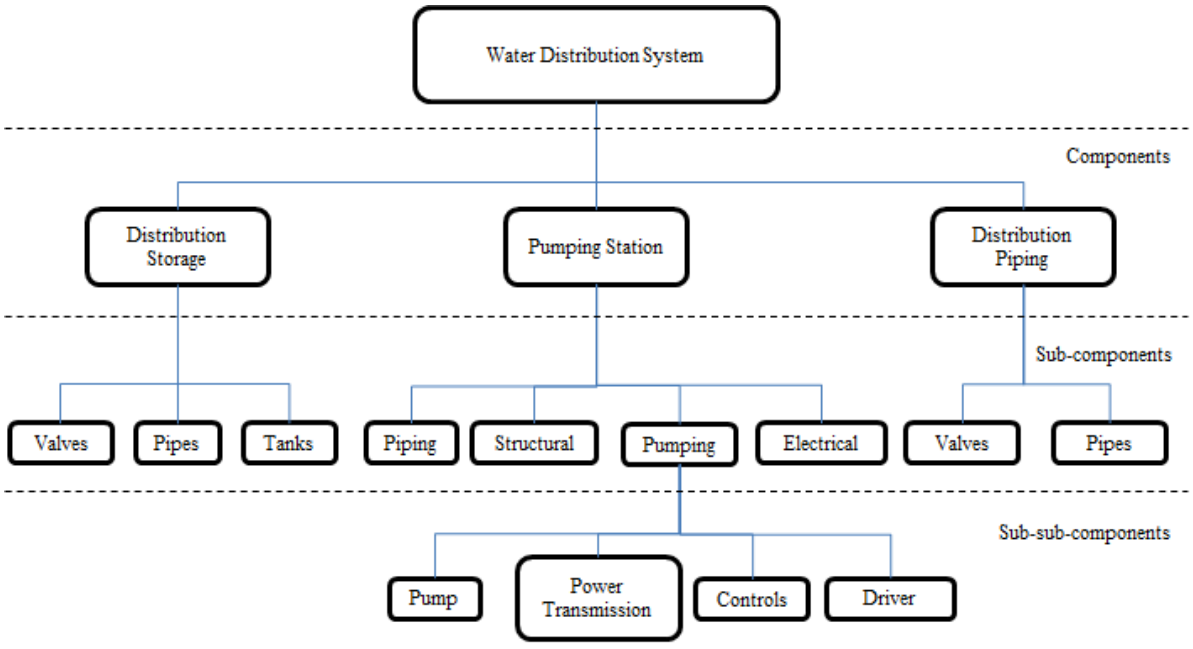

Figure 1.1: Common components of a WDN – (Figure adapted from (Mays 2010))

Typically, modeling software represents pipes and valves within a network using *links*, which are connected at junctions, or *nodes*. Customer water usage (*demands*) along a pipe is often simulated at the network nodes. Most models are skeletonized, meaning that not every pipe in the network is

included, and often small pipes delivering water to each individual user are omitted; relatively minor demands within the network (e.g. individual homes) are grouped and represented by a single node (Walski et al. 2003). Water is distributed through the network links from a storage facility (a reservoir, or tank) to the demand nodes through the use of pumping stations. WDN simulations are solved using a series of mass balance and energy conservation equations developed at each node and link in the network, respectively. These equations are mathematically defined in equations (1.1) and (1.2) which have been adapted from (Walski et al. 2003).

$$\sum_{pipes} Q_i - U = 0 \tag{1.1}$$

where Q_i represents the inflow to the node in the i-th pipe (M/T); and U represents the water used at the end node of the pipe (M/T).

$$Z_1 + \frac{P_1}{\gamma} + \frac{V_1^2}{2g} + \sum h_p = Z_2 + \frac{P_2}{\gamma} + \frac{V_2^2}{2g} + \sum h_l + \sum h_m \tag{1.2}$$

where Z represents elevation [L]; P represents pressure [$M/L^2/T^2$]; γ represents the fluid specific weight [$M/L^2/T^2$], g represents the gravitation force [L/T^2]; h_p, h_l, and h_m represent head added at pumps, head loss in pipes, and head loss due to minor losses [L].

Head added by a pump is calculated using a pump head characteristic curve which represents the non-linear relationship between pump head and discharge. Pump manufacturers provide this information, however pump curves can change over time after prolonged use of the pump. For information regarding specific pump head and flow calculations, refer to Walski et. al. (2003). Pumps are usually installed at water sources, as well as along pressure zone boundaries. For example if the elevation of one zone is significantly lower than an adjacent zone in the network, pumps are installed to boost the pressure at which the water is delivered at the higher elevation.

Minor head losses are caused by turbulence as water travels through bends or valves within the network. These losses are significantly smaller than head losses through pipes and are most often considered negligible. Head loss through pipes can be calculated using a variety of different equations; the most commonly used in North America is the Hazen Williams equation for head loss, defined in equation (1.3).

$$h_l = \frac{C_f L}{C^{1.852} D^{4.87}} Q^{1.852} \tag{1.3}$$

where C_f represents a unit conversion factor (10.7 for SI units); Q represents the flow rate [m^3/s]; D represents the internal pipe diameter [m], L represent the length of pipe (m); and C represents the Hazen-Williams C-factor [-]. Within real networks, pipes are subject to corrosion and tuberculation effects which effectively reduce the true diameter of the pipe. It is very difficult to calculate the actual internal diameter of a pipe following tuberculation effects, so WDN models typically account for these effects by altering C-factor settings. The C-factor is a pipe carrying capacity factor which is inversely related to pipe roughness. For smooth pipes, or pipes that have not experienced significant tuberculation, the C-factor is high, while rougher or severely tuberculated pipes are described using a lower C-factor (Walski et al. 2003).

A great deal of information must be defined within a WDN model to allow for accurate simulations of real-world conditions. In addition to the network topology, piping information including link diameters, lengths, and internal roughness factors (i.e. Hazen-Williams C-factors) must be defined. Moreover, pump and valve hydraulics and controls must be input into the model as well. Often pumps and valves are controlled by tank water level elevations, so it is important to also correctly describe storage volumes of each tank within a model.

Once all the necessary information is defined in the model, the network equations can be solved and the real conditions can be simulated. In order to simulate network conditions, it is necessary to assume that demands are known a priori. Typically, most modeling software used by practitioners solves for pressures and flows, while initial demand estimates are assumed static during the simulation (Tabesh et al. 2011). This is known as *demand-driven analysis*. In reality, demands are a function of the available pressures in the network, and in pressure deficient conditions, demands are reduced. Therefore, demand driven simulations can sometimes be inaccurate under conditions where pressures are too low to meet the estimated demands, such as if a pipe in the network has broken and is leaking significantly (Muranho et al. 2015). To address these issues, some researchers have begun adjusting estimated system demands as a function of the simulated pressures. This is known as a *pressure driven analysis*. Pressure driven analysis can lead to more accurate results, but this type of simulation is more complex and is generally limited to leakage assessment simulations. Due to the complexity of pressure driven simulation techniques, and the unclear applicability of these techniques to real world simulations, most practitioners prefer to use demand driven techniques. Although, this may be subject to change in the near future due to the significant amount of recent research focused

on pressure driven analysis (Savic et al. 2009; Tabesh et al. 2011; Giustolisi et al. 2014; Muranho et al. 2015).

Further to different analysis techniques, models can also be simulated in a variety of different ways. The most commonly used simulations are steady state, extended period, and transient simulations (Savic et al. 2009). Steady state simulations solve the hydraulic equations describing a network at a single snapshot in time, and the network conditions are assumed static. These types of models are typically used by designers to understand how a network might respond to extreme conditions. For operational studies analyzing how the network reacts to variable loading conditions, an extended period simulation (EPS) is required (Walski et al. 2003). An EPS is essentially a series of steady state models simulated at discrete time intervals for a specified period of time. Model results from the previous time step are used to set the boundary conditions for the next time step. Transient simulations consider unsteady flow conditions and are considered to be the most accurate type of simulations (Paluszczyszyn et al. 2015). However, these models are quite complex and are generally only utilized by researchers in specialized studies such as leak detection analyses (Savic et al. 2009; Paluszczyszyn et al. 2015).

In addition to the wide variety of simulation techniques available, numerous algorithms and software packages have been developed to solve the complex hydraulic equations defining WDN simulations (Balut and Urbaniak 2011; Paluszczyszyn et al. 2015). The most commonly used of which is the free EPANET (Rossman 2000) software package, which utilizes a global gradient algorithm method to solve the network equations (Muranho et al. 2015). Another commonly used software package is InfoWater (Innovyze 2015). InfoWater is based on EPANET simulation techniques but is integrated with geographical information systems (GIS) to allow modelers to more easily represent the physical conditions and topology of the existing network. Both of these software packages are utilized in this study.

Irrespective of the analysis technique, simulation type, or modeling software employed by practitioners, the quality of results obtained from any model is dependent on the accurate description of the model components described in figure 1.1. Due to large uncertainties associated with many model input parameters, it is vital that these parameters are properly calibrated prior to use (Engineering Computer Applications Committee 1999).

Model calibration is the process of adjusting model parameters until the discrepancies between model results and field data are minimized to some satisfactory level (Walski 1983). Ormsbee and

Lingireddy (1997) suggested the following seven step process for the calibration of hydraulic networks:

1) Identification of the intended use of the model
2) Determination of initial model parameter estimates
3) Collection of calibration data
4) Evaluation of model results
5) Macro-level calibration
6) Sensitivity analysis
7) Micro-level calibration

Since WDN models are used to aid decision makers in a variety of ways, identifying the intended use of a model is crucial to determining the type of model required (static vs. extended period simulations, water quality simulations, etc.), collecting the necessary quantity and quality of field data needed for calibration, and ensuring that the model is calibrated to the accuracy desired for its intended use (Walski 1995).

Generally, parameters describing the structure of a model (topology, network geometry and connectivity, pump hydraulics, and boundary conditions such as tank and reservoir water levels, etc.) can be directly measured with reasonable accuracy (Ormsbee 1989). Other model parameters such as the internal pipe roughness factors (C-factors) and the temporal and spatial demands throughout the network are much more difficult to measure accurately and must be estimated. C-factors are adjusted to represent energy losses within a pipe. In the short term, C-factors are considered static. However, over longer periods of time, modeled C-factor settings must be adjusted to account for pipe depreciation caused by tuberculation and corrosion. These depreciation effects are quite uncertain and can vary even within similar pipes in the same network (Lansey et al. 2001). C-factors can be back-calculated from field C-factor tests and the Hazen-Williams equation describing energy loss in a pipe. Unfortunately, field testing is quite expensive and the vast majority of C- factors within a model are often estimated based on results from a small sample of field tests and values reported from literature (Ormsbee and Lingireddy 1997).

Spatial and temporal demand distributions within a network are often estimated based on information collected from customer metered data (if available), land use characteristics, and total

inflow from pumps and tanks in the system (Walski et al. 2003). Often, demand estimates generated from customer usage data will underestimate the observed inflow into the system. There are several contributing factors, the largest of which can be attributed to network leakage. Average leakage within Canadian municipalities is approximately 13 % of total inflow (Renzetti and Dupont 2013). High pressures and aging infrastructure within a network are some of the most significant causes of leakage. When assigning spatial demand parameters within a model, it is common practice to evenly distribute leakage throughout the network. However, if information regarding the age of the network infrastructure, and/or pressures within the network are available, then this information can be used to better estimate spatial leakage allocations (Walski et al. 2003).

The quality of a model calibration is heavily dependent on the quality of the field data collected (Walski et al. 2004). Typically, data used for model calibration consists of pressures and flows collected using pressure gauges and flow recording devices installed at critical locations throughout the network. Additionally, most municipal water systems have supervisory control and data acquisition (SCADA) systems that provide tank level, pressure, and pump flow rate information at select locations in the network (Walski et al. 2003).

WDNs are generally over-designed to account for potential population growth and peak demand conditions, therefore it is important to collect calibration data when the system is stressed (e.g. under fire flows or high demand conditions) in order to ensure that the network is actually sensitive to the calibration parameters. When calibrating static simulations it is necessary to also collect data under numerous static loading conditions to confirm the robustness of any potential calibration settings identified (Ormsbee and Lingireddy 1997).

The observed field data is compared against model simulation results, and if discrepancies are particularly large, it is likely that the data pertaining to the structure of the model was either inaccurate, or incorrectly input into the model. Macro-calibration is the process of reviewing the accuracy of the aforementioned data, and validating/correcting these model inputs in order to bring the simulated and observed data sets into closer agreement (Ormsbee and Lingireddy 1997).

Smaller differences between model and field data are likely caused by inaccurate roughness settings or spatial demand allocation. The final step in model calibration deals with fine tuning these parameters until the model results reach acceptable levels of agreement with field observations. This is referred to as micro-calibration (Ormsbee and Lingireddy 1997).

Traditionally, micro-calibration has been done manually through a trial and error process. However, this is very time consuming, particularly in large networks with many pipes and nodal demands to be adjusted. Moreover, the issue of identifiability, in which an underdetermined calibration problem is being solved, further complicates this process (Walski et al. 2003). When the number of independent field observations is less than the number of calibration parameters, as is the case in the calibration of real networks, several combinations of parameters will achieve results of roughly the same quality as the correct parameter settings. However, these solutions will contain compensating errors (the incorrect adjustment of one model parameter to account for the inaccurate setting of another) (Walski et al. 2008).

Since micro-calibration is quite tedious and prone to compensating errors, it lends itself well to automated calibration approaches. In fact, the automated calibration of internal pipe roughness settings and demand data has been the focus of a great deal of research over the past few decades (Shamir 1974; Ormsbee 1989; Savic and Walters 1995; Savic et al. 2009).

Several automated calibration approaches have been developed. These can be grouped into three general categories; iterative, explicit, and implicit methods (Savic et al. 2009). Iterative procedures are essentially automated trial and error methods. Generally, these methods are only effective at calibrating very simplified networks, and have slow convergence rates (Bhave 1988). Explicit calibration methods solve an extended set of steady state mass balance and energy equations across nodes, pipes and loops in the network to generate model parameters (Ormsbee and Wood 1986). These methods are severely limited in their use due to the fact that the number of model parameters must equal the number of independent observations, there is no way to quantify uncertainty of estimated calibration parameters, and these methods generally require a high level of mathematical expertise to use. Both iterative and explicit procedures are unable to effectively and efficiently characterize large models and have no influence on the current practice of water distribution network modeling (Savic et al. 2009).

The current state of the art in water distribution network model calibration is based on the use of implicit methods, which utilize an optimization algorithm/tool coupled to a WDN model. The optimization tool sets model parameters (parameter settings are constrained by upper and lower bounds pre-specified by the user) in the model, which in turn sends results of the simulation back to the optimizer. The algorithm then uses these results to calculate a set of objective function values corresponding to this solution, and update the model parameters accordingly (Ormsbee 1989).

Defining reasonable bounds for each calibration parameter is essential to identifying high quality solutions.

All implicit calibration approaches use objective functions that are formulated to minimize the difference between observed and simulated pressure and flow data. There are several ways to accomplish this, as evidenced by the variety of objective functions that are reported in the literature (Lingireddy and Ormsbee 1999; Wu and Clark 2009; Tabesh et al. 2011), although the common theme amongst researchers is to collapse pressure and flow rate discrepancies into a single normalized objective function. Only one exception has been noted in recent literature involving a hypothetical WDN calibration research competition. Since the true settings of the hypothetical model were known a priori, the competitors were assessed on calibration and prediction errors, as well as the errors in calibrated model settings. This type of assessment forced competitors to re-evaluate the calibration objectives and many opted to solve a multi-objective calibration problem (Ostfeld et al. 2012).

In addition to the variety of applicable objective function definitions, several different optimization algorithms have been used to solve implicit calibration problems, including gradient methods which iteratively solve for the gradient of the objective function with respect to all calibration parameters (Shamir 1974; Lansey and Basnet 1991) Gauss-Newton methods, which approximate the second order Hessian matrix of the non-linear least squares objective functions (Liggett and Chen 1994; Reddy et al. 1996), as well as several other non-evolutionary methods (Ormsbee 1989; Tucciarelli et al. 1999). More recently, approaches aimed at finding approximate optimal solutions to the problems through the use of evolutionary methods have been implemented (Savic and Walters 1995; Lingireddy and Ormsbee 1999; Marchi et al. 2013). There are tradeoffs to each proposed method and no single group of optimization algorithms is unanimously preferred over another, as evidenced by the wide array of optimization algorithms utilized in recent WDN calibration literature (Ostfeld et al. 2012; Marchi et al. 2013). However, evolutionary methods tend to produce better results for larger network calibration problems than non-evolutionary approaches, but they are much more computationally expensive (Savic et al. 2009). Recently some of these advanced optimization tools have been linked to commercial hydraulic modeling software (Wu and Clark 2009), but these software packages are quite expensive (Jamasb et al. 2009).

Clearly, a great deal of research has been focused on the development of automated calibration tools (Shamir 1974; Ormsbee 1989; Lansey and Basnet 1991; Savic and Walters 1995; Reddy et al.

1996; Lingireddy and Ormsbee 1999; Walski et al. 2008; Wu and Clark 2009). Much of the research is generally focused on the development of new approaches and algorithms to automate WDN calibration, with far less attention paid to the application of these tools in real world settings; "whereas new algorithms make its appearance into water network field, little attention is paid onto real network data and only artificially created network data is used" (Puust and Vassiljev 2014). However, some researchers are beginning to address this gap in the literature through the application of these automated calibration approaches to real world large-scale WDN calibration problems (Wu and Clark 2009; de Schaetzen et al. 2011; Dini and Tabesh 2014; Puust and Vassiljev 2014; Vassiljev et al. 2015). Although, none of these studies have directly compared a manual trial and error approach against an automated approach applied to the calibration of a real network.

1.1 Problem Statement

Despite the wide availability and successful application of automated water distribution network calibration tools in numerous research settings, they are not commonly used in engineering practice (Speight and Khanal 2009); with most practitioners relying on engineering judgment and a trial-and-error approach instead. In an effort to bridge the gap between practitioners and researchers, the value of these advanced calibration approaches relative to traditional methods must be validated and quantified in a real world scenario.

1.2 Objective

The municipality of a Canadian City (City X) commissioned a local consulting company (Company Y) to calibrate the City's 24 hour EPS model of their water distribution network. The goal of the calibration was to update the existing model to include newly built areas, update system demands and demand patterns (*loading conditions)*, pump information, pipe roughness coefficients, and update pump/valve controls accordingly to match simulated tank/junction pressures, and pump flow rates to observed field conditions. This model would then be used in a variety of operational analyses.

This study builds upon this work by repeating the manual micro-calibration using an implicit automated calibration method. The results will be compared against the manually calibrated model, and the potential benefit of applying an automated approach will be assessed. No matter which method is used, the accuracy of the calibrated model is limited by the quality and quantity of field data, and a seemingly calibrated model can be full of compensating errors. Therefore, when limited field data exists, generating a single calibrated solution may not be particularly beneficial for

operational analyses. Instead, a range of feasible candidate solutions will be generated by solving an automated multi-objective micro-calibration problem. Ideally, the list of candidate solutions could be used in future operational analyses to ensure decisions are robust to several feasible solutions.

1.3 Scope

The automated WDN calibration approach applied in this study is limited to only the micro-calibration phase. Therefore, only internal pipe roughness and nodal demand parameter settings are considered in the automated calibration. Field data relating to the network structure, geometry and topology is not accessible and is assumed accurate.

The pareto-archived dynamically dimensioned search algorithm (PA-DDS) is used in the implicit calibration approach as it is parsimonious, user friendly, and has already been successfully applied to several hypothetical and bench mark water distribution network calibration and problems (Asadzadeh and Tolson 2009; Asadzadeh et al. 2011; Asadzadeh and Tolson 2013). PA-DDS is linked to the EPANET WDN modeling software through the EPANET programmer's toolkit (Rossman 1999). Both the EPANET software and programmer's toolkit are freely available and widely used in research and practical settings. All calibration results are assessed using demand driven simulations.

1.4 Outline

This thesis is outlined as follows:

Chapter 1 provides the motivation and objective of this study. It briefly describes why hydraulic network modeling is crucial for use by municipalities and why proper calibration of these models is required. Traditional approaches to hydraulic network calibration are introduced, and the applicability of automated approaches to the micro-calibration of hydraulic networks is discussed. Finally, the objective and scope of this research is defined.

Chapter 2 introduces City X's WDN EPS model and describes in detail how the model was manually calibrated. The original manual calibration objectives are defined quantitatively for use in an automated calibration procedure. Several automated calibration problems are formulated to assess the effects of calibrating to different data sets and different decision variable groupings.

Chapter 3 presents the results of an initial automated calibration effort and directly compares the solutions to the manual calibration results. Trade-off curves are presented, and time series of simulated tank levels for select solutions are analyzed. Objectives insensitive to the micro-calibration

are examined, and potential inaccuracies in static parameters not included in the calibration are identified.

Chapter 4 uses insights gained from the initial automated calibration approach to guide a manual macro-calibration of the network model. Poorly performing calibration objectives insensitive to the micro-calibration parameters are addressed, and inaccurate macro-calibration parameter settings are manually adjusted. All parameter setting adjustments and their associated effects on the model are reported.

In Chapter 5, the automated micro-calibration analysis is repeated for the adjusted model generated in chapter 4. The results are presented in a similar manner as in chapter 3, and used to define a set of high quality solutions that could potentially represent the existing network conditions.

Chapter 6 summarizes the main conclusions and recommendations of this research. Field data with the greatest potential to improve calibration results are identified for any future field studies.

Chapter 2
Manual and Automated Calibration Methods

City X's WDN model is depicted in figure 2.1. The network consists of two distinct pressure zones, 3816 nodes, 600 km of water main modeled using 4705 pipes, nineteen active wells, three elevated storage tanks, five in ground storage reservoirs, and nineteen pumping stations comprised of a total of forty nine pumps. The model is a 24 hour EPS solved with one minute hydraulic time steps. A hydraulic time step defines the times at which the set of mass balance and energy continuity equations characterizing pressures and flow within the network are re-calculated.

In the following sections, the manual calibration methodology is briefly summarized from a calibration report prepared by Company Y. The manual micro-calibration approach is then replicated in an automated multi-objective optimization problem. Several automated calibration problem formulations are presented, and sources of uncertainty inherent to the modeling software and data collection methods are discussed.

Figure 2.1: City X WDN model components; pressure zones and demand shift highlighted

2.1 Manual Calibration Methods

Using the City's GIS data base and a series of field studies, a macro-calibration of the existing InfoWater network model was completed. Network connectivity, node elevations, pipe and tank geometries, and pump curves were updated and verified. Following this, valve and pump operation settings used by the network operators on the calibration date of August 26, 2010 were translated into the InfoWater hydraulic modeling software. These settings were incorporated into the model through a series of control rules that adjust valve settings and activate/deactivate pumping stations based on certain events; most often when water levels in tanks reach a specified threshold. Some time-based rules were implemented to reflect specific operator settings on the calibration date (Company Y Consultants 2011).

The next step in the calibration process involved loading demand conditions within the network into the model. In the InfoWater software, pipes are connected at nodes, and the demands along a pipe are simulated at these nodes. In EPSs, demands are quantified through the assignment of base demands and demand patterns at each demand node within the network. Base demands define the average demand observed at the node, while the demand pattern consists of a series of demand multipliers (one for each time step of the simulation) which characterize how the water demand changes over the course of the simulation. The actual simulated nodal demand at any given time step of the EPS can therefore be calculated using equation (2.1).

$$Q_{j,t} = Q_j * M_t \tag{2.1}$$

where $Q_{j,t}$ represents the actual demand at node j at time t [l/s]; Q_j represents the base demand at node j; and M_t represents the unitless demand multiplier applied to the base demand at time t.

Base demands at each node within the network were established using averaged 2009 customer metered data. Then, SCADA data was used in a mass balance analysis to generate two distinct diurnal demand multiplier patterns, one for each pressure zone within the city. The patterns define changes in demand at each one minute time step of the 24 hour EPS. Leakage was proportionately allocated to all demand nodes within the network implicitly through the application of the demand pattern multipliers (Company Y Consultants 2011).

Field studies were then conducted to collect network pressure and flow rate information for comparison against the simulated model results. Fourteen pressure data loggers measuring instantaneous pressure information on a per minute basis were installed in various fire hydrants

throughout the network. Pressure information at all three elevated tanks, and downstream of 14 pumping stations within the network were collected using the SCADA system. Flow rates from 17 pumping stations representing flow into and out of each pressure zone in the network were also collected by the SCADA system. All of this data was used to assess the accuracy of the model simulation. Particular emphasis was placed on accurately simulating the fluctuations in tank water levels over the course of the EPS (Company Y Consultants 2011).

C-factor tests were conducted at thirty four of the 4705 pipes (<1 %) comprising the network. C-factor tests measure the head loss across a section of pipe at a known flow rate. Figure 2.2 illustrates a standard two gauge C-factor test in which temporary valve closures ensure that the discharge (Q) observed at the flowed hydrant is drawn entirely from the section of pipe being tested. Static and residual pressures are measured at hydrants 1 and 2, and the collected data is used to back calculate the internal pipe roughness setting of the measured pipe segment using equations (2.2) and (2.3).

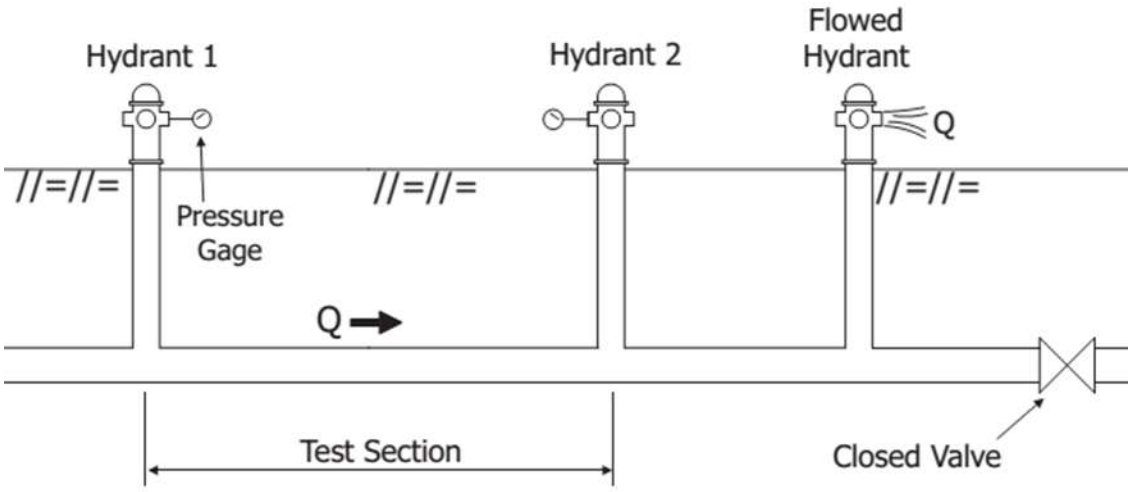

Figure 2.2: Standard C-factor test (Figure from Walski et .al. 2003)

$$C = \frac{Q}{0.278 D^{2.63} \left(\frac{h_l}{L}\right)^{0.54}} \tag{2.2}$$

$$h_l = (P_1 - P_2) + (Upstream\ Elevation - Downstream\ Elevation) \tag{2.3}$$

where C represents the Hazen-Williams C-factor [-]; Q represents the observed flow rate at the flowed hydrant [m^3/s]; D represents the nominal internal pipe diameter [m]; h_l represents the head loss observed across the pipe segment [m]; L represents the length of the pipe segment [m]; and P_1 and P_2 represent the residual pressures [m] observed at hydrants 1 and 2, respectively.

Data collected from these tests were utilized in conjunction with the Infowater 'Calibrator' tool (Innovyze 2015) to automatically adjust C-factor settings in an effort match model data to the field SCADA and pressure logger data. The Infowater calibrator tool uses an implicit calibration method by linking a genetic algorithm to the Infowater hydraulic solver. The exact problem formulation solved by the engineers is unknown, however, the 'Calibrator' tool failed to find a solution for this network, even after technical support was provided by the Innovyze software developers. Following the 'Calibrator' tool's failure, the results of the C-factor tests were used in a manual micro-calibration of the system. Five distinct pipe groupings based on pipe material and diameter were generated. Each pipe in the network belonging to a specific group was assigned a roughness value equal to the average of all field C-factor tests for that particular type of pipe. These groups, and their associated roughness coefficient settings, are presented in Table 2.1 below. In addition to these five groups, 433 pipes of unknown material and/or age within the network were assigned a C factor of 130.

Table 2.1: Manually calibrated C-factor settings

Pipe Material	Diameter (mm)	C-Factor (-)	# of pipes
Cast Iron	<=150	63.8	1344
	>150	87	584
Ductile Iron	All Diameters	132.4	651
PVC	All Diameters	140.5	1253
Hyprotec	All Diameters	138	445

Upon setting all model parameters as defined above, the calibrated model was simulated and results were graphically compared to the field data. The results of the comparison were mostly favorable; however, the model did not accurately represent tank filling and draining rates at two of the three monitoring locations (V and C elevated storage tanks). In an effort to address this problem, several alternative C-factor settings for the five pipe groups were tested, moreover additional roughness groupings accounting for the age of the network pipes were considered. These attempts were ultimately unsuccessful.

Eventually, it was concluded that demands within pressure zone one (depicted in figure 2.1) were not appropriately distributed due to the fact that the southern portion (zone 1b) was predominantly industrial with some relatively new residential developments, while the northern region (zone 1a) consisted of primarily older residential areas. The engineers assumed that during the summer months, the new residential areas may require more lawn watering than their older counterparts, and that the industrial areas may account for more water demand than originally assumed. Therefore, they shifted 20 % of the base demands originally allocated to demand nodes within zone 1a, south towards demand nodes within zone 1b. New diurnal demand patterns were created for zone 1a and zone 1b demand nodes. It is not clear how these demand patterns were generated and the information was not contained in the manual calibration report. However, upon reallocating the demands and assigning new demand patterns, the simulated results were far closer to the observed field data, and the model was considered calibrated enough for use.

Afterwards, the 2010 calibrated model parameters (C-factors and demand shift) were validated against field SCADA data collected on July 21, 2011. Validation data consisted of SCADA tank level and flow data collected at the same 3 elevated tanks and 17 pumping stations as in 2010. No pressure data was collected. The model boundary and loading conditions were updated to reflect demand and pump/valve operational data observed on the validation date, and the differences between observed and simulated 2011 results were found to be of similar quality as those achieved for the 2010 model calibration exercise. Both the calibration and validation dates were specifically chosen to be during the summer months to ensure that the network was sufficiently stressed, and that the model would be sensitive to changes in calibration parameters.

It is important to note that the demand shift required for model calibration was not based on any measured information, but rather it was assumed based on the practitioners' intimate knowledge of the system. As such, the engineers who initially calibrated the system are still interested in finding a solution that is not reliant on this demand redistribution.

2.2 Automated Calibration Methodology

The manual micro calibration approach described in section 2.1 was used to generate numerous automated calibration problem formulations. The calibration objectives and decision spaces of each problem are defined in sections 2.2.1 and 2.2.2, respectively. The software and hardware systems utilized in both the automated and manual approaches are presented in section 2.2.3.

2.2.1 Automated Calibration Objectives

The goal of the automated calibration was to replicate the manual calibration methodology as closely as possible in an automated setting in order to allow for a direct comparison of automated and manual calibration results. Thus, the manual calibration objectives had to be quantitatively described for use in an optimization procedure. The calibration objectives used in the manual approach were the minimization of differences between simulation results and field data collected on August 26, 2010. The 2010 field data consists of pressures collected from 14 pressure loggers installed throughout the network, as well as SCADA pressure data at 13 junctions and 3 elevated tanks, and SCADA flow rates collected at 17 pumping stations. The minimization objectives were achieved through a trial-and-error process and a graphical inspection of the field data vs. simulated results at each monitoring point within the network.

There are many different ways to formulate and quantify differences between simulated data and field data. However, the common theme amongst researchers is to normalize pressure and flow errors and combine them into a single minimization objective function (Ormsbee 1989; Walski et al. 2003; Wu and Clark 2009). While this method is reasonable for achieving high quality results that reduce cumulative errors in the simulation, it does not provide the user with any information regarding how pressures and flows individually respond to changes in decision variables. Furthermore, it does not afford the user the opportunity to examine objective function tradeoffs of different solutions. To allow for a meaningful examination of resulting solutions, separate objectives were defined for nodal pressure, tank pressure and flow rate differences between observed and simulated results. These three objectives were utilized within a multi-objective optimization approach to generate tradeoff information between the objectives.

When examining differences between simulated and observed pump station flow rates in an EPS, it is important to measure discrepancies in both total quantity of water pumped out of each station, as well as the times at which the pumps are operational. To quantify both of these errors, the calibration objective formulated was based on the minimization of the cumulative absolute errors between simulated and observed flows at each one minute interval of the EPS. This is described mathematically in equation (2.4).

$$Q_{Err} = \sum_{k=1}^{17} \sum_{t=0}^{T} \left| \left(Q_{k,t}^{sim} - Q_{k,t}^{obs} \right) \right| \tag{2.4}$$

where Q_{Err} represents the flow rate differences between simulated and observed data measurements, cumulated over the course of the EPS [l/s]; $Q_{k,t}^{sim}$ and $Q_{k,t}^{obs}$ represent the observed and simulated flow rates [L/s] at pump station *k* and hydraulic time step *t* [min]; and *T* represents the total number of simulated one minute time steps, 1441 in a one day simulation starting at 12 AM and ending at 12AM the following morning.

Assuming demands are correctly allocated within the model, pump flow rate errors and tank volumes are directly related. Once all demands are satisfied, any excess water that is pumped into the network will be stored in the tanks for later use. If pump station flows are unable to satisfy demands across the network, stored water in the tanks are used to compensate. Therefore, if simulated pumping rates are overestimated, then the expectation would be an over estimation in volumetric water storage in tanks within the network. Tracking differences in tank water levels independent of pump flow rate errors is essential to identifying potential errors in pump operation, and spatial and temporal demand allocation within the model. Discrepancies between simulated and observed tank water levels over the course of the EPS were quantified using cumulative absolute errors as calculated in equation (2.5). While it is acknowledged that differences in tank volumes might be more meaningful to the user, minimizing differences in cumulative tank volumes could lead the optimizer to generate solutions that favor minimizing water level discrepancies in larger tanks at the cost of misrepresenting water levels in smaller tanks. Therefore, tank water levels differences were assessed instead in order to ensure calibration efforts were equally spread across all areas of the network. The simulated nodal pressure error minimization objective is defined similarly and presented in equation (2.6).

$$H_{Err} = \sum_{i=1}^{3}\sum_{t=0}^{T}\left|\left(H_{i,t}^{sim} - H_{i,t}^{obs}\right)\right| \tag{2.5}$$

$$P_{Err} = \sum_{j=1}^{13}\sum_{t=0}^{T}\left|\left(P_{j,t}^{sim} - P_{j,t}^{obs}\right)\right| \tag{2.6}$$

where H_{Err} and P_{Err} , represent the differences between simulated and observed tank water levels and pressure heads, cumulated over the course of the EPS [m]; $H_{i,t}^{sim}$ and $H_{i,t}^{obs}$ represent the simulated and observed tank water levels [m] at tank *i* and hydraulic time step *t* [min]; $P_{j,t}^{sim}$ and $P_{j,t}^{obs}$ represent the respective simulated and observed pressure heads [m] at node *j* and hydraulic time step *t* [min]; and *T* represents the total number of simulated time steps.

Using equations (2.4) to (2.6), the calibration can be formulated as a multi-objective optimization problem presented in equation (2.7).

$$\text{minimize } F(\vec{x}) = \{f_1(\vec{x}), f_2(\vec{x}), f_3(\vec{x})\} \quad (2.7)$$
$$s.t. \vec{a} \leq \vec{x} \leq \vec{b}$$

where F represents the multi-objective minimization problem; f_1, f_2, and f_3 represent Q_{err}, H_{err}, and P_{err}, respectively; these are the cumulative differences in flow rates [l/s], tank water levels [m], and pressures [m] between simulated and observed data, calculated using equations (2.3) through (2.5), respectively; $\vec{x}$ represents the parameter settings for a particular solution; and $\vec{a}$ and $\vec{b}$ are the lower and upper bounds of the feasible parameter settings comprising the decision space. Two different decision spaces, defined in section 2.2.2, are established for use in the automated calibration formulations.

Due to different naming conventions employed by the main contractor, sub-contractor, and city officials, it was not clear at the time of this research where the 14 pressure data loggers were installed throughout the network. To avoid potential calibration errors, the pressure logger data was not included in the automated calibration objective functions. However, it is important to note that the minimization of flow and tank level simulation errors is generally more important than the minimization of pressure errors when calibrating an EPS (Walski et al. 2003). Therefore, this is not too great of a concern.

The aforementioned calibration objectives were used in conjunction with all relevant 2010 and 2011 SCADA data to formulate three different calibration objective spaces. The first of which is a tri-objective function which utilizes equations (2.4) through (2.7) to minimize discrepancies between the 2010 simulated model results and 2010 field data. This is identified as the '2010 objective space'. An alternate objective space (the '2011 objective space') is defined to minimize discrepancies between the 2011 field data and the model results simulated under 2011 boundary and loading conditions. Since no junction pressure data is available for the 2011 calibration date, this objective space is reduced to a bi-objective function which uses equations (2.5) and (2.6) to minimize tank level and pump flow rate errors in the network. Both of these objective spaces search for solutions that minimize simulation errors (or maximize model performance) in either 2010 or 2011 conditions *independently* of one another.

A third objective space is defined to simultaneously calibrate the model simulation results for both the 2010, and 2011 network conditions to their respective field data sets. This tri-objective function formulation, identified as the 'aggregate objective space', is defined using equations (2.4) through (2.7). However, the total number of one minute time steps, *T*, in the tank level and flow rate error calculations are increased to 2882, since two full days of tank water levels and flow rate observations are used for calibration purposes. The pressure objective is calculated for the 2010 simulation only, since no pressure information is available in 2011. When solving the calibration problem using the aggregate objective space, the optimization algorithm identifies a potential solution of model parameter settings which are then applied to two unique versions of the network model reflecting both the 2010, and 2011 network boundary and loading conditions. The cumulative errors observed in each of the model simulations are aggregated and passed back to the optimization algorithm, which uses these results to identify a new solution set.

2.2.2 Decision Variables

Two different sets of decision variables were generated and applied to solve the automated micro-calibration objective function formulations defined in section 2.2.1. The first of which consists of five continuous decision variables representing C-factor settings for the five pipe groups identified in the manual calibration approach, as well as one continuous decision variable representing the percentage of demand shifted from zone 1a to zone 1b. These decision variables were selected in order to emulate the manual calibration methodology in which the base demand shift and the roughness coefficients were the only parameter settings thought not to have been adequately verified in the field.

It is unclear from the manual calibration report how the demand shift was implemented. Therefore, it was assumed that the base demand at each demand node within zone 1a was reduced by 20 % and the cumulative demand was reallocated in proportion to the already existing nodal base demands in zone 1b. The demand shift was modeled using equations (2.8) through (2.10).

Demand Decrease:

$$Q_{adj,j}^{Z1_a} = \sum_{j=1}^{N1} (1 - D_s)\,(Q_{init,j}^{Z1_a}) \tag{2.8}$$

$$\Delta Q_s = \sum_{j=1}^{N1} D_s * Q_{init,j}^{Z1^b} \tag{2.9}$$

Demand Increase:

$$Q_{adj,j}^{Z1_b} = \sum_{j=1}^{N2} Q_{init,j}^{Z1_b} * \frac{\Delta Q_s}{\sum_{j=1}^{N2} Q_{init,j}^{Z1_b}} + Q_{init,j}^{Z1_b} \tag{2.10}$$

where $Q_{init,j}^{Z1_a}$ and $Q_{init,j}^{Z1^b}$ represent the original, an adjusted (decreased) base demands allocated to node *j* within zone 1a [l/s]; *N1* and *N2* represent the number of demand nodes in zone 1a and zone 1b, respectively; Q_{tot} represents the cumulative base demand transferred from zone 1a to zone 1b [l/s]; $Q_{init,j}^{Z1^b}$ and $Q_{adj,j}^{Z1_b}$ represent the original, and adjusted (increased) base demand allocated to node *j* in zone 1b [l/s]; and D_S is the decision variable setting representing the fraction of nodal base demand shifted from zone 1a to zone 1b. The D_S decision variable was unconstrained in all model calibrations; the upper and lower bounds were set from 0 to 100 %.

The upper and lower bounds of all five C-factor settings were defined so as to match the range of C-factor values obtained from all field tests of each pipe group. The C-factor settings of the 433 pipes of unknown age/material were kept static at their original setting of 130, since there was no available field data to establish alternate C-factor settings. Moreover, since there was very limited information available, it was assumed that changing the C-factors of these pipes would likely introduce uncertainty and increase the potential for compensating errors in the calibration. This group of decision variables, identified as the '5 C-factor decision space' is presented in table 2.2.

Table 2.2: Automated calibration: 5 C-factor decision space

Decision Variable	Pipe Material	Diameter (mm)	Lower Bound	Upper Bound	# of pipes
C-Factor Setting (-)	Cast Iron (CI)	<=150	57	68	1344
		>150	48	94	584
	Ductile Iron	All	116	141	651
	Polyvinyl Chloride (PVC)	All	130	149	1253
	Hyprotec Coated Iron	All	135	156	445
Demand Shift (-)	NA	NA	0	1	NA

Generally, the total number of model parameters considered for calibration is directly linked to parameter uncertainty in the calibrated model (Mallick et al. 2002). Parameter reduction through grouping C-factor settings of pipes of similar age and material is an effective way to reduce uncertainty and the potential for compensating errors, as well as deal with the identifiability issues arising in WDN calibration problems (Walski et al. 2003). However, grouping can also introduce errors in the calibration if pipes within a group should not have the same C-factor settings. Thus, it is important to identify pipe groupings that accurately and efficiently capture the full range of pipe conditions within the model network.

The 5 C-factor decision space combines 1928 cast iron pipes into only two groups. Since cast iron pipes are most susceptible to depreciation from corrosion and tuberculation (Al-Barqawi and Zayed 2006), it is unlikely that these pipe groupings accurately reflects the C-factor characteristics of cast iron pipes within the network. Therefore, an alternate decision space identified as the '13 C-factor decision space', was defined to consider both the age and diameter of cast iron pipes within the network.

The 13 C-factor decision space is identical to the 5 C-factor decision space for the PVC, ductile iron, and hyprotec lined C-factor parameters as well as the demand shift decision variable. The only difference between both decision spaces lies in the grouping of cast iron pipes within the network. The two existing cast iron pipe groupings identified in the 5 C-factor decision space are subdivided into ten pipe groupings in the 13 C-factor decision space. Due to the fact that only twelve C-factor tests were conducted on cast iron pipes in the field, it was not possible to constrain the ten newly created cast iron C-factor calibration parameters using only field data. Instead, these decision variables were bounded using literature values from Lamont (1981).

Lamont (1981) found that depreciation in a pipe is heavily dependent on local conditions, and the corrosiveness of the water source. Thus, he characterized different rates of attack on the carrying capacity of a pipe using four trends: slight, moderate, appreciable and severe attack. The relevant C-factors of various cast iron pipes under different rates of attack are presented in Table 2.3.

Cast iron pipes within the network were grouped by age using the same four categories (new, 30 years old, 60 years old, and 100 years old) defined in table 2.3. Pipes in the network that were less than 15 years old, 15 to 44 years old, 45 to 80 years of old, and greater than 80 years old were considered new, 30, 60, and 100 years old, respectively. Each of these age groupings was further sub-divided by pipe diameter as well. A minimum threshold of ten pipes per group was arbitrarily defined

in order to limit the total number of pipe groups, while still accurately characterizing aging infrastructure within the WDN. The full list of C-factor decision variables comprising the 13 C-factor decision space is defined in table 2.4.

Table 2.3: Lamont (1981) C-factor settings for cast iron pipes - Adapted from Walski et.al. (2003)

Hazen-Williams C-Factor Settings (-) for Discrete Cast Iron Pipe Diameters (mm)					
Age and Depreciation of Pipe	**76 (mm)**	**152 (mm)**	**300 (mm)**	**600 (mm)**	**1220 (mm)**
New and Smooth	129	133	138	140	141
30 years old					
Trend 1 - slight attack	100	106	112	117	120
Trend 2 - moderate attack	83	90	97	102	107
Trend 3 - appreciable attack	59	70	78	83	89
Trend 4 - severe attack	41	50	58	66	73
60 years old					
Trend 1 - slight attack	90	97	102	107	112
Trend 2 - moderate attack	69	79	85	92	96
Trend 3 - appreciable attack	49	58	66	72	78
Trend 4 - severe attack	30	39	48	56	62
100 years old					
Trend 1 - slight attack	81	89	95	100	104
Trend 2 - moderate attack	61	70	78	83	89
Trend 3 - appreciable attack	40	49	57	64	71
Trend 4 - severe attack	21	30	39	46	54

It is important to note that depreciation effects are often more severe when water hardness levels are greater than 300 ppm (James and Shahzad 2003). Since the average hardness of water sources supplying the City's WDN is approximately 460 ppm (Region of Waterloo 2011), it was assumed that the carrying capacity of pipes within the network would be subjected to higher rates of attack. The upper and lower bounds of C-factor settings generated from literature values were constrained based on this assumption.

New pipes were assumed to exhibit at most mild depreciation effects corresponding to pipes 30 years of age. No limiting assumptions were made regarding pipes 30 years of age, and the optimization algorithm could explore the entire range of depreciation values corresponding to 30 year old cast iron pipes. The range of depreciation in all pipes greater than 60 years of age were

constrained by the assumption that the depreciation in these older pipes would, at best, exhibit only moderate depreciation effects.

The upper and lower bounds of C-factor settings within each pipe group were also governed by the maximum and minimum pipe diameters comprising the group. For example, the lower bound of potential C-factor settings assigned to the new cast iron pipe group (comprised of 20 pipes ranging in diameter from 150 mm to 300 mm) was defined to include the mild depreciation effects associated with 30 year, 150 mm diameter pipes. The upper bound was set to match the C-factors associated with new pipes of a 300 mm diameter.

Table 2.4: C-factor groupings associated with the 13 C-factor grouping decision space

Type of Pipe	**Diameter (mm)**		**C-factor Setting (-)**		**# of Pipes**
	Min	**Max**	**Min**	**Max**	
Cast Iron Pipes					
New (<15 years old)	150	300	83	138	20
30 years old (15-44 year old network pipes)	50	100	41	100	12
	150	200	50	106	217
	250	400	58	112	80
60 years old (45-80 year old network pipes)	25	100	30	69	312
	150	200	39	79	851
	250	350	48	85	182
	400	600	56	92	43
100 years old (>80 years old)	25	100	21	61	69
	150	300	30	78	142
Ductile Iron	75	1000	116	141	651
Polyvinyl Chloride	100	1050	140	150	1253
Hyprotec Coated Iron	50	500	135	156	445

The 2010, 2011 and aggregate objective function formulations defined in section 2.2.1, are solved with both the 5 and 13 C-factor decision spaces in chapter 5, and only the 5 C-factor decision space in chapter 3.

2.2.3 Software/Hardware Utilized

The calibration was initially formulated by linking the PA-DDS algorithm to the EPANET toolkit using MATLAB software (The Mathworks Inc. 2015b). However, the code consistently failed to simulate the EPS. It is unclear why the code failed as MATLAB software has been used to successfully solve EPS calibration problems of smaller networks, and the static model of this network was successfully simulated in MATLAB. It is speculated that the quantity of data and size of the network were too large for computation of an EPS in MATLAB. Therefore, the code was translated to C++ (International Organization for Standardization 2015) script and compiled within the Visual Studio 2013 (Microsoft 2015) platform.

The PA-DDS multi-objective heuristic search algorithm was used in the implicit automated micro-calibration of City X's WDN model. PA-DDS is very simple relative to alternative global search algorithms as it has only one parameter, the perturbation size parameter, which is very robust to a wide variety of problems and does not require user fine-tuning (Asadzadeh and Tolson 2009). Despite it's simplicity, PA-DDS has proven to be very effective at solving large complex problems and can produce solutions of similar quality to state of the art multi objective algorithms in a fraction of the computational budget (Asadzadeh and Tolson 2013). Since PA-DDS is dynamically dimensioned, it utilizes its available computational budget very efficiently. At the start of the algorithm's search for optimal solutions, it perturbs all parameters to be exploratory. As the optimization progresses, the number of parameter perturbations are reduced and the algorithm searches more locally along the existing pareto-front.

PA-DDS archives all non-dominated solutions as it searches through the decision space. A solution is considered non-dominated if none of the objective function values can be improved without degrading some of the other objective function values. As such, the non-dominated solution set generated at the end of the calibration process are used to approximate the pareto-front of the objective space. To generate a new candidate solution, the algorithm selects one solution from the archived set of non-dominated solutions and perturbs the parameter settings. If the newly generated solution is non-dominated, it is added to the archive and selected for perturbation in the next iteration. If the solution is dominated an alternative solution is selected based on one of three available

selection metrics, random, crowding distance, and hyper-volume (Asadzadeh and Tolson 2013). The crowding distance selection metric is generally preferred to the random metric, while the hyper volume metric is generally preferred over both random and crowding distance metrics (Asadzadeh and Tolson 2013).

Unfortunately, at the time of this research the hyper volume metric was only available in MATLAB source code and was not yet implemented in C++. Since the complexity of the WDN model necessitated the use of C++ script, all calibration formulations were solved using the crowding distance selection metric. The perturbation parameter was set at 0.2.

All analysis was completed using a desktop computer with eight GBs of RAM and an eight core AMD FX-8320 processor.

2.2.4 Summary of Automated Calibration Experiments

A total of three multi-objective function formulations, and two decision spaces were defined for use in an automated micro-calibration approach. The multi-objective functions were defined to analyze the impact of calibrating the network to different boundary and loading conditions independently of one another, versus calibrating to all network conditions simultaneously. As such, the first objective formulation calibrates the network parameters to the 2010 conditions, the second calibrates to 2011 conditions, and the third calibrates the model parameters to both the 2010 and 2011 network conditions simultaneously.

The 5 C-factor decision space was defined to exactly match the manual calibration parameters. This was done to allow for a direct comparison of results achieved from both the manual and automated methods. Afterwards, a second decision space consisting of 13 C-factor groupings was generated in an attempt to more accurately represent pipe conditions within the network.

Each calibration objective function is solved with the 5 C-factor decision space in chapter 3, and the results are compared against the manual solution. Solving the micro-calibration problem in a multi-objective setting allows the user to easily identify insensitive objectives and inaccurate macro-calibration parameters. The results from this initial automated calibrate are used to update model parameters in a manual macro-calibration approach in chapter 4. The updated model is then solved with all objective function formulations and both decision spaces for a total of six unique calibration problems described in chapter 5. Each problem was solved with a budget of 10 000 iterations, corresponding to approximately 14-30 hours (depending on the problem) of computational time. The

number of iterations was selected to reflect the amount of time that engineers from Company Y would be willing to wait for a high quality solution.

2.3 Sources of Uncertainty

There are several sources of uncertainty which must be acknowledged and, if possible, addressed. Some of this uncertainty is difficult to quantify in part due to working with network models and data sets that are five years old. Additionally, as many parties were involved in the initial calibration phase (City officials, contractors and sub-contractors), and naming conventions were not consistent amongst each group, some difficulties were experienced when correlating field and model data. Many of these problems were addressed but several inaccuracies inherent to the field data, network, and modeling software persist. Sources of uncertainty specific to this problem are discussed in the following sections.

2.3.1 Uncertainty Specific to Model Inputs and Field Data

Prior to working with any model, an extensive analysis of the initial parameter settings was conducted in an attempt to revert model parameters to their reported calibration settings, and ensure that all boundary conditions were accurately set. During this process it was noted that following demand reallocation (the demand shift from zone 1a to zone 1b) in the manual calibration of the 2010 network conditions, new diurnal demand patterns were generated for zones 1a and 1b. It is unclear how these demand patterns were calculated, however they appear to produce high quality results, and so the manual solution was assessed with these new demand patterns. These new diurnal demand patterns characterizing flows in zones 1a and 1b were not included in the 2011 model loading conditions, and it was assumed that they were not used/created for the 2011 model validation date. Issues relating to diurnal demand patterns will be addressed in greater detail in chapter 4.

When analyzing the 2011 model, it was clear that the demand shift across zone 1 had already been implemented in the 2011 WDN loading conditions provided, and the original demand settings were not available. Therefore, original demand settings were back calculated by isolating and solving for the original nodal demand parameter variables in equations (2.8) through (2.10), defined in section 2.2.2. Since the exact method employed for this demand reallocation in the manual calibration was not reported, the initial base demand settings used in the 2011 model may not be exactly accurate. For the purposes of this study, the back-calculated 2011 nodal demands are assumed equal to the original demands.

All field data was also analyzed to ensure consistency across all measurements, and check for any major errors in the data. When analyzing field C-factor test data, it was noted that the observed pressure drops were quite low. While there are no set standards defining minimum observed pressure drops required for C-factor tests, Walski et.al. (2003) suggested that the recorded pressure drops should preferably be in the range of 20 PSI (~14.1m), with a minimum pressure drop of 5 PSI (~3.5m). This is done to ensure that the magnitude of measured head loss data is significantly greater than the magnitude of measurement errors. Of the 34 C-factor tests conducted, 12 tests utilized pressure drops that were less than the minimum suggested amount, and only 2 test locations forced a pressure drop that was equal to or greater than the suggested range. Even though the sub-contractor hired to complete these C-factor tests utilized pressure loggers that could accurately record pressures within 0.22 m (ADS 2009), the low magnitude of the pressure drops observed was cause for concern. To quantify the uncertainty related to pressure measurement errors in these tests, upper and lower bounds were calculated for each C-factor test using equation (2.11).

$$C_{lb} = \frac{Q}{0.278D^{2.63}((h_l + \Delta h_l) * L)^{0.54}} \; ; \; C_{ub} = \frac{Q}{0.278D^{2.63}((h_l - \Delta h_l) * L)^{0.54}} \tag{2.11}$$

where C_{lb} and C_{ub} represent the upper and lower bounds of C-factors back-calculated from field tests [-]; Q represents the observed flow rate at the flowed hydrant [m^3/s]; D represents the nominal internal pipe diameter [m]; h_l represents the head loss observed across the pipe segment [m]; L represents the length of the pipe segment [m]; and Δh_l represents the measurement error in the observed head loss, assumed constant at 0.22 m. Since the C-factor tests were conducted using 2-gauge C-factor tests, the measurement uncertainty could actually be as high as 0.44 m, but for the purposes of this analysis a measurement error of 0.22 m was used.

Upon calculating the upper and lower bounds of each of the C-factors, only 23 of the 34 field tests produced results that were accurate to within ± 15. Only C-factors calculated from these 23 tests were used to define the decision variable ranges.

Another source of uncertainty is related to the spatial allocation of leakage within this network. Unaccounted for water (or leakage) was applied in proportion to the existing demands across all nodes within the network. However, more accurate results can be achieved if leakage is allocated predominantly to areas within the network that are most likely to exhibit leakage (i.e. older parts of

the network and high pressure areas) (Walski et al. 2003). For the purposes of this study, leakage is assumed to be correctly allocated, but it is recommended that leakage allocation is re-assessed.

Prior to utilizing any SCADA data for model calibration purposes, it is essential to calibrate the SCADA instrumentation (Bentley Systems 2004). It is likely that this was done by Company Y or City officials; however, no mention of the SCADA system calibration was made in the Company Y's calibration report. For the purposes of this study, it is assumed that the instruments were properly calibrated.

Even if the instrumentation is calibrated, issues still arise due to the fact that the pressures reported by the SCADA system are instantaneous observations at each one minute time step. Therefore, this data is quite noisy, and the levels must be smoothed prior to use (Bentley Systems 2004). The method employed to smooth the data is detailed in chapter 4. Flow data reported by SCADA systems are averaged over the course of each one minute interval and were assumed accurate.

Finally, it is assumed that all network structure information is accurately input into the model. The validation of this information is not feasible and not included in the scope of this research.

2.3.2 Modeling Uncertainty

Often "significant mathematical assumptions are employed by the simulation software to make the simulation computationally tractable, yet allow the simulated results to be meaningful and useful" (Walski et al. 2003). Therefore, even if all the field data and model inputs are entirely accurate, it is highly unlikely that simulated results will perfectly match observed field conditions (Walski et al. 2003). It is important to understand the accuracy and limitations of the specific hydraulic network simulation software utilized before making decisions based on the simulated results.

The EPANET software uses a global gradient algorithm method to solve the set of mass balance equations at each node and the energy continuity equations at each link/pipe in the network (Rossman 2000). EPANET iteratively solves a linearized system of these equations to calculate nodal pressures and link flow rates within the system until a specified convergence threshold is satisfied (Muranho et al. 2015). Both the number of iterations EPANET employs and the convergence threshold settings are user specified (Rossman 2000). In EPSs, hydraulic equations are solved at each time step. Once a solution is achieved, EPANET assumes steady state conditions until the next hydraulic time step is reached. Real WDNs are actually much more complex and dynamic; however, for operational purposes EPS models provide a reasonable representation of network hydraulics (Walski et al. 2003).

Generally, hydraulic time steps are defined by the user, but an intermediate time step can be introduced in the simulation if during the course of a time step, an event occurs that would change the steady state conditions. For example, a pump controlled by a tank water level is switched on/off, or a tank becomes empty or full. If the number of intermediate time steps introduced is high, model run times increase significantly. This is often a sign of poorly designed control rules (Rossman 2000).

When extracting simulated flow rate information for comparison with field data, the instantaneous flow rates reported by EPANET at each one minute time interval were assumed static over the course of the entire minute. That is to say, the effects of the introduction of intermediate time steps on pumping flow rates averaged over a 60 second interval were assumed negligible over the course of a 24 hour EPS. This assumption was validated for several models simulated with a convergence accuracy of 0.005. Over the course of an EPS, the average discrepancy between instantaneous and averaged flow rates over a one minute interval was observed to be no greater than 0.5 %. For particularly unstable solutions in which pump settings are constantly changing over the course of a single minute, this assumption may not be valid. However, such a situation would not occur in a real WDN. If this occurs in the simulated model, then either the model network parameters or pump control rules fail to characterize the system, and a macro-calibration is required.

Since the network model was manually calibrated using InfoWater software, while the automated approach was completed using the EPANET software programmer's toolkit, the consistency of the results generated from both pieces of software was assessed in order to more accurately compare the manual and automated calibration methods. To complete this consistency assessment, a calibrated 2011 model was exported from Infowater to EPANET. The hydraulic time step of this model was set to one hour and a 24 hour EPS was run on both pieces of software. All pipe/pump flows and junction pressures of both model outputs were compared at each time step and the average relative difference between the model junction pressure and pipe flows were found to be approximately 0.06 % and 0.22 %, respectively. This level of consistency was expected due to the fact that the InfoWater software utilizes a 'modified version of the EPANET hydraulics solver' (Mala-Jetmarova et al. 2011) and as such, results generated from either software should be fairly similar.

A consistency assessment was also conducted with hydraulic time steps set to one minute. Only the agreement between the 3 tanks, 17 pipes, and 13 junctions included in the objective function formulation were assessed. The resulting average relative differences between the Infowater hydraulic solver and the EPANET solver at each time step were 1.84 %, 2.59 % and 0.67 % for simulated tank

levels, pump flow rates, and junction pressures, respectively. Thus, improvements in the objective functions were only deemed significant if they were greater than these values.

When analyzing large, complex networks with several pump/valve operation based on tank water level control rules, convergence issues can arise (Paluszczyszyn et al. 2015). In such instances, the EPANET hydraulic solver appears to randomly change pump/valve settings in search of a solution. Upon completing the simulation, EPANET will produce a summary report warning the user of the changes made in order to achieve convergence. Additional warnings include any negative pressures observed, or if the system is unstable. These issues can arise if there is a problem in the way the network is designed or operated (Rossman 2000). Unfortunately, due to the size/complexity of the City's model and the reliance on tank level based control rules, several of these warnings were observed on all attempted model runs. These warnings appeared in both the InfoWater and EPANET software packages and could not be addressed.

Regardless of the modeling software used, some of the simulated results were very sensitive to convergence accuracy settings. A sensitivity analysis of the effects of different accuracy settings on problematic solutions was completed, and results indicated that the tank level error minimization objective varied by as much as 25 % when the accuracy setting was changed from 0.005 to 0.01. Variability in the objective function values was greatly reduced at accuracy settings of 0.005 or less. Therefore, all automated model calibration analyses were completed at an accuracy setting of 0.005. Similar discrepancies were noted when comparing model C-factor settings that were rounded to the third significant digit against those that were rounded to four significant digits. Both models appear to be quite sensitive to very minor adjustments in C-factor and accuracy settings. This is likely caused by the use of tank water level based control rules which activate/deactivate pumps based on simulated tank water levels. To account for these sensitivities, the full list of non-dominated solutions generated by the implicit automated calibration method was assessed for sensitivities to C-factor settings rounded to the nearest single decimal place. All solutions that were not robust to these rounded C-factor values were removed from the non-dominated solution set.

Chapter 3
Initial Micro-Calibration Results

Ultimately the goal of any model calibration exercise is to generate robust solutions that can produce high quality simulation data under multiple loading conditions. When analyzing initial calibration results, it was noted that some of the macro-calibrated model parameters, which were held static in the automated micro-calibration, were inaccurate. These parameters greatly affected the quality of solutions generated from the micro-calibration, and were adjusted in chapter 4 in order to obtain more robust and feasible solution sets. Therefore, this chapter only assesses the initial automated calibration solutions' quality relative to the manually calibrated solution. No attempt was made to identify a 'final' set of feasible model calibrations.

Three unique calibration problems were solved using the 5 C-factor decision space so as to mimic the manual solution methods as closely as possible. Results generated from each of the three calibration problems as well as the manually calibrated solution are presented and discussed. For each problem, the multi-objective trade-off curves are plotted and compared against the manually calibrated solution. The original objectives representing cumulative errors in the system were converted into observation weighed average absolute errors (%) in order to allow all readers, even those unfamiliar with the system, to practically gauge the magnitude of simulation errors. Moreover, each solution's efficacy to both the 2010 and 2011 objective spaces was simultaneously assessed using a new bi-objective function defined in this chapter. In addition to the tradeoff curves, tank water level time series plots are generated for both the manually calibrated solution, and select results from the automated calibration. These time series are compared relative to the observed tank water levels in the field. Finally, each calibration objective's sensitivity to the micro-calibration parameters was examined, and insensitive objectives were identified for further analysis.

3.1 Trade-off Curves

The original cumulative absolute error minimization objectives presented in section 2.2.1 were formulated to characterize the simulated model errors as simply and efficiently as possible; user comprehension was not initially considered. Therefore, to allow for increased user comprehension of the simulated errors, the objective function values of all solutions generated are presented as observation weighted average absolute errors (%). The observation weighted errors were calculated a posteriori using equations (3.1) to (3.3). Calculating percent errors using these equations implicitly

weights errors between larger observed data measurements more highly than errors in smaller measurements (i.e. 10 % error in an observed flow rate of 100 l/s is weighted more heavily than a 10 % error in a flow rate of 10 l/s).

$$Q_{\%Err} = \frac{\sum_{k=1}^{17}\sum_{t=0}^{T}\left\{\left|\frac{\left(Q_{k,t}^{sim} - Q_{k,t}^{obs}\right)}{Q_{k,t}^{obs}}\right| \times 100\ \% \times Q_{k,t}^{obs}\right\}}{\sum_{k=1}^{17}\sum_{t=0}^{T}\left|Q_{k,t}^{obs}\right|} = \frac{\sum_{k=1}^{17}\sum_{t=0}^{T}\left|\left(Q_{k,t}^{sim} - Q_{k,t}^{obs}\right)\right|}{\sum_{k=1}^{17}\sum_{t=0}^{T}\left|Q_{k,t}^{obs}\right|} \times 100\% \tag{3.1}$$

$$H_{\%Err} = \frac{\sum_{i=1}^{3}\sum_{t=0}^{T}\left\{\left|\frac{\left(H_{i,t}^{sim} - H_{i,t}^{obs}\right)}{H_{i,t}^{obs}}\right| \times 100\ \% \times H_{i,t}^{obs}\right\}}{\sum_{i=1}^{3}\sum_{t=0}^{T}\left|H_{i,t}^{obs}\right|} = \frac{\sum_{i=1}^{3}\sum_{t=0}^{T}\left|\left(H_{i,t}^{sim} - H_{i,t}^{obs}\right)\right|}{\sum_{i=1}^{3}\sum_{t=0}^{T}\left|H_{i,t}^{obs}\right|} \times 100\% \tag{3.2}$$

$$P_{\%Err} = \frac{\sum_{j=1}^{13}\sum_{t=0}^{T}\left\{\left|\frac{\left(P_{j,t}^{sim} - P_{j,t}^{obs}\right)}{P_{j,t}^{obs}}\right| \times 100\ \% \times P_{j,t}^{obs}\right\}}{\sum_{j=1}^{13}\sum_{t=0}^{T}\left|\left(P_{j,t}^{obs}\right)\right|} = \frac{\sum_{j=1}^{13}\sum_{t=0}^{T}\left|\left(P_{j,t}^{sim} - P_{j,t}^{obs}\right)\right|}{\sum_{j=1}^{13}\sum_{t=0}^{T}\left|P_{j,t}^{obs}\right|} \times 100\% \tag{3.3}$$

where $Q_{\%err}$, $H_{\%err}$, and $P_{\%err}$ represent the relative percent errors of the simulated flow, tank water level, and pressure errors, respectively, between simulated and observed information in the network; all other variables have been defined in chapter 2.

The relative percent errors calculated for the manually calibrated model, simulated under 2010 loading conditions, were 3.0 %, 9.8 %, and 4.8 % for the tank levels, pump flow rates, and pressure observations within the network, respectively. It is clear that the manually calibrated solution is of a relatively high quality in both simulated tank levels and pressures. The results of the 2011 simulation were significantly worse, as the tank and pump flow rate relative percent errors were found to be 5.5 % and 23.0 %. In subsequent analysis presented in chapter 4, it is clear that these exaggerated 2011 simulation errors are caused by inaccurate macro-calibration parameter settings input in the existing 2011 network model. Given the high quality of the model simulated under 2010 network conditions, it is highly unlikely that the 2011 calibration parameters used in this research are representative of the solution achieved during initial manual calibration. It is more probable that the 2011 model parameters and loading conditions were altered post-calibration and not reverted to their original settings. Regardless, in order to allow for a direct comparison of the results, the automated calibration was completed using the same macro-calibration parameters and loading conditions that the manual calibration results were assessed with.

3.1.1 Independent Objective Formulations: 5 C-factor Decision Space

The 2010 and 2011 objective function formulations were solved in the 5 C-factor decision space, and the results are presented in this section. The resulting parameter settings generated from solving the 2010 calibration problem were validated in the 2011 WDN model conditions, and vice versa. All results are presented and compared to the manually calibrated solution in a series of multi-objective trade-off plots presented in this section.

A total of 555 non-dominated solutions were generated when solving the 2010 calibration objectives using the five C-factor decision space. 59 of the 555 solutions to the 2010 calibration problem dominate the manually calibrated solution in the 2010 objective space, while only 17 solutions dominate the manual solution in the 2011 objective space. Nine of these solutions dominate the manually calibrated objectives in both the 2010 and 2011 objective spaces. None of the automatically generated solutions were dominated by the manually calibrated result in the 2010 objective space; although 170 solutions were dominated in the 2011 objective space. Clearly, calibrating to only one loading condition independently generates high quality results for that particular simulation. However, many of these results are not robust to model simulations using alternate loading conditions.

The 2011 calibration generated only 37 non-dominated results. The large difference in the number of solutions generated between the 2010 and 2011 calibrations is likely due to the fact that the 2010 model is calibrated to tank level, flow rate, and pressure measurements, thus the optimization algorithm can explore a three dimensional objective space. The 2011 calibration problem is limited to a two dimensional objective space since no pressure data was collected in 2011. In the 2011 objectives space, only two of these solutions dominate the original manual solution, while 31 of these solutions are dominated by the manual solution. This indicates that calibrating to pressure data as well as tank levels and pump flows can improve the performance of the automated calibration methods. However, the difference in performance between the two calibration problems solved may be exaggerated due to the fact that the 2011 model contains significant demand allocation errors.

Figure 3.1 depicts the 2010 calibration objectives calculated for all 592 solutions to the independent 2010 and 2011 calibration problems, while figure 3.2 presents the same solution set in the 2011 objective space.

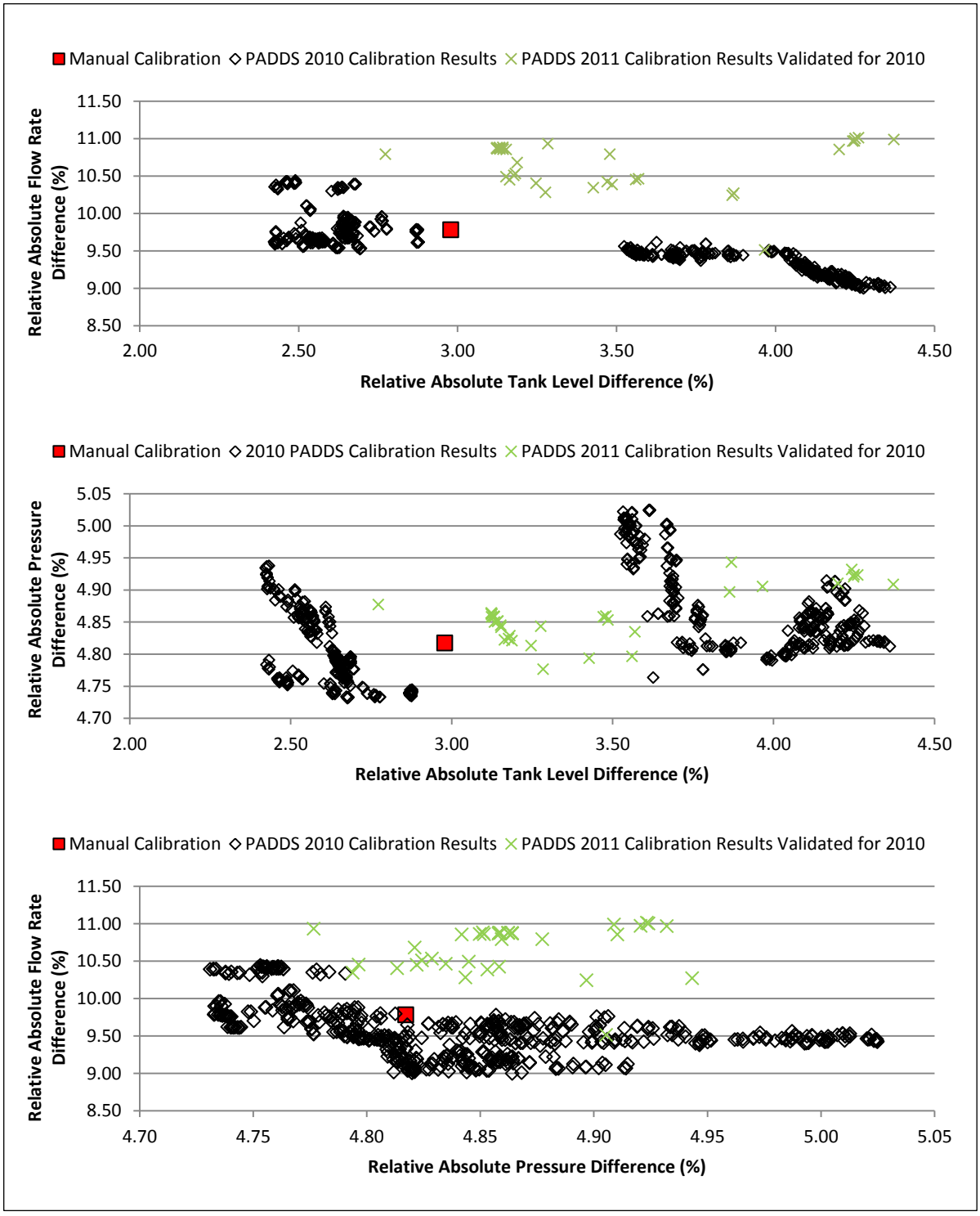

Figure 3.1: Non-dominated solutions from the 5 C-factor grouping 2010, 2011, and manual 2010 calibration formulations presented in the 2010 objective space

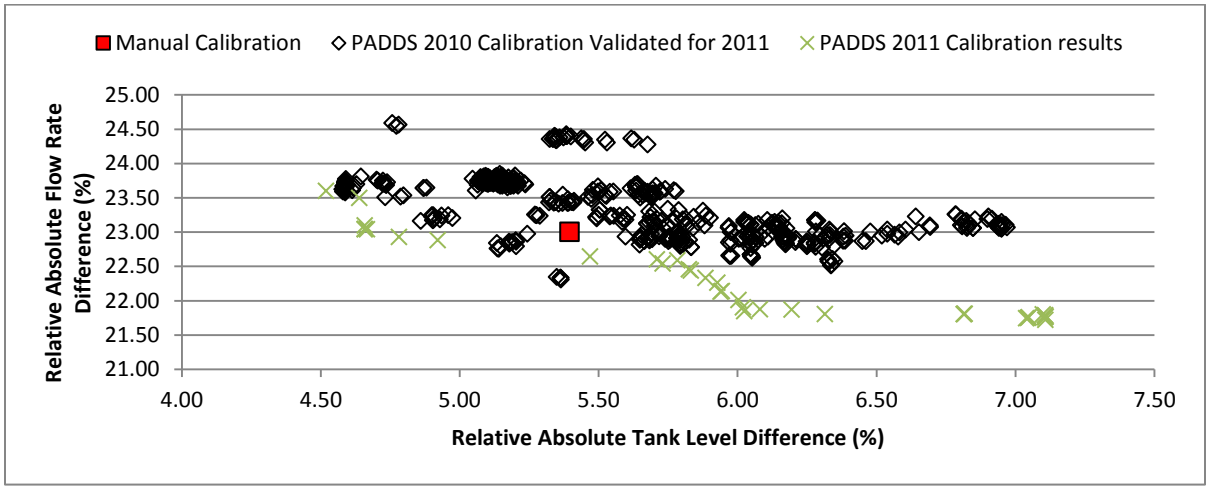

Figure 3.2: Non-dominated solutions from the 5 C-factor grouping 2011, 2010, and manual 2011 calibration formulations presented in the 2011 objective space

A visual inspection of the 2010 calibration results presented in figure 3.1 reveals two discrete clusters of solutions. The first cluster is comprised of solutions with low tank level and pressure errors, and slightly higher flow rates errors, while the second set of solutions have much higher simulated tank level errors and slightly lower flow rate errors. Pressure errors are slightly higher in the second cluster than in the first. However, this difference is almost negligible as the simulated pressures seem much less sensitive to the calibration parameters than the simulated tank water levels and pump station flow rates. The fact that the 2010 solution set is clustered in the objective space indicates that the objective space may be discontinuous, or that the optimization algorithm was able to identify two local optima. The 2011 results validated in the 2010 simulation are more continuous in the objective space than the 2010 solutions, which indicate that the latter is likely and that local optima were identified.

There are several observable tradeoffs in the generated solutions. In figure 3.1, a slight tradeoff between tank levels and pump flow rate errors, as well as pump flow rate and pressure errors is observed. A more pronounced tradeoff between tank level and junction pressures errors is noted as well. In figure 3.2, a clear tradeoff between tank levels and pump flow rates for the 2011 model calibration results is presented. In an ideal situation where all field data and macro-calibrated parameters are exactly accurate, this would not occur as model calibration should reduce all errors simultaneously. However, in a real world scenario, field measurements are never exact and it is highly unlikely that all model parameters not considered for calibration are accurate. These

inaccuracies are manifested in the micro-calibration results as the PADDS algorithm attempts to bring the simulated results closer to reality through the introduction of compensating errors and a trade-off curve is generated. Most, if not all solutions along the tradeoff curve will contain compensating errors, and any perceived improvements in objective function values may simply be a function of these errors. Congruent to ensuring agreement between simulated results and observed field data, the goal of any calibration exercise is to also identify solutions with minimal compensating errors.

Calibrating to only one day of field data can introduce significant compensating errors that reduce the robustness of the generated solutions. This is clearly demonstrated by the fact that most 2010 results perform quite poorly in the 2011 model and vice versa, although the 2010 calibration results are slightly more robust than the 2011 results. This indicates that calibrating to pressures in addition to flows and tank levels may help reduce the potential for compensating errors. However, the difference in quality of the results generated may be slightly overstated due to the fact that the 2011 model contains significant loading and boundary condition errors. Therefore, this analysis is repeated with corrected macro-calibration model parameters in Chapter 5 to verify this observation. The manually calibrated network parameters appear to be more robust than most automated calibration results generated by calibrating to only one day of data independently.

3.1.2 Aggregate Objective Formulation: 5 C-factor Decision Space

Solving the aggregate calibration problem in the 5 C-factor decision space resulted in the generation of 179 non-dominated solutions. All non-dominated solutions generated are presented in the 2010 and 2011 objective spaces in figures 3.3 and 3.4, respectively. These solutions are directly compared to the independent 2010 and 2011 calibration problem results.

68 of the 179 non-dominated aggregate calibration solutions dominate the manually calibrated result in the 2010 objective space, while 32 solutions dominate the manual solution in the 2011 objective space. 19 of these solutions dominate the manually calibrated objectives in both the 2010 and 2011 objective space. Clearly, calibrating to numerous loading conditions simultaneously is more effective at finding a larger number of robust solution sets than calibrating to only one loading condition.

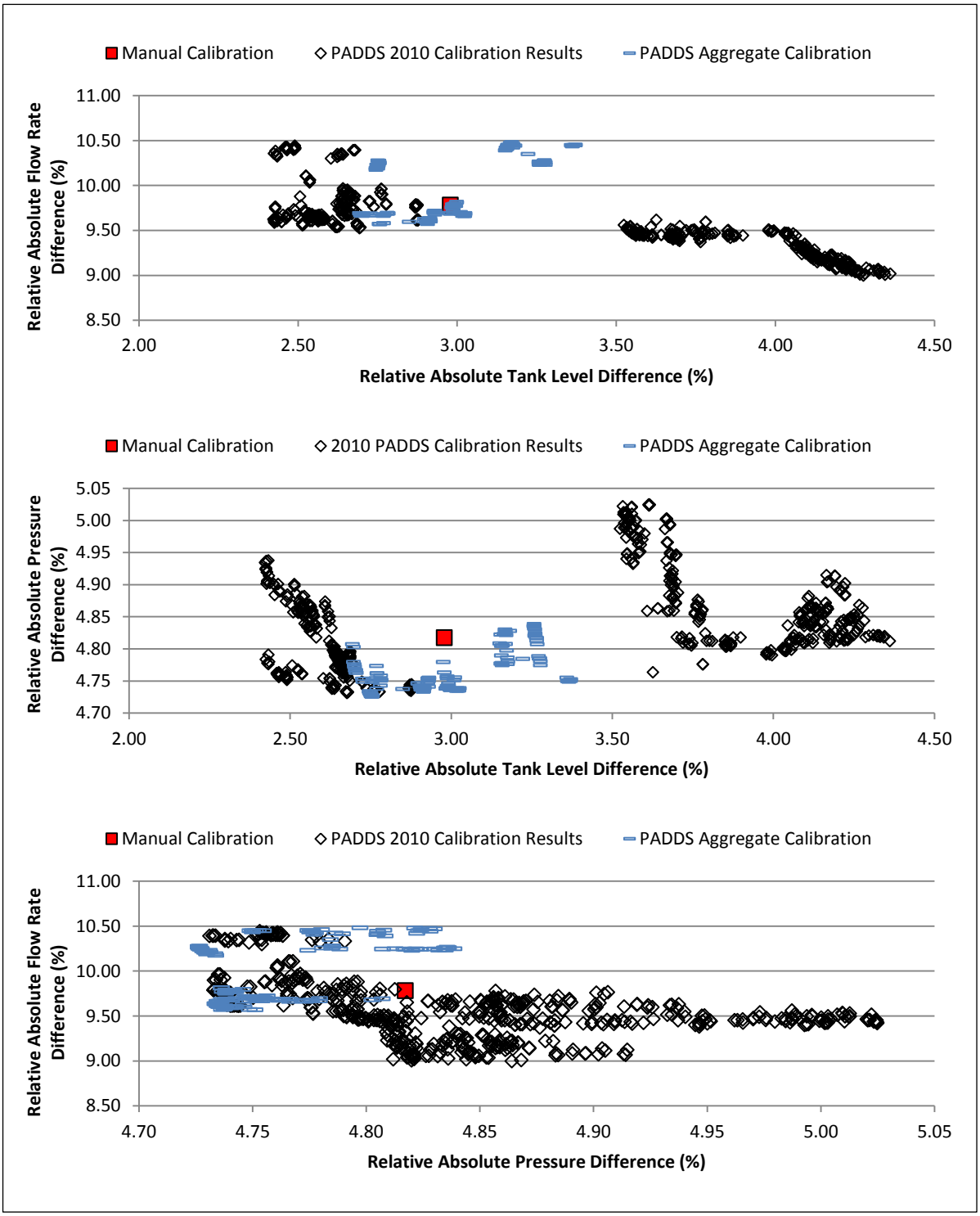

Figure 3.3: Non-dominated solutions from the 5 C-factor grouping 2010, aggregate and manual 2010 calibration formulations presented in the 2010 objective space

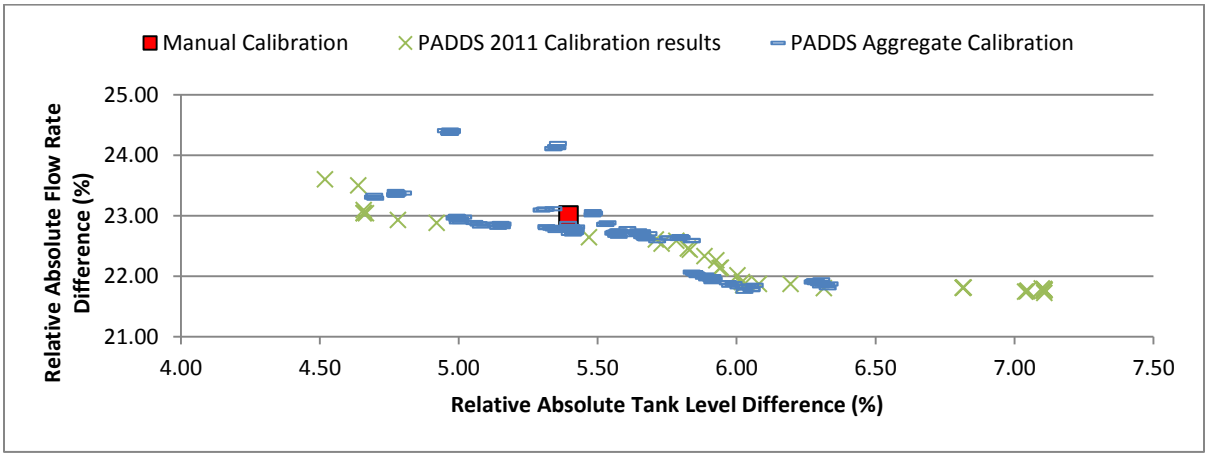

Figure 3.4: Non-dominated solutions from the 5 C-factor grouping 2011, aggregate, and manual 2011 calibration formulations presented in the 2011 objective space

Comparing the aggregate calibration results against the independent 2010 results, it is clear that the aggregate solutions are much more closely grouped. There may still be two clusters of solutions, but they are not as distinct as the clusters observed in solutions to the independent 2010 calibration problem. Moreover, there is little overlap between the independent 2010 and aggregate non-dominated solution sets. There is much greater overlap in the objective spaces of independent 2011 results and the aggregate calibration results. It is possible that given the large magnitude of errors and potential improvement in the 2011 model simulation relative to the 2010 simulation, the optimization algorithm favored solutions that minimized the 2011 simulation errors more so than the 2010 errors.

In general, the aggregate calibration seems to produce more robust solutions than solving the independent calibration problems, although it fails to identify solutions at the extreme ends of both the 2010 and 2011 objective space. It is likely that solutions in the extreme ends of the objective spaces (identified during independent model calibration) contain significant compensating errors and are not robust to different loading conditions. As such, these solutions perform poorly in the aggregate objective space, and are removed from the aggregate calibration non-dominated solution set.

3.1.3 2010 vs 2011 Performance: Bi-Objective Analysis

To further analyze the effects of calibrating to one day independently versus performing an aggregate calibration, a new objective space was formulated. The multi-objective functions characterizing relative percent error in the 2010 and 2011 model simulations were reduced to two single objective

functions defined in equations (3.4) and (3.5). The two new single objective values, representing the average relative percent error in the 2010 and 2011 model simulations, respectively, were calculated for every solution generated from all calibration problems solved. Then, each solution's overall performance in the 2010 and 2011 network conditions was evaluated in this new bi-objective setting. In this bi-objective function formulation, several results within an individual solution set were dominated. These resulted were removed, and the remaining non-dominated solutions from each calibration problem were used to generate bi-objective trade-off curves assessing each result's performance in the 2010 vs 2011 model simulations. The resulting trade-off curves are presented in figure 3.5.

$$2010_{\%Err} = \frac{Q_{\%Err} + P_{\%Err} + H_{\%Err}}{3} \tag{3.4}$$

$$2011_{\%Err} = \frac{Q_{\%Err} + H_{\%Err}}{2} \tag{3.5}$$

where $2010_{\%err}$ and $2011_{\%err}$ represent the average of all relative percent error objectives in the 2010 and 2011 objective spaces, respectively. Each objective is evenly weighted in this analysis.

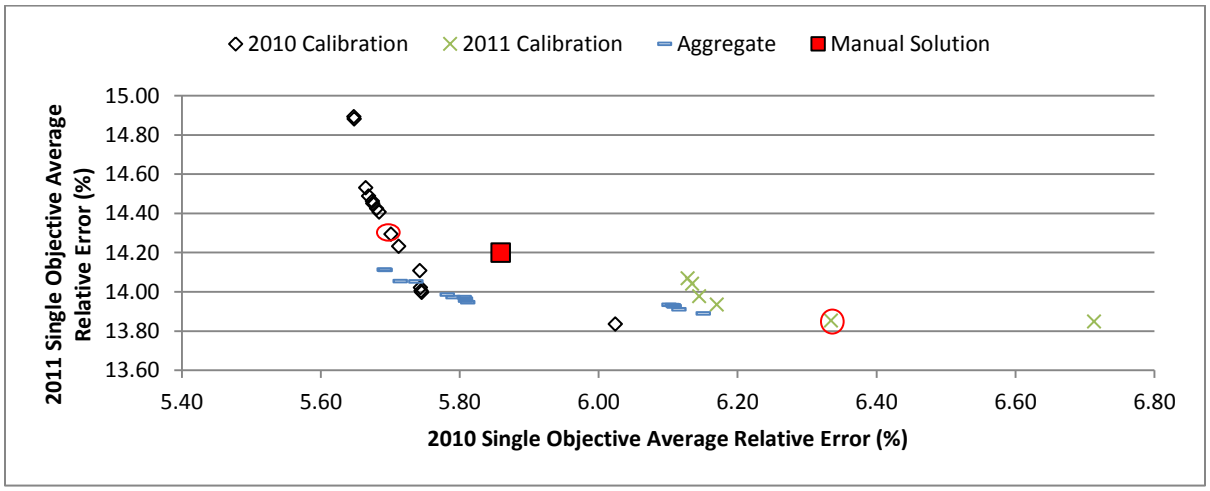

Figure 3.5: 2010 vs 2011 bi-objective analysis of non-dominated solutions from the 5 C-factor grouping 2010, 2011, and aggregate calibration formulations (solutions circled in red are selected for time series analysis)

For solutions generated in the 5 C-factor decision space, only three aggregate calibration results are dominated by the independent 2010 calibration, and no 2011 calibration results dominate the aggregate calibration results when assessing 2010 and 2011 model performance simultaneously. The independent 2010 calibration solutions are more robust than the independent 2011 calibration results,

while the aggregate calibration results are more robust than both independent calibration solutions sets. This further validates the effectiveness of an aggregate calibration approach. One solution from each of the independent calibration problems solved was selected for time series analysis of the tank water levels, or *hydraulic grade lines* (HGLs). These solutions are circled in red on figure 3.5 directly. The time series analysis is completed in section 3.2

3.2 Graphical Time Series Analysis

The automated calibration objective functions were defined in an effort to quantify the manual calibration objectives, which were based on graphical comparisons between simulated and observed data. In order to validate the initial assumption that improvements in the automated objective function values translate to improvements in the manual calibration objectives, two automatically generated solutions (identified in figure 3.5) were selected for graphical time-series analysis of the hydraulic grade lines in each tank. A hydraulic grade lines represents the water level in the tank plus the elevation of the tank. The analysis is also used to gain a more thorough understanding of the model sensitivity to the automated micro-calibration, and attempt to identify potential macro-calibration parameters that can be adjusted for solution quality improvement.

Only high quality solutions to the independent 2010 and 2011 calibration problem formulations are plotted, as these results had the greatest positive effects on the tank level objectives. Figure 3.6 presents the observed and simulated hydraulic grade line time series of the elevated storage tanks C, V, and S for one solution generated from the automated calibration of the 2010 network conditions, in addition to the manually calibrated model simulated to 2010 network conditions. Figure 3.7 presents the same information for an automated solution to the 2011 calibration problem, the manually calibrated result simulated in the 2011 network conditions, and the 2011 field conditions.

The cumulative absolute errors in simulated tank level measurements associated with the 2010 simulation of the manually calibrated model is 1234 m, which corresponds to a relative percent error between simulated and observed conditions of 3.0 %. The error associated with the automated solution presented in figure 3.6 is 1004 m, corresponding to a relative percent error of 2.4 %. Therefore, improvements are marginal, but this is expected since micro-calibration is the final, fine tuning step of a WDN calibration process.

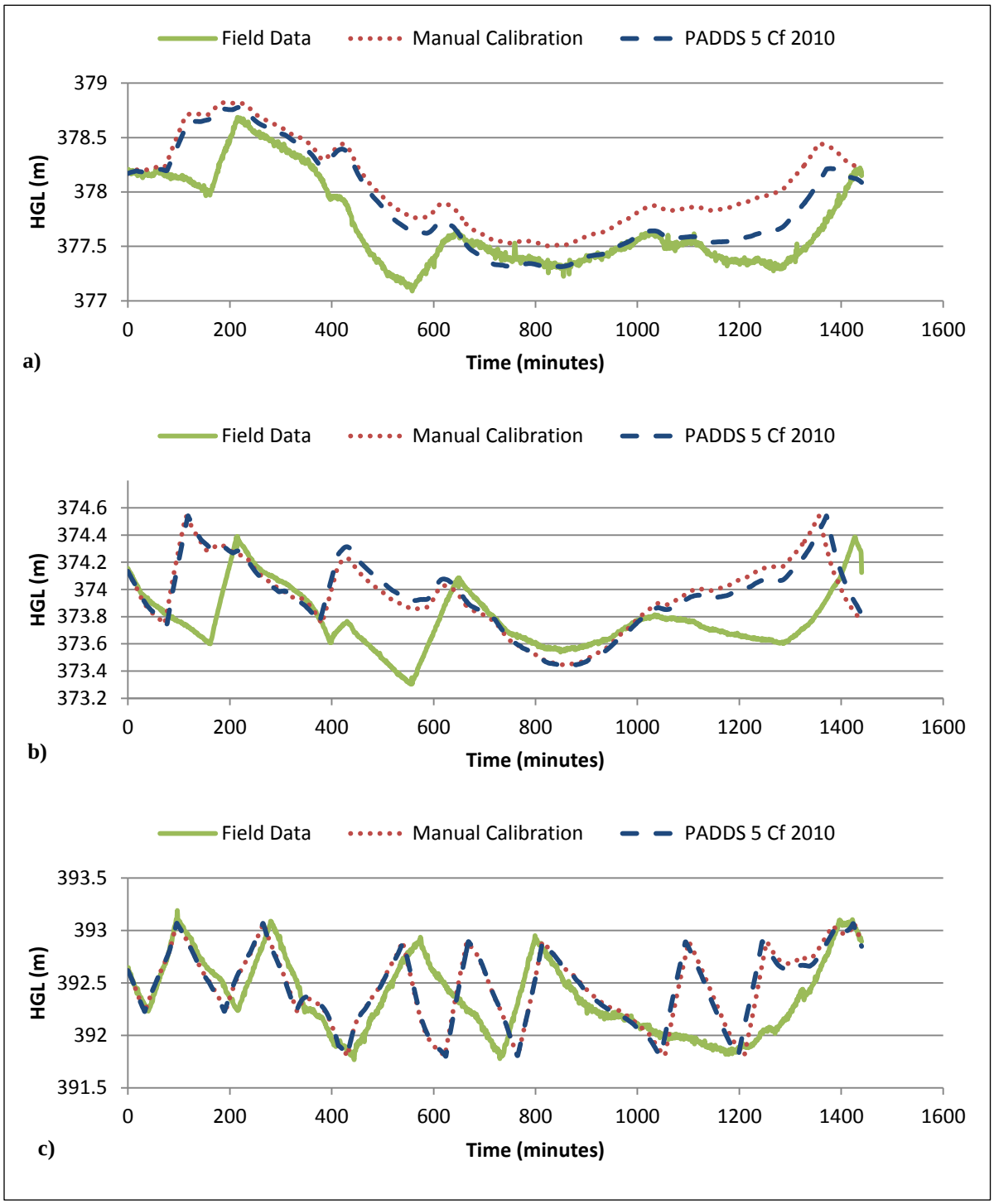

Figure 3.6: 2010 C (a), V (b) and S (c) tanks HGL time series of field observations compared to the manually calibrated and a select automatically calibrated solution in the 5 C-factor decision space

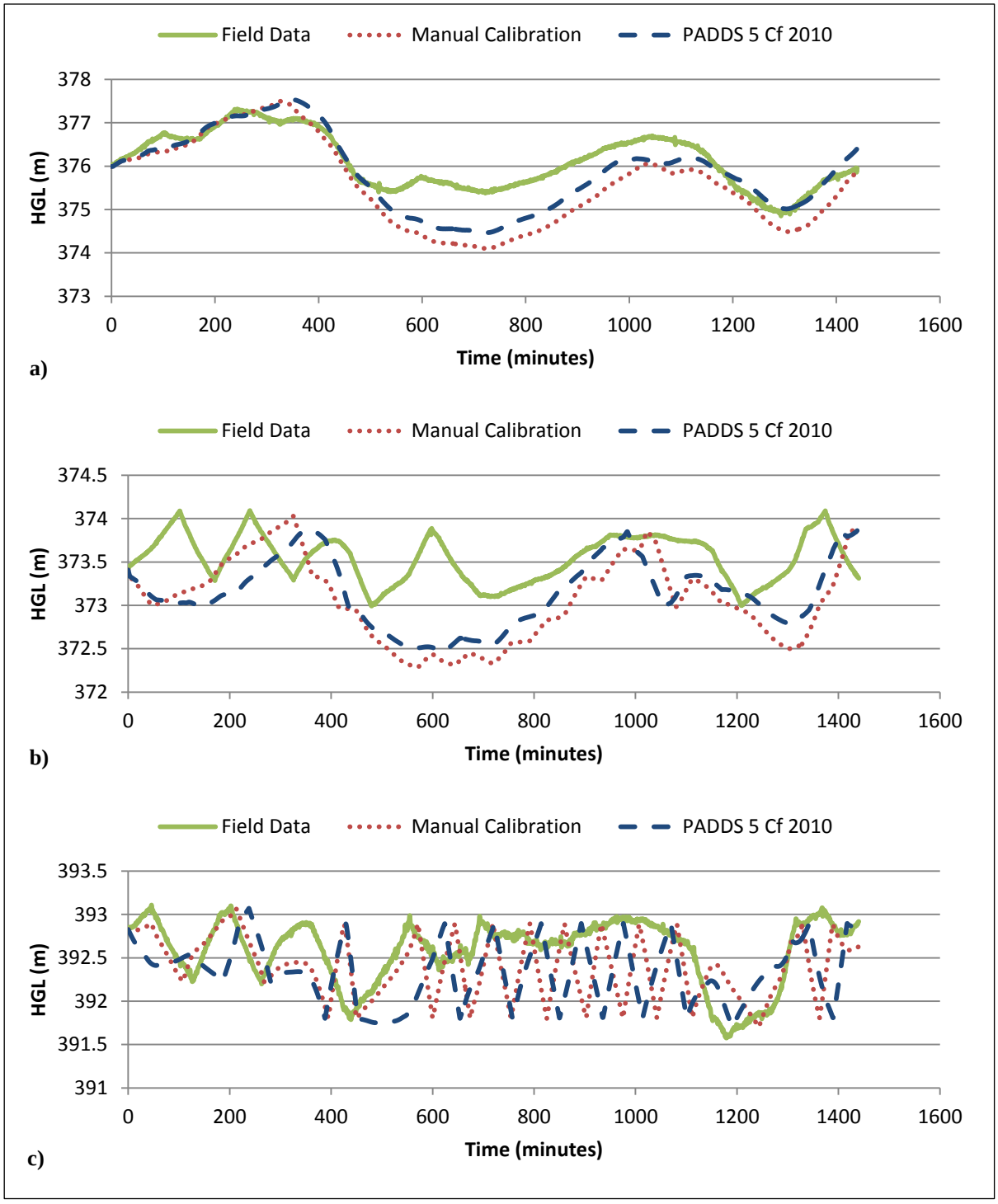

Figure 3.7: 2011 C (a), V (b) and S (c) tanks HGL time series of field observations compared to the manually calibrated and a select automatically calibrated solution in the 5 C-factor decision space

Storage tanks V and C are approximately 4500 m^3, while tank S is approximately 2200 m^3. As such, tank S drains and fills at a much quicker rate than tanks C and V and is much more sensitive to pumping operations. This is evidenced by the highly variable hydraulic grade line within the tank. It seems that water levels in tank C are most sensitive to the calibration parameters. This is expected due to the fact that the demand shift parameter was introduced specifically to bring simulated water levels of tank C into closer agreement with observed conditions.

The 2011 manual calibration objective of tank level error was calculated as 2112 m, which corresponds with a percent error of 5.4 %. The error associated with the 2011 automated calibration solution presented in figure 3.7, is 1826 m, corresponding to a relative percent error of 4.7 %. Generally the results were of significantly lower quality than the 2010 network condition model simulations, and tank S in particular was highly inaccurate. Again, results are heavily dependent on the macro-calibrated model parameters and pump controls, and it is likely that the 2011 loading conditions were altered following calibration and not reverted back to the original calibrated settings.

In general, the potential improvement in the tank water level error minimization objective are relatively low. Subsequent analysis of the network pumping rates and control rule settings in conjunction with the tank levels indicates that tank levels are most influenced by the pump control rules. For example, a major pump station becomes operational when water in tank V reaches a hydraulic grade line of approximately 373.8 meters, corresponding to a tank water level of 8.1 meters. This significantly alters the water level in the tank and simulated levels vary greatly from the observed conditions once this pump becomes operational. This is demonstrated graphically in figure 3.8, through a time series analysis of the simulated zonal inflows/outflows and tank water levels corresponding to the manually calibrated model. Altering the micro-calibration parameters can slightly alter the rate at which a tank fills/drains, which in turn affects when a pump is activated/deactivated. This can bring simulated results into closer agreement with the observed results, however improvements are marginal since the source of the error (pump operation controls) is not addressed. Improvements in all micro calibration results are quite limited by the existing pumping rules.

If the pump control rules were set accurate to the given calibration dates, this could indicate a problem in demand settings or network structure. It is unclear what the true source of error is, however it is clear that the quality of micro-calibration results are severely limited by the existing pump controls and macro-calibration parameters. Thus, an analysis of the pump controls is conducted

in chapter 4, in an effort to more closely match observed field conditions and increase micro-calibration solution quality.

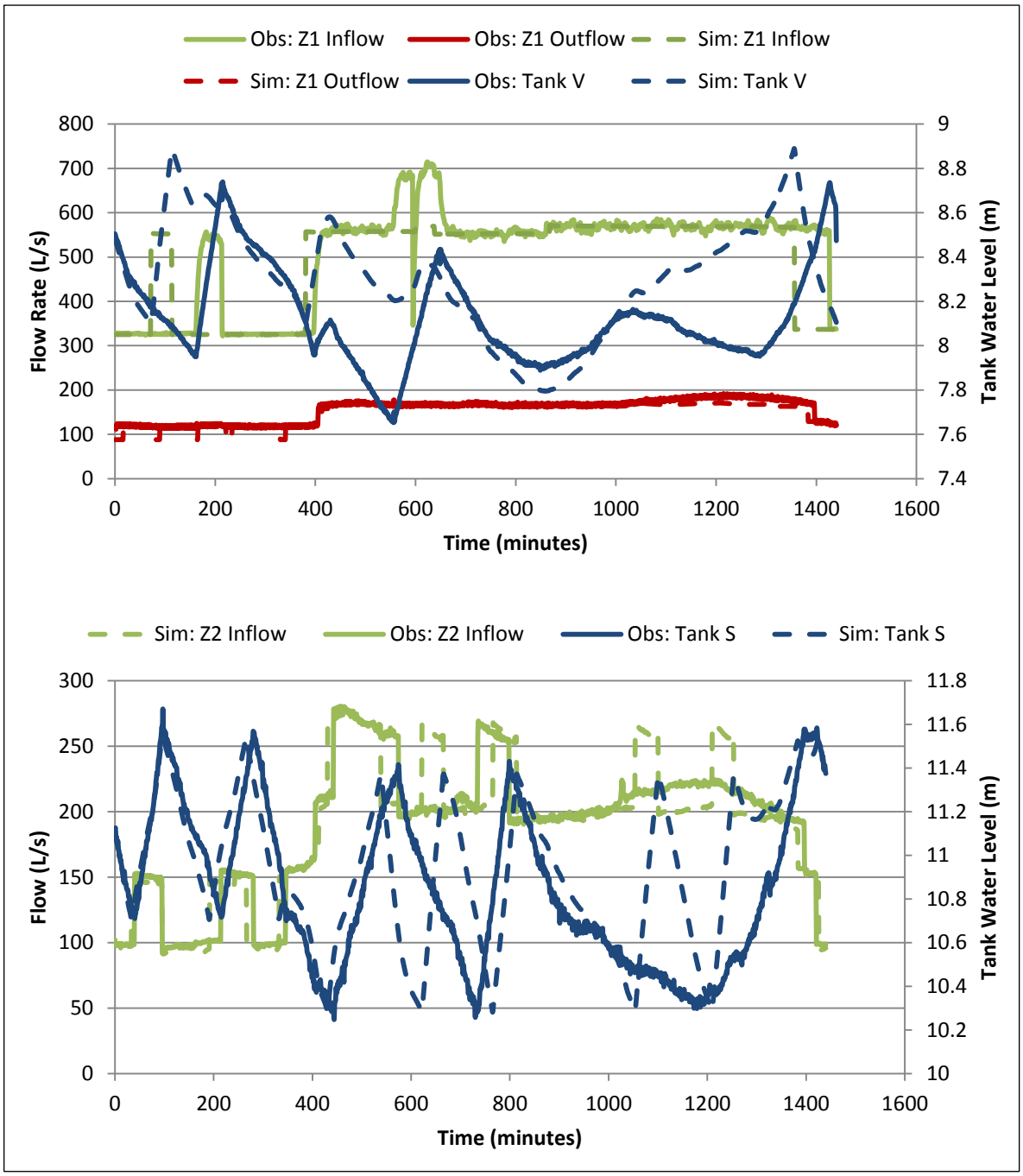

Figure 3.8: Manually calibrated simulation results vs. field observations relating zonal inflows and outflows to tank water levels

3.3 Summary Statistics

The aforementioned automated calibration formulations generate a wide range of non-dominated solutions from which a decision maker can perform operational analyses. However, no decision maker will be able to identify any decisions that adhere to all solutions, nor should they attempt to do so. This solution set should be narrowed to allow for meaningful analyses, and to attempt to remove solutions containing compensating errors. Given the fact that the initial results of the automated calibrations indicate that the macro-calibrated model parameters are inaccurate, no attempt was made to narrow the solution set to a more manageable number of solutions at this stage in the research; this is completed using results presented in chapter 5. In this chapter, solution quality is only assessed relative to the manually calibrated solution.

Summary statistics identifying the efficacy of automatically calibrated models relative to the manually calibrated model are provided. The number of non-dominated solutions generated in each calibration problem is provided in table 3.1. The number of solutions obtained from each calibration problem that either dominate, or are dominated by the manually calibrated solution is also presented in this table.

Table 3.1: Automated calibration solution summary

Solution Set	**Total # of solutions**	**Dominating Manual result in 2010 Objective Space**	**Dominating Manual Result in 2011 Objective Space**	**Dominating Manual Result in 2010 and 2011 Objective Spaces**	**Dominated by Manual Result in 2010 Objective Space**	**Dominated by Manual Result in 2011 Objective Space**
2010: 5 C-factor	555	59	17	9	0	170
2011: 5 C-factor	37	0	2	0	31	0
Aggregate: 5 C-factor	179	68	32	19	19	4

No automatically generated solutions are dominated by the manually calibrated model in both the 2010 and 2011 objective spaces, while 19 and 9 automatically generated solutions to the aggregate and 2010 calibration problems, respectively, dominate the original manual solution in both objective spaces.

No automatically generated solutions from the 2011 calibration problem dominate the manual calibration in both 2010 and 2011 objective spaces. In fact, only 2 of these automatically generated solutions dominate the original manual result in the 2011 objective space. The algorithm's inability to identify high quality solutions for the 2011 model simulation, even when only calibrating to 2011 data, may be due to the fact that no pressure data was used in the calibration, or it could be caused by the fact that the macro-calibration parameters may be inaccurate. Considering the inaccurate 2011 loading conditions it is difficult to draw more meaningful conclusions; however it is clear that the optimization algorithm can identify a wide range of solutions, many of which can improve upon the quality of a manually calibrated solution. In order to identify the cause of the poor performance of the 2011 automated calibration results, the macro-calibration parameters were updated and the micro-calibration analysis was repeated. Results are presented in chapters 4 and 5.

Statistics summarizing calibration objective performance across the entire range of non-dominated solution sets for all three calibration problems are provided in table 3.2. Since the magnitude of improvements of a micro-calibration exercise is relatively minor, the performance of each solution is measured by the *relative percent improvement* over the manually calibrated solution objective function calculations. The minimum, maximum, and standard deviation of objective function changes relative to the manual solution are tabulated. The tank error objective is most sensitive, while flow and pressure errors are relatively insensitive to the micro-calibration parameters. The insensitive flow rate error objective is based on the existing pump controls. Therefore, these controls are addressed in a manual macro-calibration in chapter 4 in order to provide the algorithm the best possible opportunity to identify solutions void of compensating errors.

Simulated pressures are insensitive to the calibration parameters due to the fact that the available pressure measurements used for 2010 calibration purposes are obtained a short distance downstream of pumps within the network. Therefore, the potential impact of calibrated C-factor settings on these pressures is severely limited. It is expected that a greater improvement in the simulated pressures would be observed if calibration pressure data was taken further downstream of pump stations at various locations throughout the network. For more significant improvements in pressure readings at the existing monitoring points, pump operations and hydraulic curves must be adjusted. Neither parameter was considered in the micro-calibration analysis.

More significant improvements in the tank level objectives may be achieved by adjusting macro-calibration parameters. This is attempted in chapters 4 and 5.

Table 3.2: Automated calibration solution objective function change relative to manual Solution

Solution Set	ΔTank Objective (%)			ΔFlow Objective (%)			ΔPressure Objective (%)		
	Min	Max	Std Dev	Min	Max	Std Dev	Min	Max	Std Dev
2010: 5 C-factor	-46.4	18.5	23.1	-6.8	8.0	3.5	-4.3	1.8	1.5
2011: 5 C-factor	-31.7	-1.4	16.7	1.6	5.6	2.6	NA	NA	NA
Aggregate: 5 C-factor	-2.4	17.6	5.8	-3.7	3.7	1.9	0.2	2.5	0.7

3.4 Results Summary

Ultimately, not a great deal of emphasis can be placed on the algorithm's ability to generate solutions robust to different loading conditions as it appears as though one, or maybe both of the models contain errors in the previously assumed accurate parameters. It is clear, however, that solving a multi-objective implicit automated calibration problem can produce a wide range of solutions regardless of loading conditions. Moreover, an analysis of the objective function tradeoffs and insensitive objectives can be useful when identifying inaccuracies in exiting parameter settings. A total of 28 solutions generated from solving the 2010 and aggregate calibration problems dominate the original manual solution in both 2010 and 2011 simulation objective. The benefit of calibrating to both days simultaneously has been established, and the C++ script generated can be easily manipulated to calibrate to more data as it becomes available.

The relative percent errors between simulated and observed 2010 data calculated for the manually calibrated solution are 3.0 %, 9.8 %, and 4.8 % for the tank levels, pump flow rates, and pressure observations within the network, respectively. This indicates that the manual solution is already of high quality; however the pump flows appear to be both inaccurate, and insensitive to the micro-calibration analysis. This greatly hinders the potential improvement in the simulated tank levels. Despite these inaccurate settings, a large number of unique automated micro-calibration solutions were generated. Given the nature of a micro-calibration, the magnitude of objective function improvements in the automatically generated solutions were marginal and severely limited by existing model parameter settings.

The relative percent errors for the 2011 simulation of the manually calibrated model are 5.4 % and 23.0 %, for the tank level, and pump flow rate errors, respectively. It is unlikely that these results accurately represent the manual calibration effort and are likely a function of data management issues exasperated from working with data sets that are 5 years old. That said, it is clear that results generated from calibrating to the 2011 model are of lower quality than those generated from solving the 2010 calibration problem, and correcting the 2011 model is crucial to achieving more reasonable results.

Due to the significant error in 2011 loading conditions and pump operations in the 2010 and 2011 network conditions, it is difficult to derive any more meaningful conclusions from the automated results generated in this chapter. A manual macro-calibration of model parameters is completed in chapter 4, and the automated micro-calibration is attempted once more with the adjusted model parameters in chapter 5. Additional insights are provided using these new results in chapter 5.

Chapter 4
Manual Adjustment of Model Parameters

The analysis of initial micro-calibration results revealed potential errors in the operation of the pumping stations. The existing pump control rules are based on tank water levels, and as such pump operation varies in each simulation as C-factors and demand shift parameters are adjusted. These rules were implemented to allow for a more robust model which could respond to various loading conditions. However, if the water level based controls were inaccurately reported or incorrectly input into the model, then the use of these rules could severely hinder any calibration efforts. This adds a source of uncertainty to the model parameters and increases the potential of the introduction of compensating errors during calibration. Moreover, a significant number of tank water-level based control rules in a complex model can cause significant convergence issues in EPANET (Paluszczyszyn et al. 2015). For example, solutions can vary significantly by only changing the fourth decimal place of modeled C-factor settings. To address these concerns, SCADA data was used to create new time-based pump control rules which more accurately characterize pump operation on the given calibration dates.

Following control rule adjustment, erroneous demand pattern multiplier settings were identified and new demand pattern curves were created to match available SCADA data. Graphical analysis of tank water level time series indicated that further potential improvements in simulated tank levels could be achieved through the application of a new demand shift across the network. This demand shift was identified for use as a micro-calibration parameter in chapter 5. All model adjustments were assessed using the existing manually calibrated C-factor and demand shift settings.

4.1 Control Rule Adjustment

The existing network is divided into two pressure zones. The quantity of water flowing into and out of each zone is controlled by 17 pump stations and a series of flow control valves (FCVs) and pressure reducing valves (PRVs) installed along the boundaries of these zones. The pump stations, PRVs, and FCVs are remotely controlled by system operators using controls which activate and deactivate pumps and adjust valve settings throughout the day. During the manual calibration, the operating control rules employed by the system operators were input in the model network, and the micro calibration was completed with these controls. A total of 77 and 75 control rules adjusting valve/pump operational settings based on the simulated tank levels were implemented in the 2010 and

2011 model networks, respectively. Although these rules match operator reported settings on the given calibration dates, they may not accurately reflect network conditions due to inaccurate logging of pump switch settings or inaccurate tank or reservoir level sensors (Walski et al. 2003). This source of error is both unnecessary and hinders the automated algorithm's search for calibrated C-factors and spatial demand adjustments.

To address these concerns and more accurately reflect network conditions, new control rules were created using information collected from SCADA systems along the boundaries of each zone. Using SCADA data, the total quantity of water discharged into each zone, and the time at which it is discharged is known a priori and can be modeled explicitly using time based control rules.

An example pump station (the university pump station) is depicted in figure 4.1. The network structure was altered slightly from 2010 to 2011, and the inlet valve depicted in figure 4.1 is a new addition to the 2011 model network. This may correspond to a newly installed valve in the real system, or an update to the model which was missing in the 2010 network. Regardless, the figure represents a typical pumping station for which SCADA data representing zonal inflow and outflow is recorded. The data is comprised of averaged flows over a one minute time interval, and is assumed accurate. Most pump stations in the network are comprised of several pumps, and the available data does not identify which pumps are active; only a total flow rate out of the pump station is provided. The actual active pumps at any given time step were corroborated using the total flow rate reported from SCADA systems, and the existing pump discharge-head curves input in the model network. Generally SCADA data at well pumps was not available, however these pumps only control water pumped directly into reservoir storage and not yet introduced to the distribution system. Data is available for all inflows and outflows directly along the boundaries of the distribution system, with the exception of information at the university inlet valve. At this location, SCADA data was not available and the modeled control rules were assumed accurate representations of field conditions.

Using the SCADA flow data, new pump/valve operational control rules were created. All pump start/stop times were explicitly defined using time based control rules. If the observed discharge at any given pump station was relatively static, only one control rule was established at the flow control valves downstream of the pumping stations, and the flow was set equal to the average flow rate over the course of the simulation. If discharges were more variable, the average flow rates at each 15 minute interval of the 24 hour time period were calculated, and new 15 minute control rules were applied to capture the variability in pumping rates. A total of 283 and 275 time based control rules

were created to more accurately reflect network conditions in the 2010 and 2011 model boundary conditions.

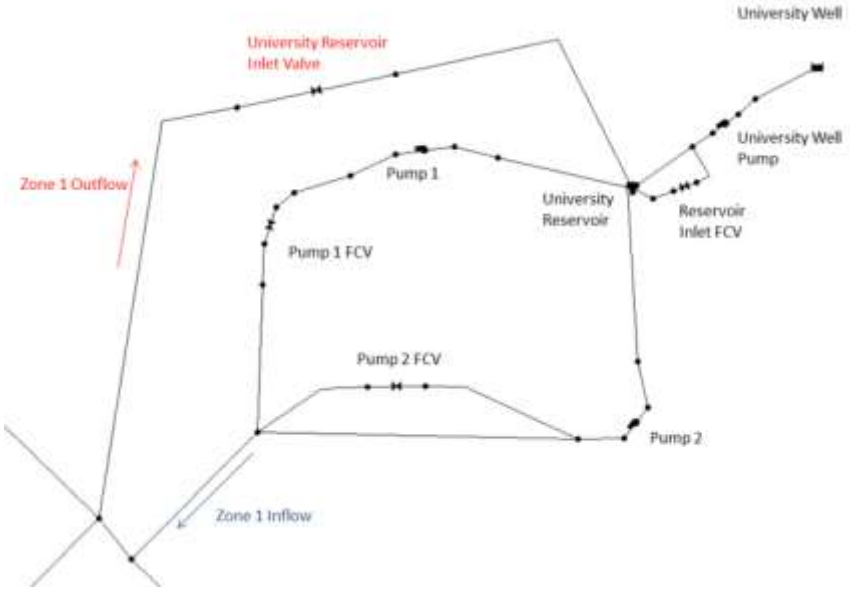

Figure 4.1: University pumping station model components and inflows/outflows

Of course, controlling pump activity does not guarantee an exact match between simulated and field conditions due to inherent differences in the simulated and real pump systems. Moreover, as discussed in section 2.3.2, the EPANET modeling software can alter pump controls if it cannot converge to a solution under existing conditions. Therefore, an iterative process increased the specificity of the control rules until observable improvements in simulated pump operations were marginal and remaining errors were assumed inherent to the calibrated pump curves and modeling limitations. Using the relative percent flow error calculation defined in chapter 3.1, the percent errors of the simulated flows under existing pump controls was 9.8 % and 23.0 %, in the 2010 and 2011 manually calibrated model simulations, respectively. Upon changing the control rules to time-based settings, pump flow errors were reduced to 2.8 % in the 2010 simulation, while the 2011 model actually failed to simulate the entire EPS due to the fact that demands were inaccurately set in the model.

Unfortunately the improvement in the 2010 simulated flow objective did not correlate to an improvement in simulated tank levels. In fact, tank errors actually increased to 6.7 %. Although, a comparison of the tank level time series (provided in figure 4.2) shows that the simulated water levels

in tanks C and V more accurately follow the filling and draining patterns observed in the field. The simulated results for S tank also more closely resembles the filling and draining patterns observed in the field; however the rate at which the tank fills/drains in the simulation is significantly greater than the observed conditions.

Assuming the network structure and field data are accurate, the increased error in 2010 simulated tank levels could be due to any number of reasons, including inaccurate C-factor settings along the flow paths into/out of the tanks, and/or spatial and temporal demand distributions. The C-factor settings, and to a lesser extent the spatial distribution of demands are considered in subsequent micro-calibration analyses, while the temporal demands are held static. Since temporal demands are not considered in the micro-calibration it is important to ensure that these modeled parameter settings are as accurate as possible and not a major contributing factor in the simulated tank level errors. Therefore, in section 4.2, the zonal demand patterns were re-calculated using the SCADA data of zonal inflows and outflows, as well as SCADA tank levels over the course of the simulation. This was done to validate the initial calculations and reduce potential sources of error not related to the micro-calibration parameters.

The 2011 simulated tank level time series, provided in figure 4.3, are drastically different in pattern and magnitude than the observed field conditions. This is a clear indication that demands are not accurately set in the model. The 2011 loading conditions are almost definitely not representative of the parameter settings applied in the manually calibrated model, and it is very likely that the demand settings have been altered at some point since it was initially calibrated. In any event, the spatial variation in base demand settings was consistent with the 2010 model, and therefore it was assumed that only the simulated diurnal demand patterns were inaccurate. These are corrected in section 4.2 and the adjusted 2011 demand settings are more likely attuned to the initial manual calibration efforts.

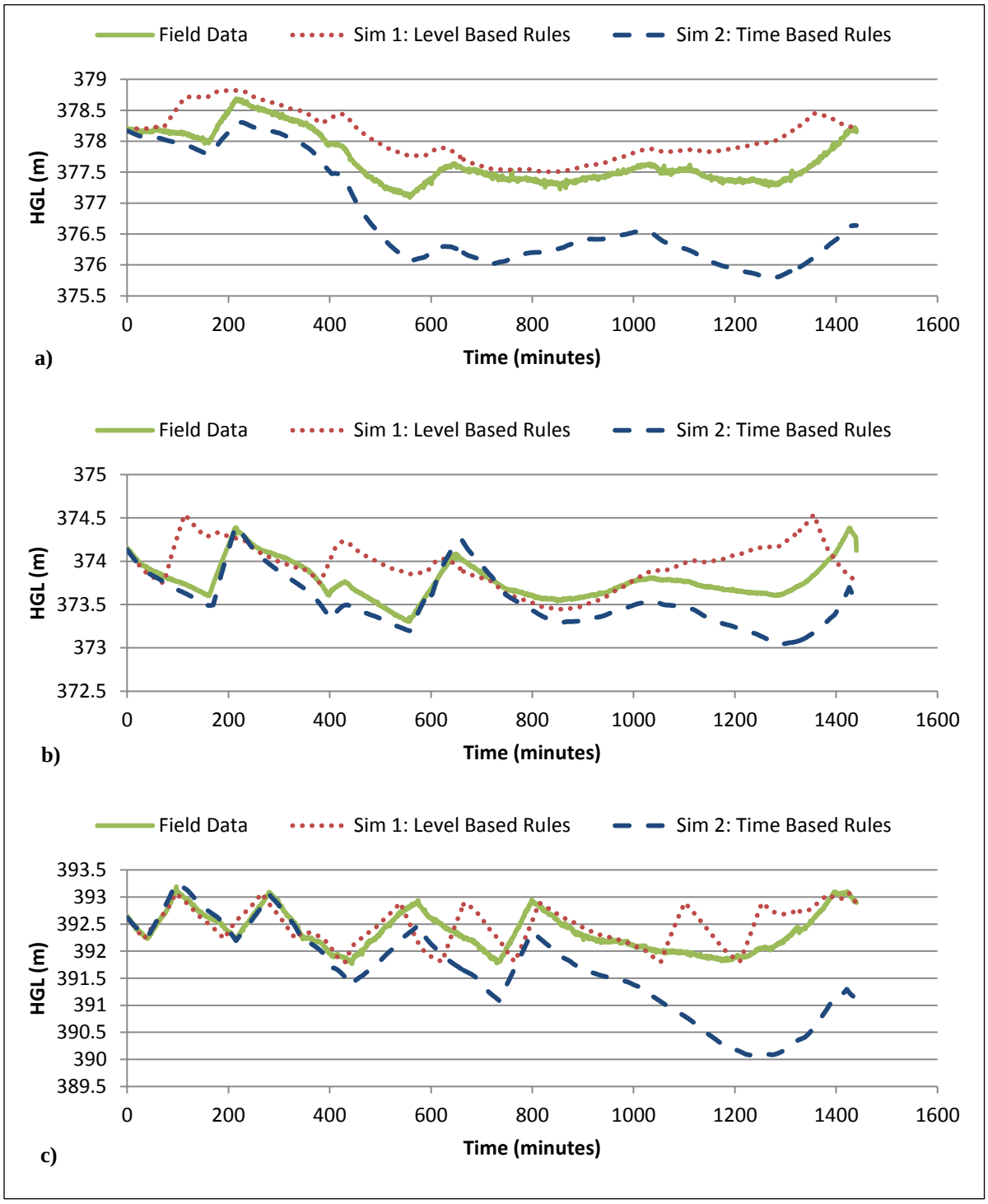

Figure 4.2: C (a), V (b), and S (c) tanks HGL time series for manually calibrated 2010 model with original and adjusted control rules

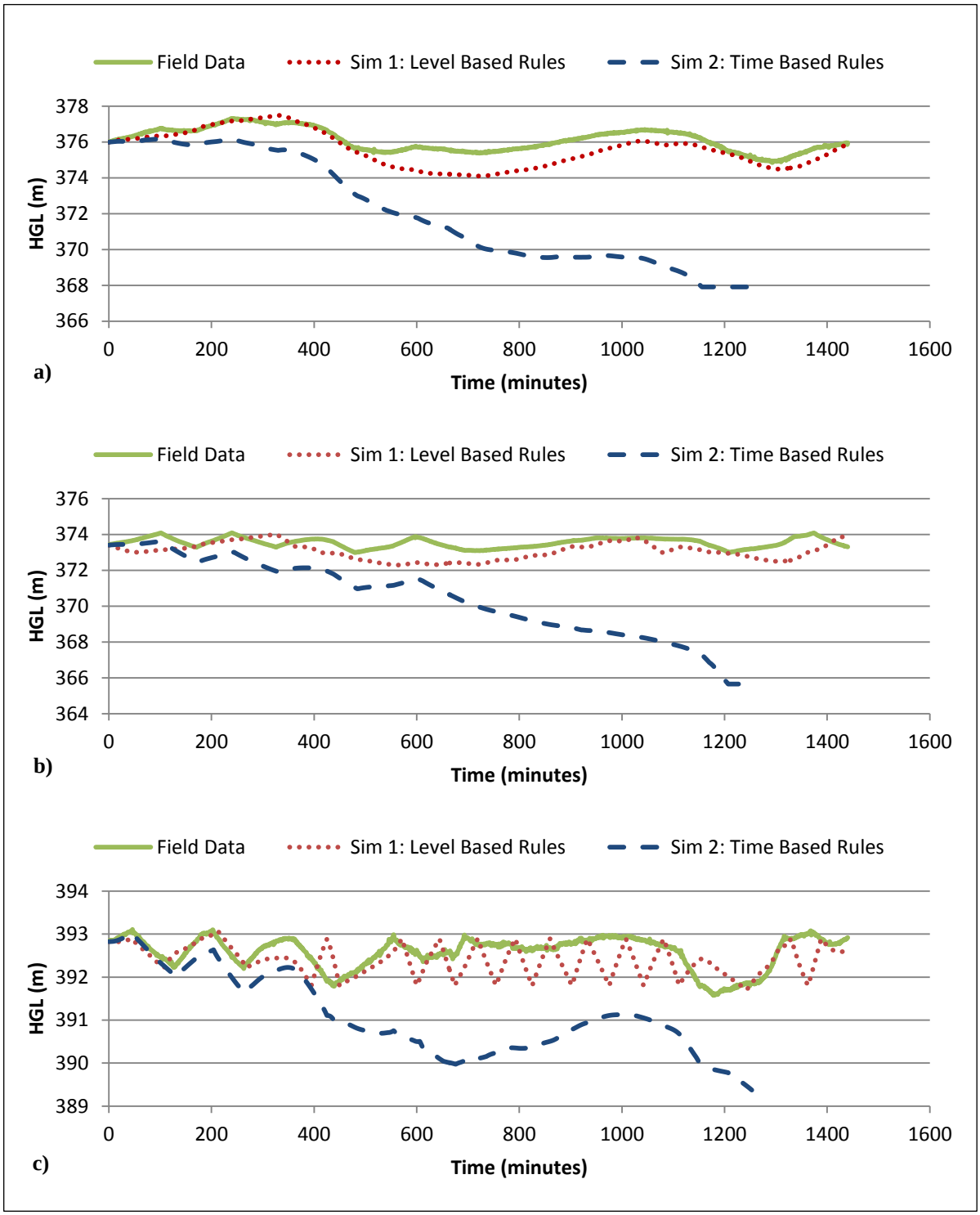

Figure 4.3: C (a), V (b), and S (c) tanks HGL time series for manually calibrated 2011 model with original and adjusted control rules

4.2 Demand Pattern Adjustment

New zonal demand pattern multipliers were created using SCADA measurements of inflows and outflows into each zone, the existing base demand settings at all nodes comprising zones 1 and 2, and the instantaneous SCADA measurements of tank water levels for all three tanks within zones 1 and 2. Since the SCADA tank level data is comprised of instantaneous measurements at each minute, there are several oscillations in the data that prevent it from being directly used in diurnal demand calculations. In fact, the noise in the data is so large at some points that if it were used directly in diurnal demand calculations at each one minute time step, it would lead to negative demand observations; this is clearly inaccurate. Therefore, as is common practice (Walski et al. 2003; Bentley Systems 2004), the SCADA data was smoothed to remove the noise.

Although several literature sources recommend smoothing instantaneous SCADA data, no smoothing methods are recommended. For this research, the time series of tank level data was smoothed in MATLAB using the locally weighted scatter plot smooth (LOWESS) function (The Mathworks Inc. 2015a). This function performs a weighted linear regression to smooth data points within a pre-specified span of the data set. The data point being smoothed has the largest weight and the most influence on the fit, while the weights of data points further away are reduced as a function of their distance from the smoothed data point. The span represents the percent of all 1441 tank level time series data points used in the regression. In order to respect the water balance as much as possible, the span was iteratively increased by 0.1 % until all calculated demands based on the tank levels were non-negative. Spans of 0.3 %, and 0.7 % (corresponding to approximately 5, and 10 minutes of data, respectively) were required to adequately smooth the 2010 and 2011 tank water level information, respectively. Total diurnal zonal demands over the course of each one minute interval were calculated using equations (4.1) and (4.2).

$$V_{Z1,\Delta t} = \left(Q_{Z1,in} - Q_{Z1,out}\right) * \Delta t - \Delta V_V - \Delta V_C \tag{4.1}$$

$$V_{Z2,\Delta t} = \left(Q_{Z2,in} - Q_{Z2,out}\right) * \Delta t - \Delta V_S \tag{4.2}$$

where $V_{Z1\Delta,t}$, and $V_{Z2,\Delta t}$, represent the volume of water withdrawn from the system in zone 1 and zone 2, respectively over the course of the one minute time step [m^3]; $Q_{Z1,in}$, and $Q_{Z2,in}$, represent the volumetric flow rate of water discharged into zones 1 and 2, respectively [m^3/min], these flow rates

are assumed static over a one minute time step; $Q_{Z1,out}$, *and* $Q_{Z2,out}$, represent the volumetric flow rate of water pumped out of zones 1 and 2, respectively [m^3/min]; ΔV_V, ΔV_C, and ΔV_S, represent the change in volume of V, C, and S tanks, respectively [m^3]; and Δt represents the time step length which is set to one minute to match available field data. The total zonal demands over the 24 hour simulation period are simply summations of the aforementioned calculations at all one minute time steps. The total zonal inflows and outflows for both the manually calibrated model as well as the observed data are provided in table 4.1.

The base demand parameter settings implemented in each model were used in conjunction with the diurnal zonal demands to generate new demand pattern multipliers to model the 2010 and 2011 EPSs. The base demands in zones 1 and 2 of the 2010 model were 21.3, and 11.3 m^3 per minute, respectively. The 2011 demands in zones 1 and 2 were 29.2, and 13.5 m^3 per minute, respectively. The new demand pattern multipliers at each time step were calculated using equations (4.3) and (4.4).

$$M_{Z1,t} = \frac{V_{Z1,\Delta t}}{Q_{Z1} * \Delta t} \tag{4.3}$$

$$M_{Z2,t} = \frac{V_{Z2,\Delta t}}{Q_{Z2} * \Delta t} \tag{4.4}$$

where $V_{Z1,\Delta t}$, and $V_{Z2,\Delta t}$ represent the actual volume of water consumed in zones 1 and 2 over the one minute time step Δt at time t [l/s]; Q_{Z1}, and Q_{Z2} represent the base demands in zones 1 and 2; and $M_{Z1,t}$, and $M_{Z2,t}$ represent the unitless demand multipliers applied to the zone 1 and zone 2 base demands at time t. A total of 1440 demand multipliers are calculated for each zone in each model, and demands are assumed static over the course of a one minute time step.

Since new control rules and diurnal demand patterns were established, the need to implement the demand shift from zone 1a to zone 1b, depicted in figure 4.4, was re-assessed. The adjusted models were simulated with, and without the demand shift implemented to re-evaluate the network sensitivity to this parameter. All simulated 2010 and 2011 tank level time series are depicted in figures 4.5 and 4.6.

Table 4.1: Observed zonal flux and demand calculated from 2010 and 2011 SCADA data

Zonal Inflow/Outflow and Demands	**Cumulative Observed Discharge: 2010 (m^3)**	**Cumulative Observed Discharge: 2011 (m^3)**
Z1 Inflow	44043.8	52186.6
Z1 Outflow	13404.8	19952.9
Z1 Tank Inflow	-20.2	-107.1
Z2 Inflow	16286.5	19388.5
Z2 Tank Inflow	48.0	13.6
Z1 Demand	30659.3	32340.8
Z2 Demand	16238.5	19375.0
Total Demand	46897.7	51715.8

In general, this demand shift appears to introduce a compensating error to the model network. In all cases, the demand shift brings the simulated water levels in C tank into closer agreement with the observed tank levels; however the shift reduces the quality of the simulated water levels in V tank. This is to be expected due to the fact that demands are shifted away from V tank, and towards C tank, as depicted in figure 4.4. This demand shift, which may have appeared necessary under the previous control rule settings, demonstrates how easily compensating errors can propagate throughout every step of the calibration.

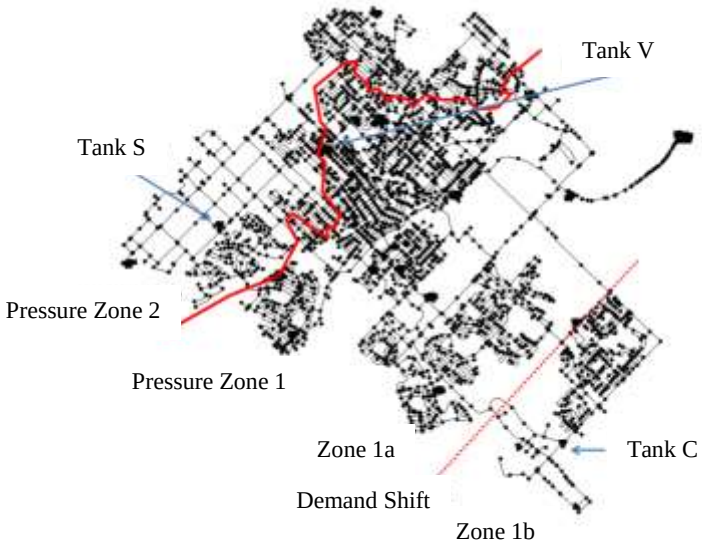

Figure 4.4: Zone 1 demand shift and network tanks

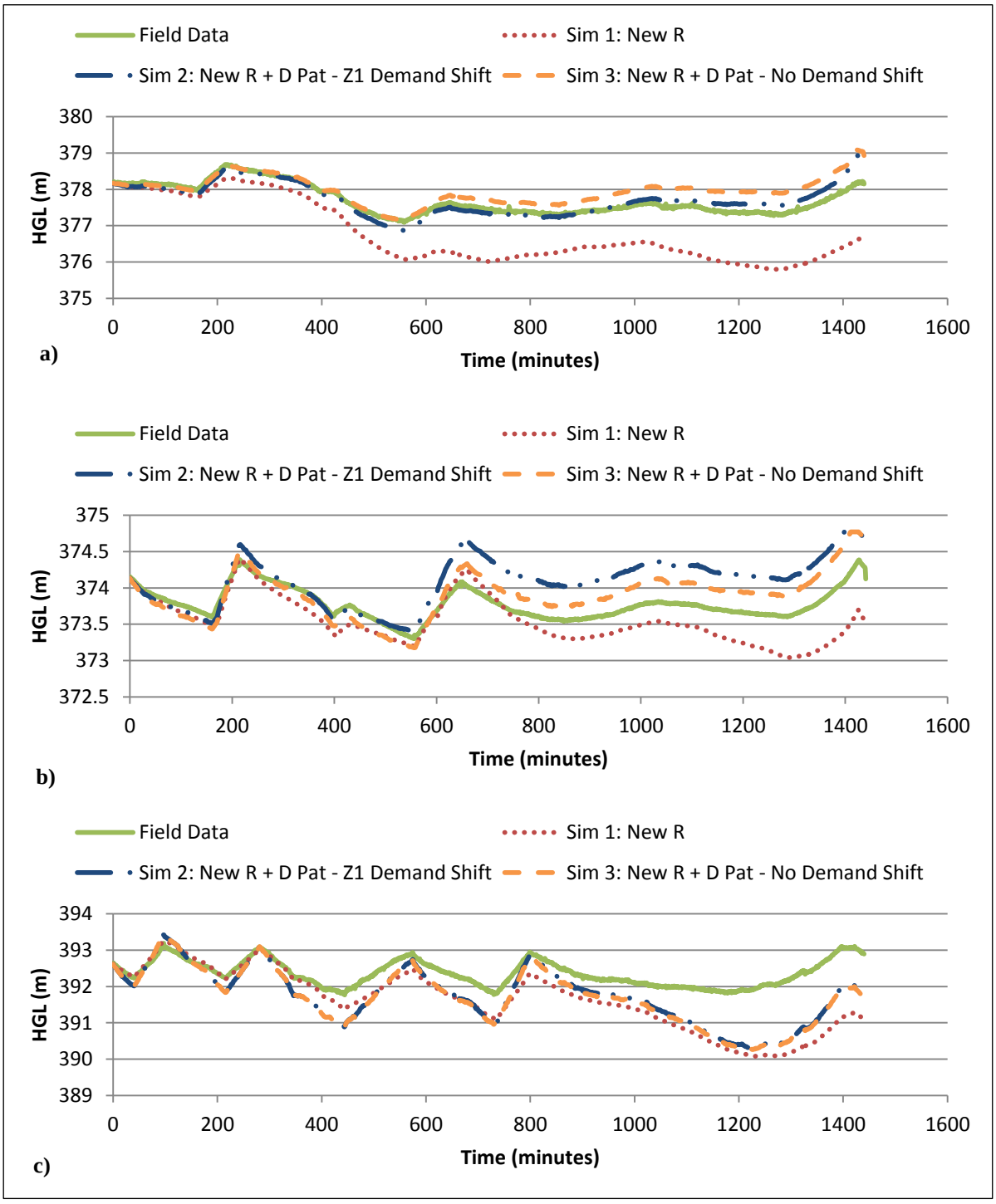

Figure 4.5: C (a), V (b), and S (c) tanks HGL time series for the manually calibrated 2010 model with adjusted control rules – zone 1 demand shift analysis

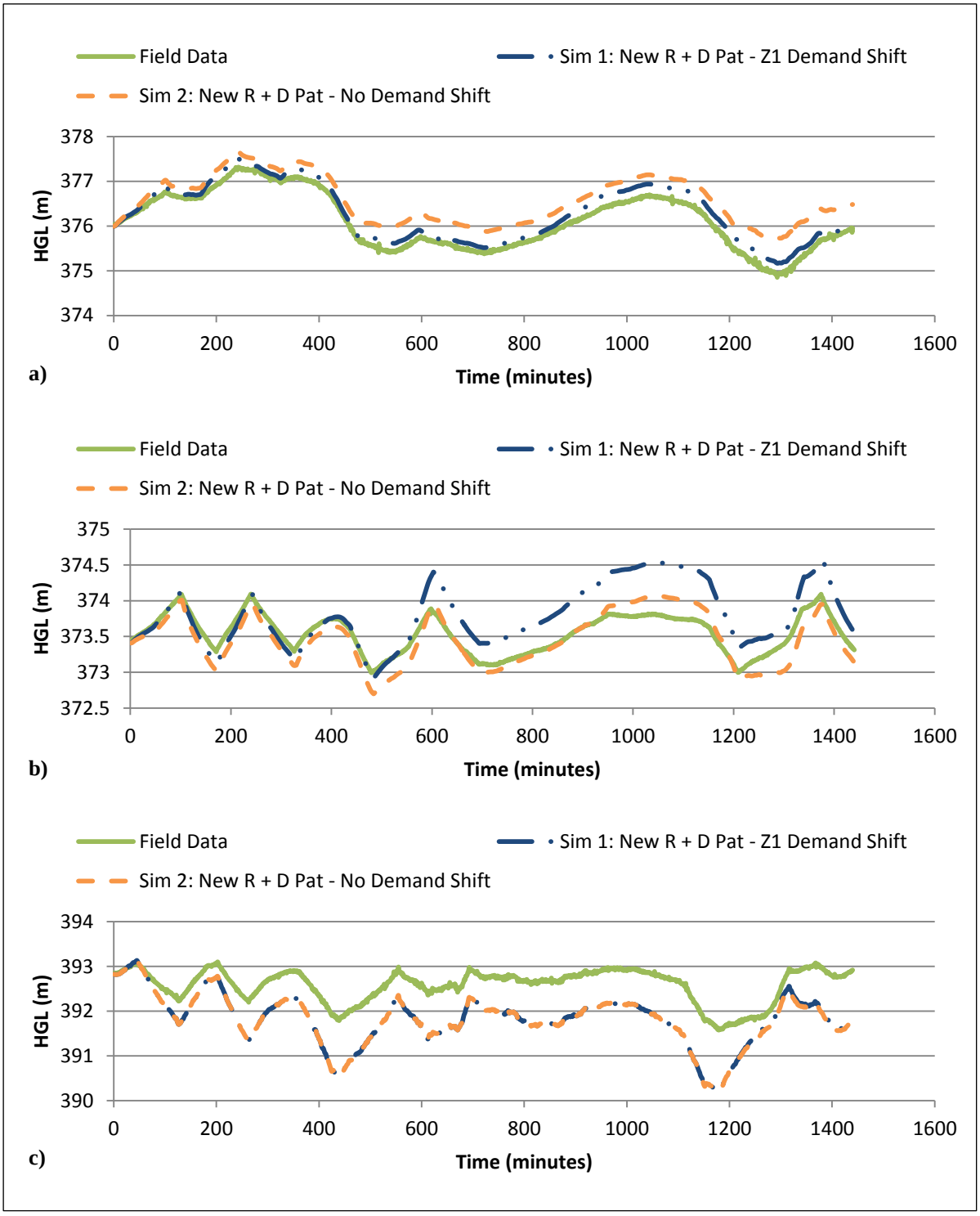

Figure 4.6: C (a), V (b), and S (c) tanks HGL time series for the manually calibrated 2011 model with adjusted control rules – zone 1 demand shift analysis

Water levels in tanks V and C indicate the need to model at least two unique diurnal demand curves per zone to more accurately capture differences in industrial, commercial and residential water usage throughout the network. The simulated water levels in each tank modeled without the zone 1 base demand shift implemented, are consistently less than observed conditions in the early morning hours (12 AM to approximately 9 AM), and higher than observed conditions throughout the rest of the day. This correlates with an overestimation of demands in the morning, and under estimation of demands in the evening. It is likely that the introduction of new demand patterns based on water users would bring the tank levels into much closer agreement with the observed conditions than any shift in base demands.

Since tank S operates in the upper pressure zone (zone 2), the simulated tank levels are relatively unaffected by the demand shift. It is clear, however that the base demands in close proximity to the tank S may be overestimated as evidenced by the fact that in both 2010 and 2011 simulations, tank S water levels are consistently lower than field conditions throughout the entire EPS. Therefore, a new shift in base demands within zone 2 is identified and analyzed in section 4.3.

4.3 Zone 2 Demand Shift Analysis

During model calibration, initial estimates of demand should be adjusted within reason to match field conditions, as it is never exactly known what may have occurred on a particular day (Walski et al. 2003). Since both selected calibration dates occur in the summer months, while the base demands are averaged from yearly customer demand data, it is possible that demands distributed near tank S are more susceptible to seasonal variation and the average base demands do not accurately capture the summer time network conditions. Therefore, the effect of shifting demands from nodes near tank S towards nodes further away in zone 2 was assessed.

When implementing any demand shift, it is important to respect the zonal water balance previously calculated in section 4.2. As such, demands could only be shifted within the upper pressure zone. Nodal demands within a 3.5 km radius of tank S were assumed to have the largest influence on water levels within the tank. Therefore, base demands of nodes located within a 3.5 km radius of tank S were shifted to nodal demands in the remainder of the upper zone, in accordance with equations (2.8) to (2.10) defined in chapter 2.2.2. The new demand shift applied to demands within zone 2 is depicted in figure 4.7.

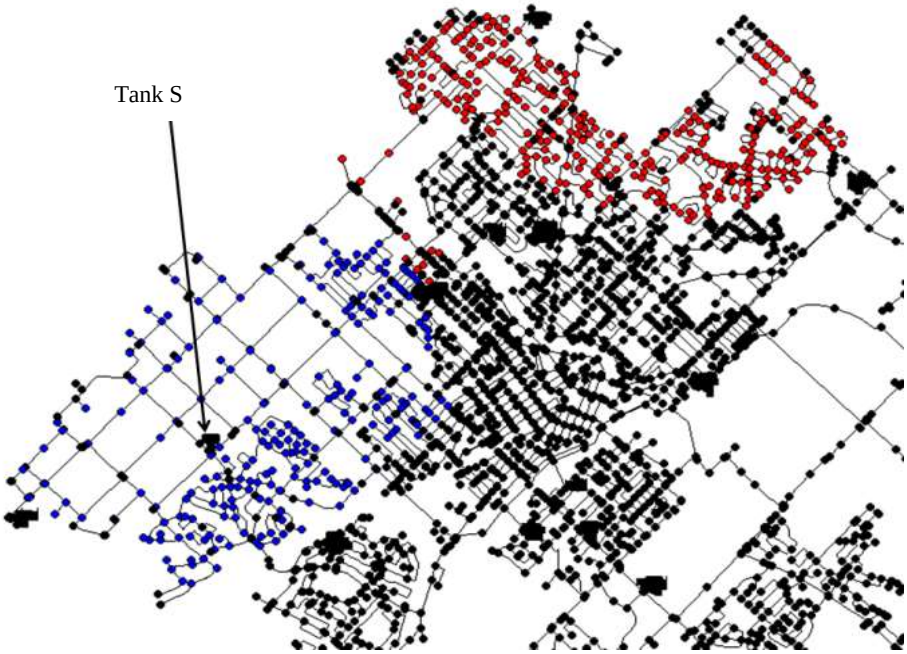

Figure 4.7: Zone 2 demand shift - decreasing base demands coloured blue; increasing demands coloured red

Using the manually calibrated C-factor settings with adjusted control rules and diurnal demand curves, network response to increasing the percentage of demand shifted was assessed. The demands were iteratively increased by 1 % using adjusted C++ code, and the network response was measured. Implementing a 6 % demand shift across demand nodes within zone 2 resulted in the greatest error reduction in simulated tank water levels in both the 2010 and 2011 network conditions. Simulated water levels in S tank are provided in figure 4.8. Since tanks V and C are located in zone 1, the demand shift in zone 2 had negligible effects on these tanks in the simulation. At this stage, the solution quality was very high in both the 2010 and 2011 objective spaces, and it was assumed that any additional improvements in solution quality would not be worth the investment in time.

An attempt was made to revert the updated time based control rules back to the original level based rules; however the solution quality degraded significantly. Since it was clear that the tank level based controls could not accurately capture the network conditions, the time based controls were re-applied and all manual calibration efforts were concluded.

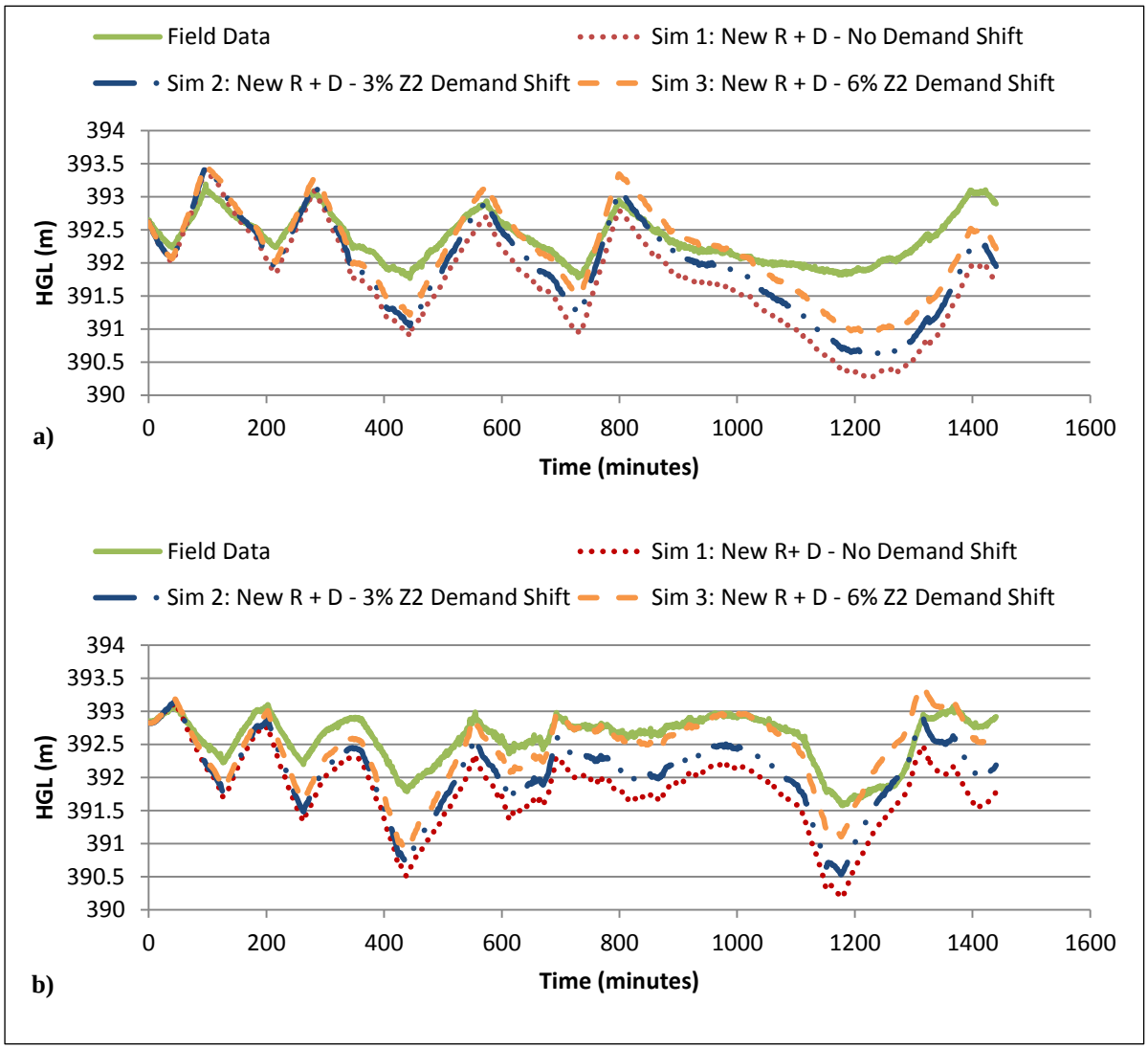

Figure 4.8: 2010 (a) and 2011 (b) simulated HGL time series of S tank for the manually calibrated model with adjusted control rules and diurnal demand curves – zone 2 demand shift analysis

4.4 Result Summary and Adjusted Micro-Calibration Problem Formulation

The water level based control rules were replaced by time based controls, and inaccurate model parameters describing diurnal demands were corrected. Following these model parameter adjustments, the shift in demands along zone 1 was identified as a compensating error that was initially deemed necessary due to the inaccurate modeling of pump operations. Moreover, it was noted that a shift in the demand allocations within zone 2 could significantly improve simulation result quality. Through an iterative trial and error search, a demand shift setting of 6 % was found to

generate robust and high quality simulation results in both the 2010 and 2011 objective spaces. In the 2010 objective space, the relative percent error objective function values are 3.0 %, 2.7 %, and 4.6 % for the tank level, flow rate and pressure errors, respectively. In the 2011 objective space, the relative percent error objective function values are 3.1 % and 3.9 %, for the tank levels and flow rate errors, respectively. Applying demand shifts greater than 9 % resulted in a significant degradation of solution quality.

At this stage, an attempt was made to revert the time based control rules back to the initial level based controls, however the solution quality deteriorated significantly and it was very clear that the tank level based controls did not adequately characterize the network. As such, the time based controls were re-applied, and it was deemed that there would be minimal benefit to continuing the calibration efforts manually.

Although this solution was only achieved from insights gained through the initial automated micro-calibration results, and automated tools were used to aid in the search for appropriate model adjustments, this result was still technically generated through a manual trial and error method. Moreover, the C-factor parameters were set in accordance with the C-factor settings implemented in Company Y's initial manual calibration efforts. Therefore, these model parameter settings are considered manually calibrated.

Chapter 5
Micro-Calibration Results of Manually Adjusted Model

In an effort to enhance the quality of the manually calibrated solution described in chapter 4, as well as quantify parameter uncertainty, six automated micro-calibration problems were formulated and solved. The 5 C-factor and 13 C-factor decision spaces described in chapter 2 were adjusted to replace the demand shift parameter within zone 1, with a demand shift along zone 2. During manual parameter adjustment it was noted that solutions with a zone 2 demand shift setting of greater than 9 % significantly reduced solution quality; therefore, this parameter was bounded from 0 to 10 %. Then, the 2010, 2011 and aggregate objective function formulations defined in chapter 2 were solved with the adjusted 5 and 13 C-factor decision spaces.

Despite manually adjusting the model WDN pump operations to match the observed field conditions using time based controls, the discharges at each pumping station can still vary as a function of C-factor settings and pressures within the network. Moreover, EPANET can alter pump settings in the simulation as it converges to a solution. Therefore simulated pump flow rates are still quite variable, and the automated calibration objectives still include the flow rate error minimization objective to account for this.

Results are compared to the manual macro-calibration solution identified in chapter 4, and presented in a similar manner as in chapter 3. Since the benefit of solving the aggregate problem has already been established, it is only briefly discussed in this chapter. Differences in solution quality achieved from calibrating the model with 5 C-factor parameters versus 13 C-factor parameters are analyzed using a series of trade off curves. Moreover, each solution's efficacy to both the 2010 and 2011 objective spaces was simultaneously assessed using the bi-objective function defined in chapter 3. Then, the data presented in the trade-off curves is summarized and presented in tabular form. In addition to the tradeoff curves, time series plots of zonal inflows/outflows and tank water levels are generated for one result from the automated calibration. These time series are compared to the observed inflows/outflows and tank water levels in the field. Finally, a methodology for reducing the non-dominated set of solutions to a more manageable number is presented, and a final set of potential model calibration solutions is identified for future use.

5.1 Trade-off Analysis

Since the benefit of applying an aggregate calibration has already been established in chapter 3, the tradeoffs depicted in this chapter are presented in a manner that demonstrates the difference in solution quality obtained from using the 5 C-factor vs the 13 C-factor decision space.

5.1.1 2010 Calibration – 5 C-factor vs 13 C-factor

The independent 2010 calibration problem was solved using both the 5 and 13 C-factor decision spaces. A total of 1667 non-dominated solutions were generated to the 2010 objective formulation problem solved in the 5 C-factor decision space, while 2250 solutions were generated when the problem was solved in the 13 C-factor decision space. All automatically generated solutions are presented in the 2010 objective space in figure 5.1. Moreover, the manually calibrated solution generated in chapter 4 is presented on the same figure to allow for a direct comparison of results. Afterwards, the same solutions are validated for 2011 network conditions, and the validation results in the 2011 objective space are presented in figure 5.2.

Analyzing the results presented in figure 5.1, it is clear that all automatically generated solutions perform well in the 2010 objective space regardless of the decision space used in the calibration formulation. However, the 5 C-factor solution set is much more clustered in the 2010 objective space, while the 13 C-factor solutions produce a much wider range of objective function values. The 5 C-factor solutions seem to perform marginally better in the flow rate objective; however the 13 C-factor solutions are of a much higher quality in the pressure objective. The improved pressure performance is expected since the C-factors directly impact head loss and pressures throughout the network. The validation results presented in figure 5.2 seem to indicate that neither solution set is more robust to different loading conditions than the other.

In the 2010 objective space, 133 and 276 solutions generated in the 5 and 13 C-factor decision spaces, respectively, dominate the manually calibrated solution; and no automated solutions are dominated by the manual calibration result. In the 2011 objective space, 681 and 895 solutions obtained in the 5 and 13 C-factor decision spaces, respectively, are dominated by the manual solution. Only one of the 2250 solutions generated in the 13 C-factor decision space dominates the manual solution in the 2011 objective space, and none of the 5 C-factor solutions dominate the manually calibrated solution. All automatically generated solutions neither dominate, nor are dominated by the manually calibrated solution in both objective spaces.

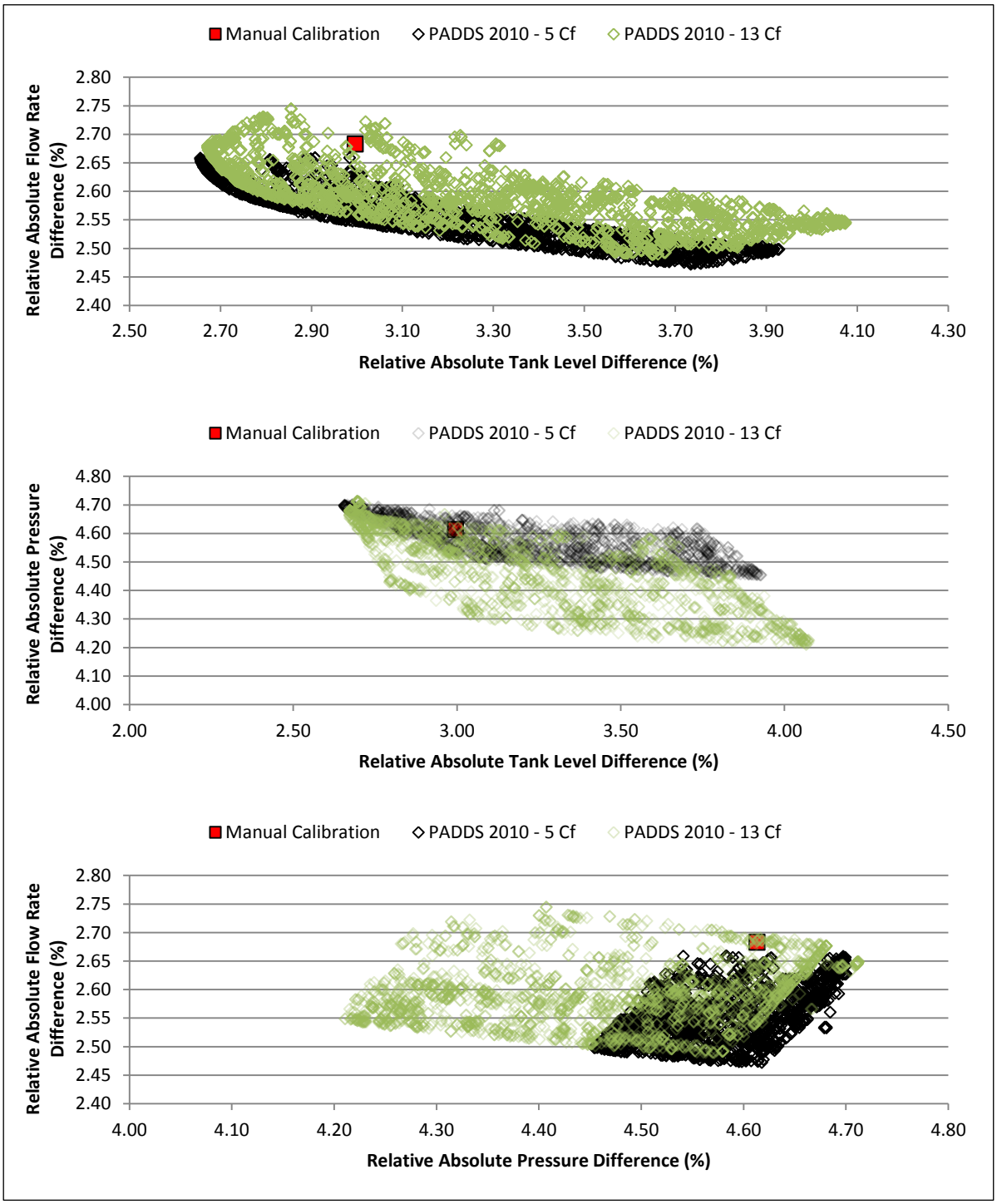

Figure 5.1: Non-dominated solutions from the 2010 5 C-factor and 13 C-factor decision space calibration formulations presented in the 2010 objective space

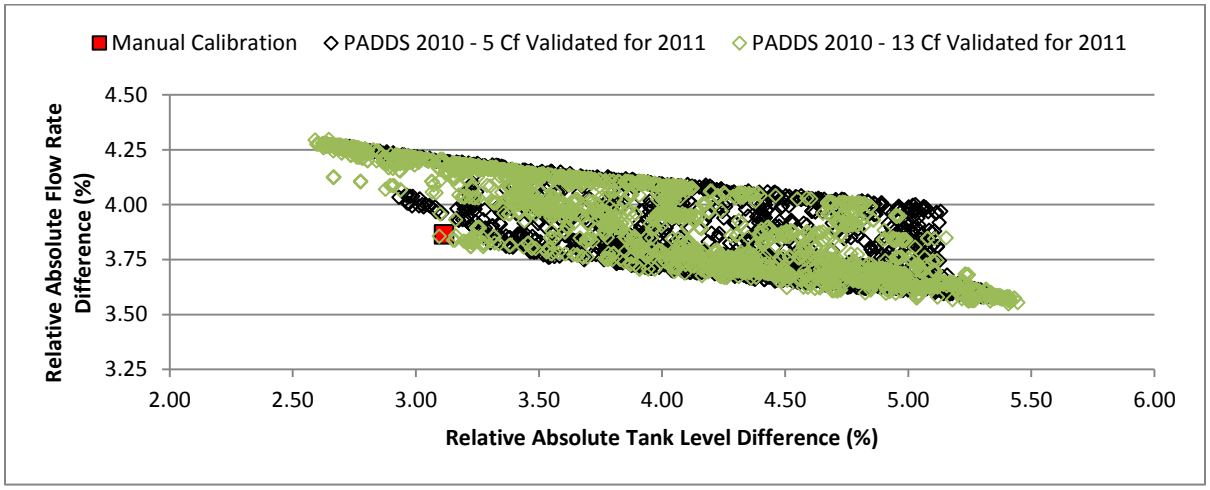

Figure 5.2: Non-dominated solutions from the 2010 5 C-factor and 13 C-factor decision space calibration formulations validated in the 2011 objective space

5.1.2 2011 Calibration: 5 C-factor vs 13 C-factor

The independent 2011 calibration problem was solved using both the 5 and 13 C-factor decision spaces. A total of 145 non-dominated solutions were generated to the 2011 objective formulation problem solved in the 5 C-factor decision space, while 132 solutions were generated when the problem was solved in the 13 C-factor decision space. All automatically generated results are compared to the manually calibrated solution from chapter 4 in figures 5.3 and 5.4.

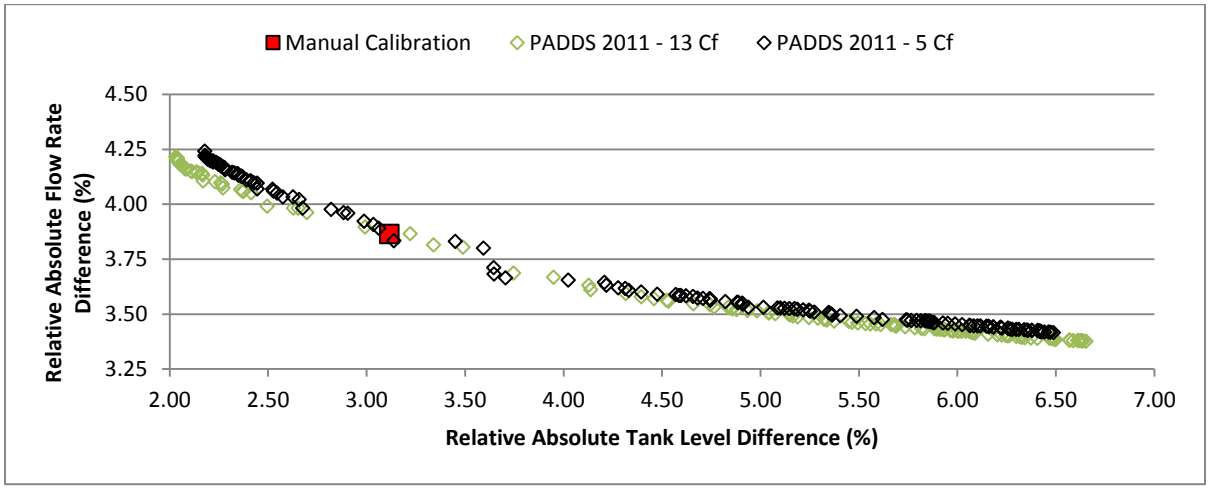

Figure 5.3: Non-dominated solutions from the 2011 5 C-factor and 13 C-factor decision space calibration formulations presented in the 2011 objective space

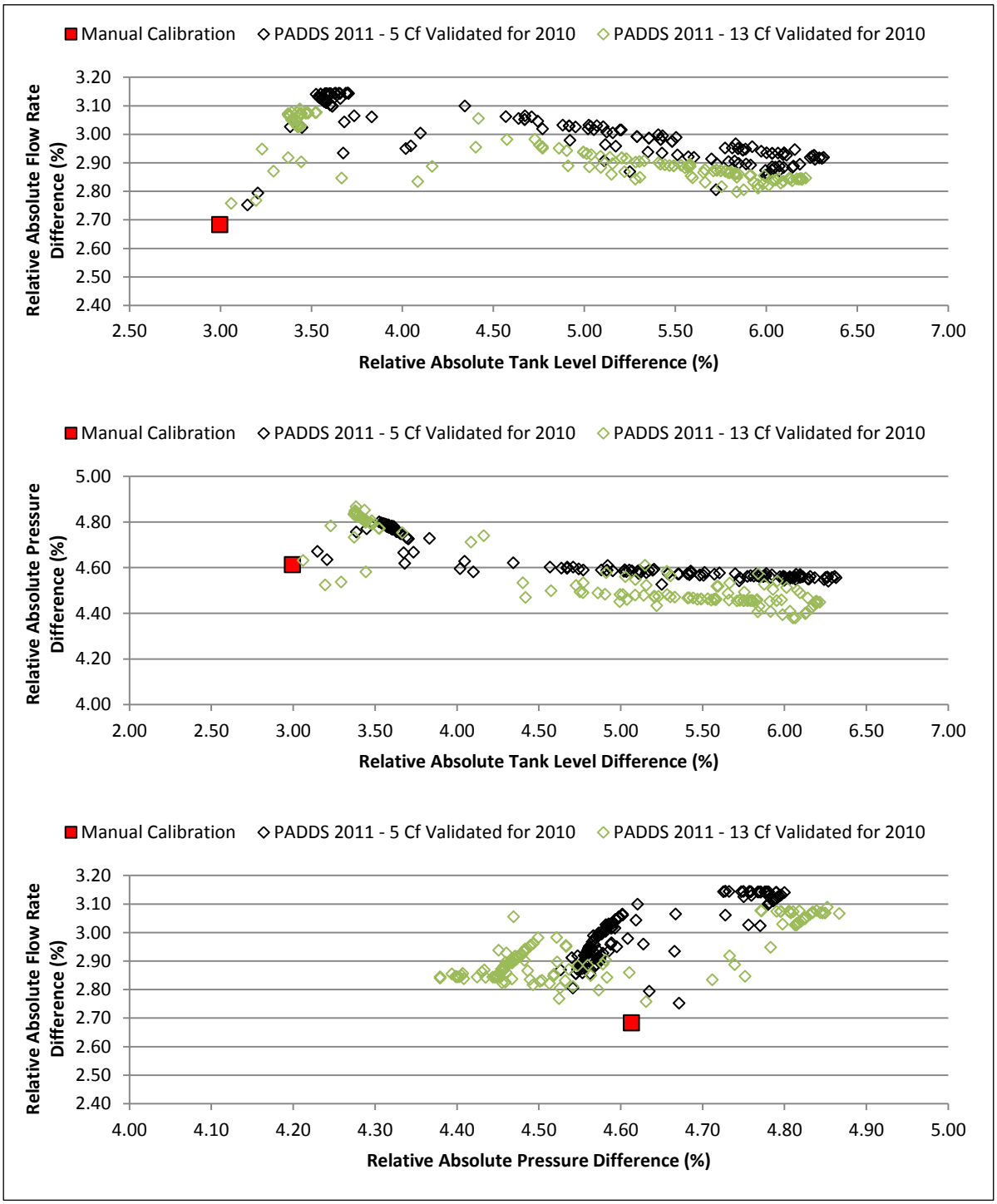

Figure 5.4: Non-dominated solutions from the 2011 5 C-factor and 13 C-factor decision space calibration formulations validated in the 2010 objective space

The calibration results are presented in the 2011 objective space in figure 5.3, while the validation results for the 2010 network conditions are presented in figure 5.4. Analyzing the results presented in figure 5.3, it is clear that the manually calibrated solution is located very near the pareto-front of the 2011 objective space. In fact, none of the automatically generated solutions dominate the manual result in the 2011 objective space.

It is also clear that the 13 C-factor solution set is mostly superior to the 5 C-factor solution set. In general, a network model is most sensitive to changes in C-factor settings when the network is stressed (i.e. demands are high) (Ormsbee and Lingireddy 1997; Walski et al. 2003). Since the 2011 network demands are approximately 10 % greater than the 2010 demand conditions, it is possible that the 2011 model is more responsive to changes in C-factor settings. This may explain why describing the 2011 network conditions using 13 C-factor settings leads to a more accurate representation of the real network than only using 5 C-factor settings. Of course, any increase in performance in the 2011 conditions could simply be the result of compensating errors and over-calibration to one set of model loading conditions. Therefore, it is necessary to examine the validation results and ensure that perceived improvements in the 2011 objective space do not lead to a loss of quality in the 2010 objective space.

The validation results depicted in figure 5.4 indicate that neither solution set performs particularly well in the 2010 objective space. However, the 13 C-factor solutions are slightly more robust to simulations in the 2010 network conditions than the 5 C-factor solutions. It is clear that the using 13 C-factor parameters to describe the 2011 network conditions does not lead to a reduction in model robustness. In fact, the quality of the validation results is actually greater when the calibration problem is solved in the 13 C-factor decision space.

In the micro-calibration results presented in chapter 3, it was evident that the independent 2011 calibration results were of lesser quality than the independent 2010 calibration results. Walski (2008) reported that the quality of any calibration results are limited by the quantity and quality of the field data collected. As such, it was posited that the difference in result quality could be attributed to the fact that the 2011 model is only calibrated to observed tank water levels and flow rates, while the 2010 network conditions are calibrated to observed tank levels, flows and pressure data within the network. This could not be validated given the fact that the 2011 loading conditions were not accurately set in the micro calibration analysis presented in chapter 3. Therefore, upon adjustment of

the 2011 WDN model parameters, the micro-calibration analysis was repeated in an effort to verify this assumption.

Similar to the results obtained in chapter 3, solutions generated from independently calibrating to the corrected 2011 network conditions are generally less robust than those generated from solving the 2010 network calibration problem. Moreover, none of the solutions generated from solving the 2011 problem dominate the manual solution in the 2011 objective space. This can be partially attributed to the fact that the 2011 calibration objective values associated with the manually calibrated solution are very near the pareto-front. However, since several solutions generated from solving the independent 2010 and aggregate calibration problems dominate the manual result in the 2011 objective space, it is clear that solving the independent 2011 calibration problem is less effective than solving the independent 2010 or aggregate calibration problems. This could be caused by the difference in structure of the objective formulations (bi vs tri-objective), or not calibrating to pressures within the network in addition to the tank levels and flow rate information. Based on evidence from the literature review (Walski et al. 2008), it is assumed that the missing pressure data is the main contributing factor to the deterioration of the results; however this was not conclusively validated due to time constraints. This could be validated by solving 2 bi-objective 2010 calibration problems, the first combining pressure and tank level errors into one objective, and another which omits the pressure errors entirely. The differences in solution quality could be used to isolate the source of the problem.

5.1.3 Aggregate Calibration: 5 C-factor vs. 13 C-factor

A total of 1380 and 1618 non-dominated solutions were generated to the aggregate calibration problem solved using the 5 and 13 C-factor decision spaces, respectively. All automatically generated solutions are presented in the 2010 objective space in figure 5.5. Additionally, the manually calibrated solution generated in chapter 4 is presented on the same figure. The same solutions were validated for the 2011 network conditions, and the validation results in the 2011 objective space are presented in figure 5.6.

Regarding the efficacy of results generated from solving the aggregate calibration in the 5 and 13 C-factor decision spaces, the conclusions are very similar to those established from analyzing the results to the independent 2010 and 2011 calibration problems. In the 2010 objective space, the 13 C-factor solutions performed better than the 5 C-factor solution set in the pressure objective; however this increased pressure objective performance is associated with a decreased performance in the flow

rate objective. In the 2011 objective space, the 13 C-factor results were superior to the 5 C-factor results.

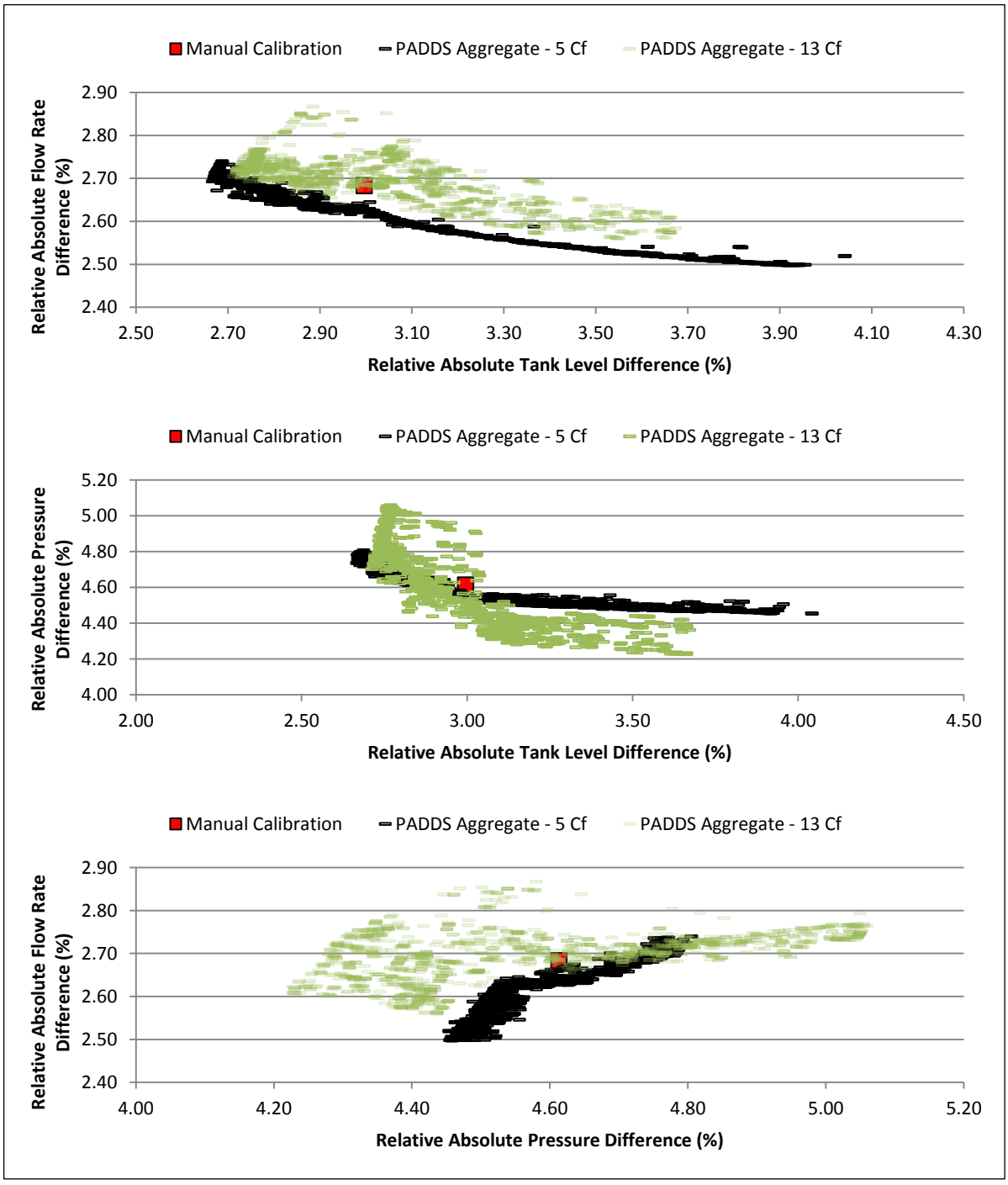

Figure 5.5: Non-dominated solutions of the aggregate 5 C-factor and 13 C-factor decision space calibration formulations presented in the 2010 Objective Space

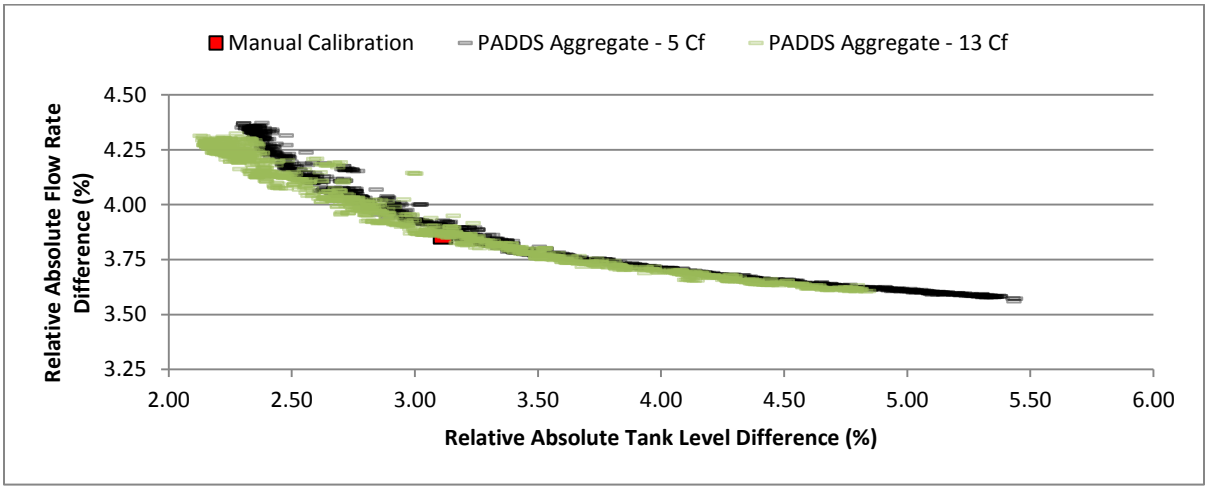

Figure 5.6: Non-dominated solutions of the aggregate 5 C-factor and 13 C-factor decision space calibration formulations presented in the 2011 Objective Space

In the 2010 objective space, 226 and 12 solutions to the aggregate calibration problem solved in the 5 and 13 C-factor decision spaces, respectively, dominate the manual solution. In the 2011 objective space, none of the 5 C-factor solutions, and only 10 solutions generated in the 13 C-factor decision space dominate the manual solution. The manually calibrated solution neither dominates, nor is dominated by any of the automatically generated solutions in both objective spaces. Clearly the manually calibrated model, which was generated using the results obtained from the initial micro-calibration analysis, is very near the approximate pareto-front, particularly in the 2011 objective space.

5.1.4 Bi-Objective Trade-off Analysis

In order to assess each solution's quality in the 2010 and 2011 network conditions simultaneously, the objective functions associated with all calibration results were re-formulated using the bi-objective function formulation defined in chapter 3. All 2010 and 2011 calibration objectives were equally weighted and collapsed into two single objective functions representing the overall solution quality in the 2010 and 2011 objective spaces, respectively. In this new objective function formulation, all dominated results within each solution set were removed, and the remaining non-dominated results from each calibration problem are presented in figure 5.7. The remaining non-dominated solutions are comprised of a total of 46 and 43 solutions in the 5 and 13 C-factor decision spaces, respectively. These results are plotted in the bi-objective space in figure 5.7.

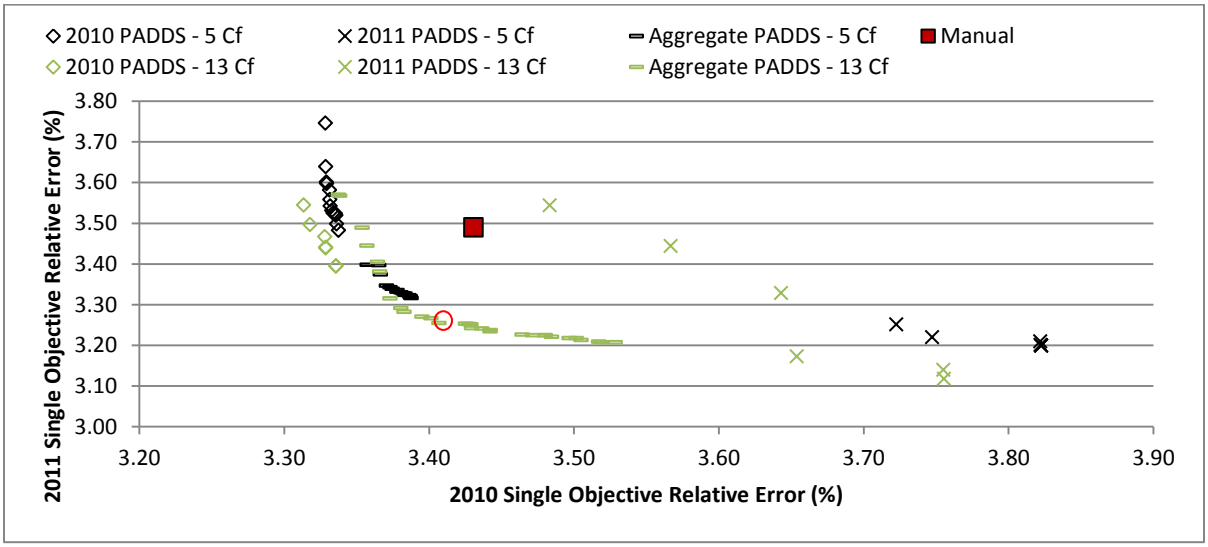

Figure 5.7: 2010 vs 2011 bi-objective analysis of non-dominated solutions from the 2010, 2011 and aggregate calibration formulations in the 5 and 13 C-factor decision spaces (solution circled in red selected for time series analysis)

In the bi-objective formulation, the 13 C-factor solutions generally outperform the 5 C-factor results from each calibration problem. In fact, the non-dominated 13 C-factor solutions to the 2010, and 2011 independent calibration problems dominate the corresponding 5 C-factor solution sets entirely. Moreover, only 3 of the 30 results to the aggregate calibration solved in the 13 C-factor decision space are dominated by solutions in the 5 C-factor set. Whereas 14 of the 24 results in the 5 C-factor solution set are dominated by solutions in the 13 C-factor solution set. This verifies the previous observations that solutions obtained in the 13 C-factor space generate significant improvements in the pressure objective at the cost of marginal losses in the flow rate objective. If the three objectives describing simulation errors in the 2010 objective space were weighted differently as they were collapsed into a single objective, then the 13 C-factor solution set may not be as dominant.

The solution with the lowest collective average of 2010 and 2011 simulation errors was selected for time series analysis of zonal inflows and outflow as well as simulated tank levels. The analysis is completed in section 5.2.

5.1.5 Trade-off Summary Statistics

A significant number of non-dominated solutions were generated in each automated calibration problem solved. Due to the sheer number of solutions generated and the presentation of the tri-

objective surface using a series of two dimensional plots, it difficult to assess how well each solution set performs relative to each other from the graphical analysis alone. Therefore, for each calibration problem solved in both the 5 and 13 C-factor decision spaces, both solution sets were quantitatively compared against each other to identify the number of dominated results in each solution set. The number of 5 C-factor solutions dominated by results from the 13 C-factor solution set, and vice versa is presented in table 5.1.

Table 5.1: 5 C-factor vs. 13 C-factor solution set comparison for 2010, 2011 and aggregate objective function formulations

Objective Formulation	2010		2011		Aggregate	
Decision Space	5 C-factor	13 C-factor	5 C-factor	13 C-factor	5 C-factor	13 C-factor
Solutions Generated	1667	2250	145	132	1379	1618
Number of Solutions Dominated in 2010 Objective Space by Solution Set from Alternate Decision Space	474	229	144	101	841	1113
Number of Solutions Dominated in 2011 Objective Space by Solution set from Alternate Decision Space	1636	2214	135	3	1369	1446
Number of Solutions Dominated in 2010 and 2011 Objective Spaces by Solution set from Alternate Decision Space	446	229	134	1	831	974
Number of Solutions Non-Dominated by alternate Decision Space Solution Set in at Least One Objective Space	1193	2021	10	129	548	644

In general, there is little difference between the quality of results generated in the 5 and 13 C-factor decision spaces. The only exception is in the solutions generated to the 2011 calibration problem. As discussed in section 5.1.2, it is likely that the increased demands in the 2011 network conditions result in an increased sensitivity to the C-factor parameter settings. In conditions of increased demands it seems that using the 13 C-factor decision space to characterize network conditions can

lead to higher quality simulations. This should be validated using additional field data results collected during peak demands or fire flows.

5.2 Time Series Analysis

The automatically generated solution with the lowest average relative percent error in both the 2010 and 2011 objective spaces was selected for additional analysis. The time series of observed and simulated zonal inflows/outflows as well as tank levels within zones 1 and 2 are all provided on the same figures. The 2010 and 2011 results are presented in figures 5.8 and 5.9, respectively.

The simulation results for the selected model parameters have greatly improved upon the initial manually calibrated solution, presented in chapter 3.2. The relative percent errors associated of the manual solution provided by Company Y, simulated under 2010 loading conditions, were 3.0 %, 9.8 %, and 4.8 % for the tank levels, pump flow rates, and pressure observations, respectively. The simulated errors in the 2010 network conditions for the automatically generated solution presented in this section are 2.8 %, 2.8 %, and 4.6 % for the same observations, respectively. Clearly, the results have greatly improved in the quantified optimization objectives and the automated result presented dominates the original manual solution. This correlates to a significant improvement in the graphical time series of simulated tank levels and pump flow rates. The simulated values are much more aligned with observed field conditions. However, as previously mentioned in chapter 4, it is quite clear that a single demand pattern multiplier for each zone is not sufficient to accurately capture the demand conditions within the network. As such, all automatically generated micro-calibration results suffer from this limitation, and any objective improvements are limited by the macro-calibration settings. When compared to the manual result in chapter 4, the automated result neither dominates, nor is dominated by the manually calibrated solution.

The automated solution presented in this section is just one of several thousand unique automatically generated solutions to this problem. Due to the nature of micro-calibration analysis, the objective function values of all results are not drastically different from one another, and the vast majority of automatically calibrated results are very similar in quality to this solution. However, even though the objective function values and simulation results are similar, the parameter values associated with each solution are very different. The wide range of different parameter values in all automatically generated results represents the significant uncertainty in the micro-calibration parameters.

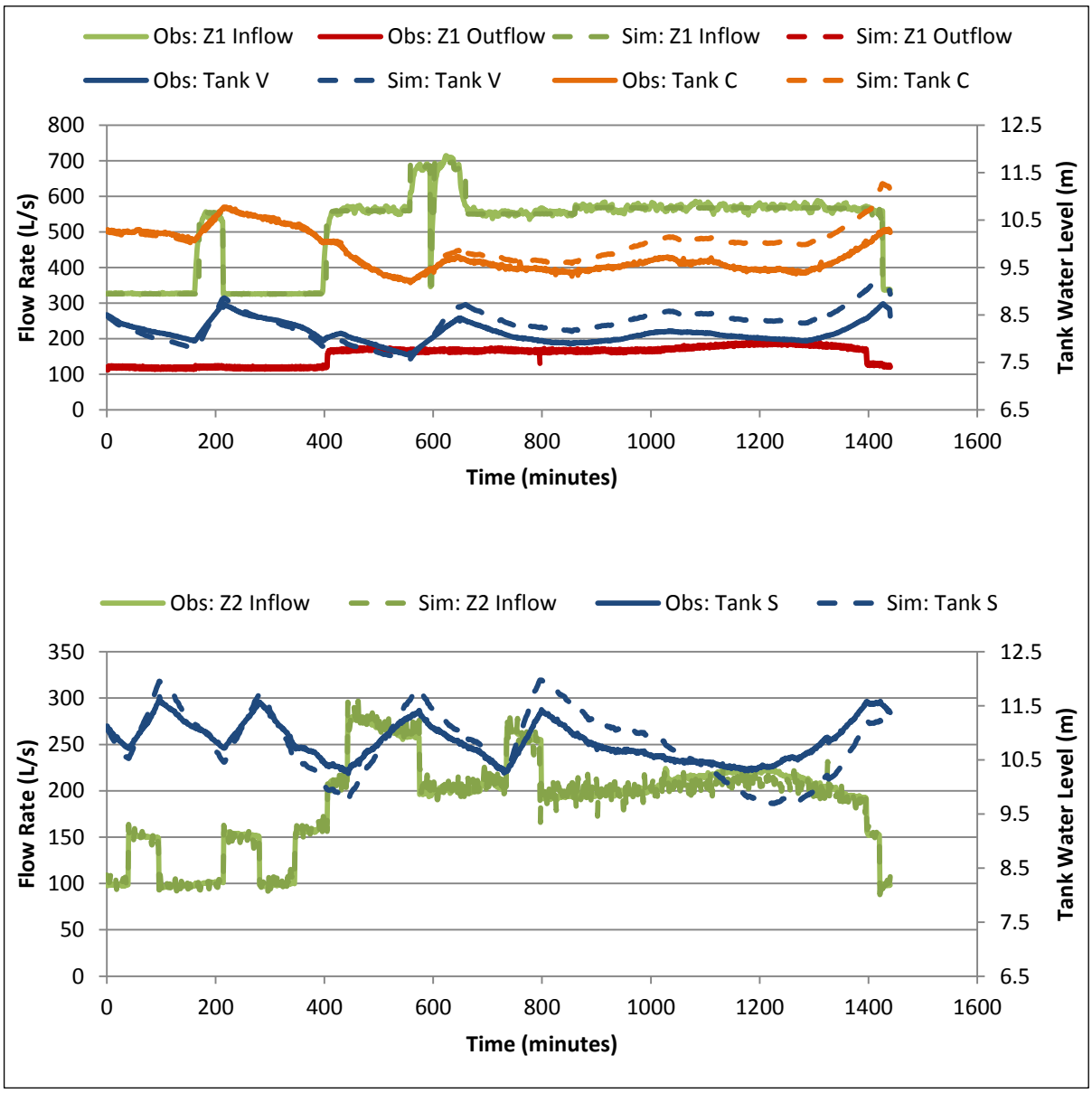

Figure 5.8: Zonal inflow/outflow and tank water level time series of observed field data vs. an automatically generated solution simulated in 2010 network conditions

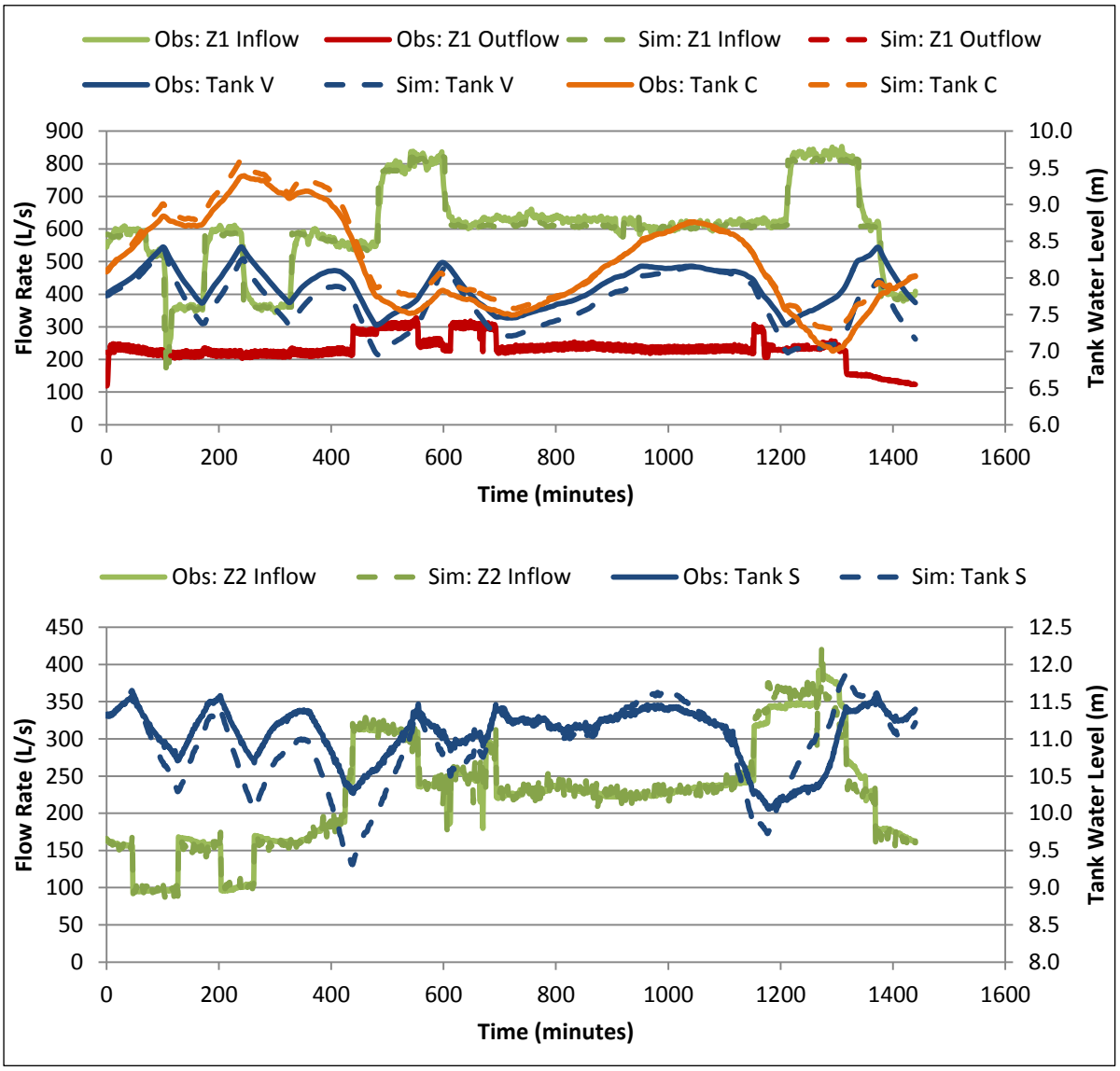

Figure 5.9: Zonal inflow/outflow and tank water level time series of observed field data vs. an automatically generated solution simulated in 2011 network conditions

5.3 Final Solution Set

The goal of any calibration exercise is to identify potential model parameter values that can produce high quality simulation data under multiple loading conditions. Clearly, using automated calibration tools is a very effective method of generating a large set of robust solutions. Unfortunately, given the limited quantity of field data used in this calibration exercise, the uncertainty in the model parameter settings is quite large, and several thousand unique non-dominated solutions are identified by the

PADDS algorithm. This solution set must be reduced to a more manageable number in order to allow for any meaningful hydraulic analyses.

When narrowing the number of solutions generated, it is most important to ensure that all models identified in the reduced solution set describe the real network conditions accurately enough for decision makers to rely on the simulated model results; "The true test of model calibration is that the end user … of the model results feels comfortable using the model to assist in decision-making" (Walski et al. 2003). Since, Company Y's manually calibrated model was considered effective enough to aid in operational analyses; this solution will act as the lower bound for any acceptable designs. Only the subset of solutions that are non-dominated by the original manually calibrated model are considered for inclusion in the final solution set. Unfortunately, this does not help narrow the number of solutions down since all of the automatically generated solutions in this chapter are non-dominated by the initial manual calibration solution.

Since all results generated are of sufficient quality for decision makers, the number of solutions representing model uncertainty was filtered using the results from the bi-objective analysis completed in section 5.1.4. All 2010 and 2011 objective function values were equally weighted and collapsed into two single objective function values. The single objective values corresponding to all solutions generated were calculated, and all dominated solutions within each solution set were removed. This greatly reduced the number of solutions considered for analysis.

The remaining 89 non-dominated solutions from all six calibration problems solved were used to approximate the bi-objective pareto-front in both the 5 and 13 C-factor decision spaces. Although the independent 2010 and 2011 calibration results are not as robust as the aggregate solutions, the validation results of each calibration problem are still non-dominated by the initial manually calibrated solution. Therefore, these solutions can still be relied upon by decision makers. Moreover, including the independent calibration results ensures that the pareto-front generated is wide enough to capture the full range of uncertainty in model parameter values.

A total of 46 and 43 solutions in the 5 and 13 C-factor decision spaces, respectively, were included in the final solution set. The minimum, maximum, mean and standard deviation of each parameter within the 5 and 13 C-factor results comprising the final solution set are presented in tables 5.2 and 5.3, respectively.

Table 5.2: Final solution set - parameter variability and summary statistics of the 46 unique solutions generated in the 5 C-factor decision space

Paramater	Minimum	Maximum	Average	Standard Deviation
CI <150 mm (-)	57.0	68.0	62.9	4.6
CI>150 mm (-)	58.0	94.0	88.8	11.8
DI (-)	116.0	127.3	118.3	2.7
PVC (-)	130.0	138.9	131.2	2.1
Hyprotec (-)	135.0	147.6	136.1	2.8
Demand Shift (%)	6.1	9.0	7.73	0.76

The parameters in the 5 C-factor decision space are much less variable than the 13 C-factor parameter values. This is expected, since uncertainty in parameter settings is generally associated with an increase in the number of parameters (Mallick et al. 2002). Using only 5 C-factors implicitly limits the range of effective parameter settings; however describing the network using only 5 C-factors may limit the solution quality in extreme demand conditions, as discussed in section 5.1.2. In both the 5 and 13 C-factor decision spaces, the most variable parameter values are generally the cast iron pipes groups within the network. The demand shift parameter is consistently in the range of approximately 5 and 9 %. This clearly shows that demands near S tank are overestimated as the most robust solutions consistently implement a demand shift of at least 5 %. This demand shift was assumed from a very limited knowledge of the network and although it is effective in both the 2010 and 2011 loading conditions, the shift must be validated by practitioners familiar with the system. Moreover, additional field data in zone 2 must be collected to identify the cause of this demand shift (i.e. leak in the network, differences in summer water usage, etc.)

The parameter values and objective function values associated with this reduced solution set are provided in Appendix A. The remaining automatically generated solutions are not included in this report, but they have been archived for future use. Since the entire solution set is archived, any decision maker can easily generate a different set of reduced solutions based on their own weighting of the initial tri and bi-objective values describing errors in the 2010 and 2011 network conditions.

Table 5.3: Final solution set - parameter variability and summary statistics of the 43 unique solutions generated in the 13 C-factor decision space

Parameter	Minimum	Maximum	Average	Standard Deviation
CI: New (<15 years old) (-)	83.0	138.0	113.8	9.8
CI: 15 - 44 Years Old < 100 mm (-)	41.0	100.0	74.0	16.7
CI: 15 - 44 Years Old >100 mm <=200 mm (-)	57.1	105.3	80.5	13.2
CI: 15 - 44 Years Old >=250 mm <=400 mm (-)	61.5	112.0	109.6	8.2
CI: 45-80 Years Old < 100 mm (-)	30.0	65.1	38.2	8.9
CI: 45-80 Years Old >100 mm <=200 mm (-)	39.0	79.0	59.1	14.9
CI: 45-80 Years Old >=250 mm <=350 mm (-)	48.0	85.0	61.9	16.0
CI: 45-80 Years Old >=400 mm <=600 mm (-)	66.1	92.0	89.5	6.9
CI: > 80 Years Old >=25 mm <=100 mm (-)	21.0	52.3	28.0	10.1
CI: > 80 Years Old >=150 mm <=300 mm (-)	30.6	78.0	56.9	11.9
DI (-)	116.0	132.3	118.8	3.1
PVC (-)	140.0	149.2	141.2	1.7
Hyprotec (-)	135.0	153.4	137.2	4.1
Demand Shift (%)	5.1	8.9	7.4	0.9

5.4 Results Summary

The manually calibrated solution generated in chapter 4 was found to be very near the approximate pareto-front of the 2010 and 2011 objective spaces. Clearly, a manual calibration effort guided by results from automated calibration tools can lead to a very high quality solution. However, given the limited quantity of available field data, and the identifiability issues inherent to real world calibration problems, the uncertainty in the calibrated model parameters is very high. Therefore, even if a single high quality solution is manually generated, it is improbable that this solution can be used to

accurately simulate various loading conditions. To account for this, the uncertainty in the model parameters must be quantified through the generation of a large set of feasible model parameter values.

In order to quantify parameter uncertainty, six calibration problem formulations were solved using the PADDS optimization algorithm, and several thousand unique calibration results were generated. The quality of all solutions describing the network in the 5 C-factor decision space were directly compared to the solutions describing the network in the 13 C-factor decision space. In the 2010 objective space, the 13 C-factor solutions generally improve model performance in the pressure objective; however this improvement coincides with a slight degradation in the flow error minimization objective. Describing the model using 13 C-factor parameter settings results in a much wider range of solutions in the objective space, whereas the 5 C-factor solutions are much more clustered. In the 2011 objective space, the 13 C-factor results consistently improve model performance relative to the 5 C-factor solutions. This is likely a function of the increased demands on the 2011 calibration date. Moreover, while describing the model using 13 C-factors can lead to more accurate simulation results in some cases, the 13 C-factor solution sets contain greater parameter uncertainty than the corresponding 5 C-factor solution sets.

Since neither the 5 C-factor, nor the 13 C-factor decision space was consistently more effective at describing model conditions, all automatically generated solutions were analyzed and only the most robust solutions generated in both decision spaces comprise the final solution set. Robust solutions were identified through a bi-objective trade-off analysis of simulation performance in the 2010 network conditions relative to the performance in the 2011 conditions. A total of 46 and 43 solutions from 5 and 13 C-factor decision spaces, respectively, were identified as the most robust solutions. In addition to robustness, these solutions were selected to span a wide range of the bi-objective tradeoff surface in an effort to capture and quantify the uncertainty in the model parameter settings.

The most uncertain model parameters in both decision spaces were the cast iron C-factor settings. This is expected given the large number of cast iron pipes of varying ages and diameters within the network. Moreover, the uncertainty in this parameter is increased due to the fact that cast iron pipes are most susceptible to the non-linear corrosion and tuberculation effects. The most robust results were achieved with demand shift parameter settings ranging from 5 to 9 percent. Without having full knowledge of system conditions and a clear understanding of the original leakage assessment, it is difficult to justify this shift in demands. However, since applying the demand shift produces the

highest quality simulation results in both the independent and aggregate calibration problems, it is clear that in the existing macro-calibrated network conditions, the demands near S tank are over estimated.

Since the nodal demands were generated from averaged yearly customer information, while both calibration dates were specifically selected to be during summer months, it is possible that the demand shift could be related to variances in summer and winter usage. Moreover, the demand shift could be indicative of a leak in the network in pressure zone 2. It is unclear what the source could be, but it is important to investigate this demand shift in the field. Even though the demand shift in zone 2 appears necessary in this desktop modeling study, it must be validated in the field to ensure that the shift is not simply another compensating error introduced into the network.

Chapter 6
Conclusions and Recommendations

Manual WDN micro-calibration approaches are quite tedious, and prone to compensating errors. Moreover, a traditional manual approach will not effectively quantify the uncertainty in calibrated model parameters. To account for this, several automated tools have been developed and used in research settings, but they are much less used in practice. Company Y attempted to use one of these automated tools (the built-in InfoWater calibrator tool) in their calibration effort of City X's WDN model. However, the algorithm failed to identify any solutions to the network, even after technical support was provided by InfoWater software developers. Thus, Company Y resorted to a manual calibration effort to identify a high quality solution which was subsequently used in operational analyses.

The same calibration problem was resolved automatically using the PADDS optimization algorithm and several solutions were generated. However, these solutions only marginally improved upon the quality of the initial manually calibrated result. In order to achieve greater improvements in the model simulations, the results obtained from the automated micro-calibration efforts were used to guide a manual macro-calibration of model parameters. This led to significant improvement in the WDN model simulation quality. Moreover, the assumed demand shift within zone 1 was identified as inaccurate and a manifestation of compensating errors in Company Y's manual calibration efforts. An alternate shift in demands along zone 2 was analyzed, and it seemed to produce high quality results during initial manual analysis.

In order to validate the proposed zone 2 demand shift, as well as quantify parameter uncertainty, the adjusted model was re-calibrated using the automated calibration tools. Several thousand unique solutions of similar quality were identified. This solution set was reduced to 89 unique and robust solutions describing model parameter uncertainty. The initial manually calibrated model provided by Company Y is dominated by 75 of these solutions.

In all 89 solutions, a demand shift along zone 2 of at least 5 % was implemented. This indicates that initial demand estimates in zone 2 are slightly inaccurate, and must be verified in the field. This demand shift may be related to initial leakage allocation assessments, and as described in section 2.3.1, it is recommended that leakage allocation is re-assessed and applied to areas within the network that are more likely to exhibit leakage (Walski et al. 2003). Moreover, since the cast iron pipe C-

factor settings are very uncertain, it is suggested that additional C-factor tests are conducted on several cast iron pipes within the network. The results generated seem to be very robust and of high quality, however any perceived improvements must be validated and justified by practitioners who are familiar with the system. It is recommended that experienced modelers review the final set of solutions and ensure that all model parameter settings identified could feasibly represent the real network conditions.

This research would not have been possible without the significant work and effort put forth by the practitioners who initially calibrated the model. Barring the 2011 simulation results, which were likely adjusted a posteriori and not reverted to the original calibrated settings, it is clear that the initial calibration effort resulted in a high quality and robust solution. That said, the use of automated tools coupled with a manual macro-calibration effort is a very effective and efficient way of improving solution quality, identifying errors, and quantifying uncertainty in calibration parameters. The PADDS algorithm's applicability to WDN calibration problems was clearly demonstrated as the algorithm generated several robust and high quality solutions to a problem in which other optimization algorithms failed. Generating a range of solutions for more experienced practitioners to validate and analyze is a key feature of this research.

Ideally more flow and pressure data should be collected at various locations and peak demand times (e.g. fire flow analysis) within the network. The data can be used in a meaningful assessment of the difference in simulation quality between models describing network C-factors using 5 parameters, and those that use 13 parameters. Moreover, the field data can be used to identify some invalid solutions in the final solution set generated, and reduce model uncertainty. Until then, it is recommended that decision makers apply decisions that are robust to as many of the potential solutions as possible.

To achieve robust solutions, it is recommended that any future calibration exercises are formulated to balance model efficacy across multiple loading conditions (e.g. 2010 vs 2011). This is similar to the bi-objective analyses presented in sections 3.1.3 and 5.1.4, where the cumulative errors in both 2010 and 2011 loading conditions were compared against one another. This calibration framework can be easily adjusted to include additional calibration data and model loading conditions.

In order to reduce uncertainty and the potential for compensating errors in all future calibrations of model C-factor and demand parameter settings, pump and valve operations should be modeled using time-based control rules. Additionally, it is recommended that the City officials or engineers at

Company Y calibrate the SCADA instrumentation associated with pump operations, as it is clear that the level-based pump control rules provided by the network operators do not match the observed conditions. This may simply be a typographical error by the operators, or it could be a systematic issue relating to the instrumentation. In any event, the effects of pumping controls are very apparent in the model simulations and it is crucial that any future control rules input into the model are accurate representations of the real network conditions.

Finally, it is recommended that more data regarding water usage in the network is collected. This data is required to establish additional diurnal curves capturing differences between industrial, commercial and residential water usage rates in the network. Implementing these additional curves would greatly improve simulation quality.

Whittemore (2001) stated that "Model efficacy depends heavily on experience and, in this sense, can be described as an art. While model formulation is more related to science, calibration has aspects more related to art. Good calibrations are more than curve fitting exercises that simply align model simulations with constituent behavior". It is clear that automated methods cannot replace the judgement of an experienced practitioner, and engineering judgment must be applied to any calibration procedure. One cannot simply rely on automated tools to generate robust solution sets. Automated calibration procedures are simply tools, which when intelligently applied by experienced practitioners can generate robust solutions in an efficient manner. If the correct tools are applied, and the calibration problem is well formulated, automated approaches can greatly reduce calibration time and effort and significantly increase solution quality.

Appendix A

Calibration Parameters for Final Solution Set

5 C-Factor Solutions:

Solution Set	Model Parameter Setting						2010 Objective Values			2011 Objective Values	
	CI <150 mm (-)	CI>150 mm (-)	DI (-)	PVC (-)	HYP (-)	Demaand Shift (%)	Cumulative Tank Errors (m)	Cumulative Flow Rate Errors (l/s)	Cumulative Pressure Errors (m)	Cumulative Tank Errors (m)	Cumulative Flow Rate Errors (l/s)
Independent 2010 Calibration Problem Solutions	68.0	94.0	116.0	130.0	135.0	7.56	1101.0	29829.8	52711.9	1057.0	61511.1
	68.0	94.0	116.0	130.1	135.0	7.42	1101.7	29778.3	52687.8	1094.3	61220.0
	68.0	94.0	116.0	136.4	135.3	7.18	1101.8	29777.9	52700.9	1068.9	61529.0
	67.3	94.0	116.0	131.7	135.0	7.30	1102.0	29755.5	52691.3	1096.6	61190.2
	67.6	94.0	116.0	134.5	135.0	7.18	1102.0	29748.2	52694.3	1097.0	61238.8
	68.0	94.0	116.0	131.4	135.0	7.29	1102.1	29741.6	52650.4	1099.3	61185.6
	68.0	94.0	116.0	130.0	135.0	7.29	1102.5	29722.0	52628.2	1105.9	61134.4
	68.0	94.0	116.0	130.1	135.0	7.17	1103.4	29679.0	52608.5	1115.4	61084.0
	67.6	94.0	116.0	131.4	135.0	6.97	1104.3	29642.3	52610.5	1130.6	60992.9
	67.1	94.0	116.0	132.4	135.0	6.77	1106.4	29580.3	52614.0	1152.0	60873.6
	68.0	94.0	116.0	131.4	135.0	6.70	1107.7	29544.0	52542.5	1166.8	60772.4
	68.0	94.0	116.0	131.4	136.0	6.70	1108.1	29542.5	52527.1	1170.2	60771.2
	68.0	94.0	116.0	130.0	135.0	6.70	1108.7	29517.2	52520.1	1204.1	60621.3
	67.6	94.0	116.0	130.0	147.5	6.20	1121.7	29397.6	52281.6	1295.5	60320.9

Independent 2011 Calibration Problem Solutions	57.0	58.0	117.6	130.0	135.0	9.00	1461.4	35237.1	53863.3	852.7	61186.8
	57.0	58.0	117.6	130.0	135.0	8.80	1466.6	35143.9	53816.6	852.8	60918.7
	57.0	58.0	117.6	130.0	135.0	8.70	1469.7	35100.4	53793.5	853.4	60836.7
	57.0	58.0	117.6	130.0	135.0	8.70	1469.7	35100.4	53793.5	853.8	60831.9
	57.0	62.4	117.6	130.0	135.0	7.90	1429.4	33922.8	53529.7	893.1	59973.7
	57.0	64.5	121.8	130.0	137.3	8.70	1403.0	33961.2	53369.3	935.8	59308.3
	63.9	75.4	127.3	138.9	147.6	6.30	1329.0	31349.7	52010.6	1169.4	56584.3
	58.8	78.2	127.3	136.7	136.2	6.10	1305.0	30879.2	52418.6	1187.8	56389.5
Aggregate Calibration Problem Solutions	57.8	94.0	117.3	130.0	135.0	8.50	1115.1	30228.2	53479.4	932.3	61613.6
	57.0	94.0	117.7	130.0	135.0	8.50	1117.9	30236.6	53522.0	931.1	61414.8
	57.0	94.0	117.7	130.0	135.0	8.50	1117.9	30236.6	53522.0	931.1	61414.8
	57.0	94.0	117.8	130.0	135.6	8.50	1118.7	30229.3	53505.6	934.2	61375.0
	60.4	94.0	117.3	130.0	135.0	8.40	1114.5	30179.6	53251.1	944.0	61533.3
	58.1	94.0	118.2	130.0	135.0	8.40	1120.7	30188.9	53372.8	942.4	61159.2
	57.0	94.0	118.5	130.0	135.0	8.40	1122.6	30196.8	53448.6	940.1	61012.6
	60.4	94.0	118.2	130.0	135.0	8.40	1120.7	30182.1	53187.5	951.7	61162.1
	57.8	94.0	118.3	130.5	135.0	8.20	1119.7	30130.0	53360.9	956.3	60823.3
	64.9	94.0	116.0	135.9	135.7	8.10	1105.4	30222.3	53144.2	969.8	62253.0
	59.7	94.0	118.5	130.0	135.0	8.30	1121.7	30149.6	53200.8	953.4	60976.9
	66.6	94.0	117.3	130.0	135.0	8.40	1114.1	30238.3	52930.0	969.4	61615.9
	60.3	94.0	118.2	130.0	135.0	8.20	1118.8	30107.4	53156.0	964.6	60880.4
	61.5	94.0	118.2	130.0	135.0	8.20	1119.0	30105.6	53067.9	968.3	60873.1
	58.8	94.0	119.7	130.0	135.3	8.20	1129.0	30120.6	53167.5	965.3	60423.9
	57.8	94.0	119.9	130.5	135.0	8.20	1130.6	30130.6	53251.6	963.3	60371.3
	62.7	94.0	117.1	130.0	135.0	7.90	1109.4	29980.2	53005.7	1001.3	61128.2
	61.7	94.0	120.5	130.0	135.3	8.00	1132.7	30032.5	52854.9	989.8	60032.1

65.0	94.0	119.2	131.7	138.9	7.40	1124.6	29829.9	52593.0	1058.0	60027.6
65.0	94.0	119.2	131.7	140.0	7.40	1125.1	29819.0	52544.0	1061.9	60017.2
67.5	94.0	121.3	134.2	135.3	7.20	1136.4	29783.3	52367.1	1063.6	59258.4
68.0	94.0	119.5	131.4	142.5	7.40	1127.9	29804.1	52322.0	1076.5	59918.9
67.8	94.0	122.5	131.9	135.0	7.20	1144.1	29747.2	52244.1	1076.8	58768.4
68.0	94.0	123.1	131.9	135.3	7.20	1147.8	29750.7	52192.0	1081.2	58572.6

13 C-Factor Solutions:

Solution Set	DV Setting														2010 Objective Values			2011 Objective Values	
	CI: New (<15 years old) (-)	CI: 15 - 44 Years Old < 100 mm (-)	CI: 15 - 44 Years Old >100 mm <=200 mm (-)	CI: 15 - 44 Years Old >=250 mm <=400 mm (-)	CI: 45-80 Years Old < 100 mm (-)	CI: 45-80 Years Old >100 mm <=200 mm (-)	CI: 45-80 Years Old >=250 mm <=350 mm (-)	CI: 45-80 Years Old >=400 mm <=600 mm (-)	CI: > 80 Years Old >=25 mm <=100 mm (-)	CI: > 80 Years Old >=150 mm <=300 mm (-)	DI (-)	PVC (-)	Hyp (-)	Demand Shift (%)	Tank Level Errors (m)	Flow Rate Errors (l/s)	Pressure Errors (m)	Tank Errors (m)	Flow Rate Errors (l/s)
Independent 2010 Calibration Problem Solutions	102.3	100.0	87.4	112.0	65.1	78.1	53.7	92.0	21.0	64.9	116.0	149.2	135.7	7.09	1143.2	30522.3	50559.2	1056.3	61097.7
	122.2	44.9	100.0	108.8	47.9	79.0	48.0	92.0	49.1	78.0	116.3	141.5	142.7	7.19	1158.2	30637.8	49694.2	1088.8	60747.7
	136.1	55.9	101.7	112.0	58.5	79.0	48.0	92.0	35.3	60.8	117.0	141.9	138.0	6.46	1165.9	30403.3	49577.7	1149.1	59909.8
	122.2	41.0	105.3	112.0	46.9	78.5	48.0	92.0	51.3	78.0	120.1	140.7	145.6	7.54	1183.6	30795.8	49456.0	1043.1	59506.7
	122.2	71.7	105.3	112.0	46.9	78.5	48.0	92.0	51.3	78.0	120.1	140.7	145.6	7.54	1183.7	30796.2	49455.7	1043.1	59500.8
	122.2	44.9	105.3	112.0	46.9	78.5	48.0	92.0	51.3	78.0	120.1	140.7	145.6	7.13	1183.8	30631.9	49376.8	1086.2	59190.5
	122.2	56.1	105.3	112.0	46.9	78.5	48.0	92.0	51.3	78.0	120.1	140.7	145.6	7.13	1183.8	30628.4	49376.6	1086.2	59232.6
Independent	83.0	56.7	91.9	112.0	30.0	39.0	48.7	66.1	22.5	58.8	118.5	140.0	135.0	8.90	1405.2	34237.1	54142.2	803.4	60333.6

2010 Calibration Problem Solutions	87.5	56.7	90.2	112.0	30.0	39.0	48.7	66.1	22.5	76.1	118.5	140.0	135.0	8.50	1419.2	33960.0	54028.0	835.0	59817.9
	101.4	77.3	68.5	112.0	30.0	39.1	49.5	75.9	39.4	62.8	122.0	140.0	135.0	8.20	1338.9	33085.0	53671.1	888.8	58782.9
	134.8	88.0	89.9	112.0	36.1	53.0	51.2	69.6	22.1	56.5	123.5	144.2	135.0	7.00	1427.7	32573.2	51412.5	1055.2	57149.5
	116.1	76.8	59.3	93.8	47.6	53.1	50.1	77.9	52.3	68.5	129.0	143.0	153.4	7.30	1364.9	32208.7	50908.8	1171.0	56212.0
	99.5	96.7	57.1	61.5	60.6	60.0	70.6	90.4	23.9	72.0	132.3	143.2	137.2	5.10	1268.5	30948.1	51966.6	1260.8	55770.5
Aggregate Calibration Problem Solutions	112.2	98.5	86.1	112.0	30.0	39.0	85.0	92.0	21.0	50.5	118.1	140.3	135.0	7.40	1148.8	31063.2	56621.3	839.2	61609.8
	112.2	99.4	87.4	112.0	30.0	39.0	85.0	92.0	21.0	50.5	118.1	140.3	135.0	7.04	1146.2	30863.4	56501.2	846.3	61391.0
	120.3	79.4	96.1	111.8	31.5	39.0	80.6	92.0	22.3	48.0	118.1	140.0	135.0	7.17	1151.9	31051.9	56213.3	843.3	61459.2
	112.2	99.4	74.0	112.0	30.0	41.9	85.0	92.0	21.0	50.5	118.1	140.3	135.0	7.40	1146.4	30966.0	55987.6	843.9	61583.3
	115.5	92.1	98.7	111.6	30.0	41.6	85.0	92.0	21.0	51.7	118.1	140.7	135.0	7.40	1145.4	30946.1	55761.2	847.1	61603.7
	115.5	92.1	84.9	111.6	30.0	41.6	85.0	92.0	21.0	51.7	118.1	140.7	135.0	7.40	1145.7	30960.4	55896.8	846.6	61621.1
	112.2	99.4	74.0	112.0	30.0	44.4	85.0	92.0	21.0	50.5	118.1	140.3	135.0	7.40	1144.0	30898.1	55437.2	857.0	61347.5
	113.0	69.3	91.5	112.0	30.0	49.4	83.5	92.0	21.0	52.7	117.7	140.0	135.0	7.30	1136.9	30648.9	54255.8	871.0	61417.5
	112.2	99.4	74.0	112.0	30.0	44.3	85.0	92.0	21.0	54.9	118.1	140.3	135.0	7.40	1142.6	30800.4	55426.1	860.5	61314.4
	112.2	99.4	74.0	112.0	30.0	44.3	85.0	92.0	21.0	54.9	118.1	140.3	135.0	7.40	1142.6	30800.4	55426.1	860.5	61314.4
	113.0	69.3	91.5	112.0	30.0	49.4	69.3	92.0	25.8	35.0	117.7	140.0	135.0	7.30	1164.8	31472.4	53613.0	853.6	61629.1
	112.2	99.4	73.0	112.0	30.0	44.9	77.3	92.0	21.0	62.4	118.1	140.3	135.0	7.40	1148.3	30838.7	54927.9	867.7	61052.8
	116.5	81.9	74.0	112.0	30.0	55.3	81.6	92.0	21.0	48.0	118.1	140.9	135.0	7.40	1141.3	30698.6	53707.4	879.5	61428.9
	112.0	64.2	70.0	111.0	37.7	55.1	48.8	92.0	25.0	61.6	116.7	141.1	135.0	8.67	1185.4	31954.3	51384.5	861.1	62070.0
	112.0	64.2	70.0	111.0	37.7	55.1	48.8	92.0	25.0	61.6	116.9	141.1	135.0	8.67	1186.4	31953.3	51369.3	858.2	61913.8
	112.0	64.2	70.0	111.0	42.0	55.1	48.8	92.0	25.0	61.6	116.9	141.1	135.0	8.67	1185.4	31927.5	51355.9	865.8	61929.3
	117.3	76.1	78.2	108.5	31.1	68.6	83.7	92.0	32.8	48.0	116.9	140.0	135.0	7.06	1124.4	30345.2	52761.8	924.6	61561.9
	112.0	64.2	70.0	111.0	42.0	61.5	48.8	92.0	25.0	61.6	116.9	141.1	135.0	8.67	1178.9	31772.2	51000.8	875.5	61633.9
	112.0	64.2	70.0	111.0	42.0	65.6	48.8	92.0	25.0	61.6	116.9	141.1	135.0	8.82	1177.4	31750.3	50876.0	882.5	61709.1
	112.0	64.2	70.0	111.0	42.0	65.6	48.8	92.0	25.0	61.6	116.9	141.1	135.0	8.67	1175.5	31634.4	50837.7	887.5	61648.1
	112.0	59.2	70.0	112.0	42.0	77.3	48.8	92.0	25.0	59.3	116.9	140.9	135.0	8.82	1169.6	31501.6	50634.8	902.6	61689.9

	113.7	64.2	70.0	112.0	34.8	53.1	48.8	92.0	21.0	48.0	119.3	141.1	138.1	8.17	1205.8	31965.7	51269.9	887.0	60614.4
	112.0	64.2	70.0	112.0	34.8	53.1	48.8	92.0	28.5	48.0	119.3	141.1	138.1	8.17	1206.1	31965.1	51259.3	889.4	60609.4
	114.1	76.1	73.4	108.5	34.3	70.1	59.6	92.0	22.3	48.0	119.2	140.0	135.5	7.50	1167.0	30918.0	51367.7	931.3	60374.3
	114.1	69.5	73.4	108.5	34.3	70.1	72.9	92.0	22.3	48.0	119.2	140.0	135.5	6.35	1149.2	30213.5	51982.5	1023.7	59829.4
	112.0	78.6	70.0	112.0	42.0	76.3	48.8	92.0	25.0	30.6	116.9	141.1	138.1	6.48	1174.3	31166.3	50303.8	1017.9	60711.2
	138.0	71.2	78.9	98.3	36.4	79.0	79.8	92.0	27.7	32.4	117.8	146.0	135.5	5.05	1138.5	30217.9	51972.2	1055.8	60469.0
	112.0	64.2	70.0	112.0	42.0	76.3	48.8	92.0	25.0	48.0	116.9	142.9	138.1	6.48	1169.6	30595.8	50120.2	1170.5	59777.0
	112.0	64.2	70.0	112.0	42.0	76.3	48.8	92.0	25.0	48.0	116.9	141.1	138.1	6.48	1170.2	30573.1	50099.8	1173.7	59743.6
	112.0	65.4	70.0	112.0	42.0	76.3	48.8	92.0	25.0	48.0	121.8	141.1	138.1	6.48	1200.2	30605.3	49808.0	1156.6	58034.9

Bibliography

ADS. (2009). "ADS PrimeLog User Manual." *Rep. No. QR 775015 A0,* ADS LLC, 4940 Research Drive, Huntsville, Alabama 35805.

Asadzadeh, M., Tolson, B., and McKillop, R. (2011). "A Two Stage Optimization Approach for Calibrating Water Distribution Systems." American Society of Civil Engineers, 1682-1694.

Asadzadeh, M., and Tolson, B. (2013). "Pareto archived dynamically dimensioned search with hypervolume-based selection for multi-objective optimization." *Engineering Optimization,* 45(12), 1489-1509.

Asadzadeh, M., and Tolson, B. A. (2009). "A New Multi-objective Algorithm, Pareto Archived DDS." *Proceedings of the 11th Annual Conference Companion on Genetic and Evolutionary Computation Conference: Late Breaking Papers,* ACM, New York, NY, USA, 1963-1966.

Balut, A., and Urbaniak, A. (2011). "Management of water pipeline networks supported by hydraulic models and information systems." *Carpathian Control Conference (ICCC), 2011 12th International,* 16-21.

Bentley Systems. (2004). "SCADA.Model Integration: The Rules for Success." .

Bhave, P. (1988). "Calibrating Water Distribution Network Models." *J.Environ.Eng.,* 114(1), 120-136.

Company Y Consultants. (2011). "City X Water Distribution System Calibration Study." .

de Schaetzen, W., Hung, J., Clark, S., Gottfred, C., Acosta, B., and Reynolds, P. (2011). "How Much Is "Your Un-Calibrated Model" Costing Your Utility? Ten Lessons Learned from Calibrating the CRD Water Model." American Society of Civil Engineers, 1053-1065.

Dini, M., and Tabesh, M. (2014). "A New Method for Simultaneous Calibration of Demand Pattern and Hazen-Williams Coefficients in Water Distribution Systems." *Water Resour.Manage.,* 28(7), 2021-2034.

Engineering Computer Applications Committee. (1999). "Calibration Guidelines for Water Distribution System Modeling." *American Water Works Association ImTech Conference,* .

Giustolisi, O., Berardi, L., Laucelli, D., Savic, D., Walski, T., and Brunone, B. (2014). "Battle of Background Leakage Assessment for Water Networks (BBLAWN) at WDSA Conference 2014." *Procedia Engineering,* 89(0), 4-12.

Innovyze. (2015). "InfoWater." .

International Organization for Standardization. (2015). "*ISO International Standard ISO/IEC 14882:2014(E) – Programming Language C++*." https://isocpp.org/std/the-standard (November 21, 2015).

Jamasb, M., Tabesh, M., and Rahimi, M. (2009). "Calibration of EPANET Using Genetic Algorithm." American Society of Civil Engineers, 1-9.

James, W., and Shahzad, A. (2003). "Water Distribution Losses Caused by Encrustation and Biofouling: Theoretical Study Applied to Walkerton, ON." *Bridges*, 10(40685), 142.

Lamont, P. A. (1981). "Common pipe flow formulas compared with the theory of roughness." *Journal (American Water Works Association)*, 274-280.

Lansey, K., and Basnet, C. (1991). "Parameter Estimation for Water Distribution Networks." *J.Water Resour.Plann.Manage.*, 117(1), 126-144.

Lansey, K., El-Shorbagy, W., Ahmed, I., Araujo, J., and Haan, C. (2001). "Calibration Assessment and Data Collection for Water Distribution Networks." *J.Hydraul.Eng.*, 127(4), 270-279.

Liggett, J., and Chen, L. (1994). "Inverse Transient Analysis in Pipe Networks." *J.Hydraul.Eng.*, 120(8), 934-955.

Lingireddy, S., and Ormsbee, L. (1999). "Optimal Network Calibration Model Based on Genetic Algorithms." American Society of Civil Engineers, 1-8.

Mala-Jetmarova, H., Schwarz, S., Barton, A., Le Roux, S., Smalley, P., and Gerke, S. (2011). "Development of hydraulic models for a complex and large scale water distribution system in regional Australia." *Proceedings of the MODSIM, International Congress on Modelling and Simulation*, .

Mallick, K. N., Ahmed, I., Tickle, K. S., and Lansey, K. E. (2002). "Determining pipe groupings for water distribution networks." *J.Water Resour.Plann.Manage.*, 128(2), 130-139.

Marchi, A., Salomons, E., Ostfeld, A., Kapelan, Z., Simpson, A. R., Zecchin, A. C., Maier, H. R., Wu, Z. Y., Elsayed, S. M., and Song, Y. (2013). "Battle of the water networks II." *J.Water Resour.Plann.Manage.*, 140(7), 04014009.

Mays, L. W. (2010). *Water Resources Engineering.* John Wiley \& Sons, .

Microsoft. (2015). "Visual Studio 2013." .

Muranho, J., Ferreira, A., Sousa, J., Gomes, A., and Marques, A. S. (2015). "Convergence issues in the EPANET solver." *Procedia Engineering*, 119 700-709.

Ormsbee, L. E., and Lingireddy, S. (1997). "Calibration of hydraulic network models." *Journal AWWA*, 89(2), 42-50.

Ormsbee, L. (1989). "Implicit Network Calibration." *J.Water Resour.Plann.Manage.*, 115(2), 243-257.

Ormsbee, L., and Wood, D. (1986). "Explicit Pipe Network Calibration." *J.Water Resour.Plann.Manage.*, 112(2), 166-182.

Ostfeld, A., Salomons, E., Ormsbee, L., Uber, J. G., Bros, C. M., Kalungi, P., Burd, R., Zazula-Coetzee, B., Belrain, T., Kang, D., Lansey, K., Shen, H., McBean, E., Wu, Z. Y., Walski, T., Alvisi, S., Franchini, M., Johnson, J. P., Barkdoll, B. D., Ghimire, S. R., Koppel, T., Vassiljev, A., Kim, J. H., Yoo, D. G., Chung, G., Diao, K., Zhou, Y., Li, J., Liu, Z., Chang, K., Gao, J., Qu, S., Yuan, Y., Prasad, T. D., Laucelli, D., Berardi, L., Giustolisi, O., Lyroudia Vamvakeridou, L. S., Kapelan, Z., Savic, D., Barbaro, G., Asadzadeh, M., Tolson, B. A., and McKillop, R. (2012). "Battle of the water calibration networks." *J.Water Resour.Plann.Manage.*, 138(5), 523-532.

Paluszczyszyn, D., Skworcow, P., and Ulanicki, B. (2015). "Modelling and Simulation of Water Distribution Systems with Quantised State System Methods." *Procedia Engineering*, 119 554-563.

Puust, R., and Vassiljev, A. (2014). "Real Water Network Comparative Calibration Studies Considering the Whole Process from Engineer's Perspective." *Procedia Engineering*, 89 702-709.

Reddy, P., Sridharan, K., and Rao, P. (1996). "WLS Method for Parameter Estimation in Water Distribution Networks." *J.Water Resour.Plann.Manage.*, 122(3), 157-164.

Region of Waterloo. (2011). "Residential Water Softener Performance Study." *Rep. No. 950174*, Waterloo.

Renzetti, S., and Dupont, D. (2013). "Buried Treasure: The Economics of Leak Detection and Water Loss Prevention in Ontario." *Rep. No. ESRC-2013-001*, Environmental Sustainability Research Centre, St. Catharines, Ontario, Canada, L2S 3A1.

Rossman, L. A. (2000). "EPANET 2 Users Manual, US Environmental Protection Agency." *Water Supply and Water Resources Division, National Risk Management Research Laboratory, Cincinnati, OH*, 45268.

Rossman, L. A. (1999). "The epanet programmer's toolkit for analysis of water distribution systems." *ASCE 29th Annual Water Resources Planning and Management Conference*, 39-48.

Savic, D. A., and Walters, G. A. (1995). "Genetic algorithm techniques for calibrating network models." *Report*, 95 12.

Savic, D. A., Kapelan, Z. S., and Jonkergouw, P. M. R. (2009). "Quo vadis water distribution model calibration?" *Urban Water Journal*, 6(1), 3-22.

Shamir, U. (1974). "Optimal Design and Operation of Water Distribution Systems." *Water Resour.Res.*, 10(1), 27-36.

Tabesh, M., Jamasb, M., and Moeini, R. (2011). "Calibration of water distribution hydraulic models: A comparison between pressure dependent and demand driven analyses." *Urban Water Journal*, 8(2), 93-102.

The Mathworks Inc. (2015a). "Filtering and Smoothing Data." http://www.mathworks.com/help/curvefit/smoothing-data.html#bq_6zbc (11/30, 2015).

The Mathworks Inc. (2015b). "MATLAB r2012a." .

Tucciarelli, T., Criminisi, A., and Termini, D. (1999). "Leak Analysis in Pipeline Systems by Means of Optimal Valve Regulation." *J.Hydraul.Eng.*, 125(3), 277-285.

Vassiljev, A., Koor, M., and Koppel, T. (2015). "Real-time demands and calibration of water distribution systems." *Adv.Eng.Software*, 89 108-113.

Walski, T. M., Chase, D. V., Savic, D. A., Grayman, W. M., Beckwith, S., and Koelle, E. (2003). "Advanced water distribution modeling and management." *Advanced Water Distribution Modeling and Management*, Haestad Methods Press, Waterbury,Connecticut,USA, .

Walski, T. (1995). "Standards for model calibration." *Proceedings of the AWWA Computer Conference. American Water Works Association, Norfolk, Virginia*, .

Walski, T. (1983). "Technique for Calibrating Network Models." *J.Water Resour.Plann.Manage.*, 109(4), 360-372.

Walski, T., DeFrank, N., Voglino, T., Wood, R., and Whitman, B. (2008). "Determining the Accuracy of Automated Calibration of Pipe Network Models." American Society of Civil Engineers, 1-18.

Walski, T., Wu, Z., and Hartell, W. (2004). "Performance of Automated Calibration for Water Distribution Systems." American Society of Civil Engineers, 1-10.

Whittemore, R. (2001). "Is the Time Right for Consensus on Model Calibration Guidance?" *J.Environ.Eng.*, 127(2), 95-96.

Wu, Z., and Clark, C. (2009). "Evolving Effective Hydraulic Model for Municipal Water Systems." *Water Resour.Manage.*, 23(1), 117-136.